Statistical graph models of temporal brain networks

Catalina Obando Forero

Sorbonne Université

École Doctorale d'Informatique, de Télécommunication et d'Électronique (EDITE)

ARAMIS LAB à l'Institut du Cerveau et de la Moelle épinière (ICM)

STATISTICAL GRAPH MODELS OF TEMPORAL BRAIN NETWORKS

MODELISATION STATISTIQUE DE GRAPHE POUR L`ETUDE DE RESEAUX DYNAMIQUES DU CERVEAU

CATALINA OBANDO

Thèse de doctorat d'informatique

Dirigée par *Fabrizio De Vico Fallani*

Présentée et soutenue publiquement le 6 *DECEMBRE 2018*

Devant un jury composé de :

- *Mme. Sophie ACHARD*
  DR, CNRS – Université de Grenoble, Rapporteur
- *M. Vito LATORA*
  Full professor, Queen Mary University of London, Rapporteur
- *M. Andrea GABRIELLI*
  Chercheur, CNR – Institute of Complex Systems (ISC), Examinateur
- *M. Matthieu LATAPY*
  DR, Sorbonne Université, Examinateur
- *Mme. Charlotte ROSSO*
  MCU-PH, Sorbonne Université, Examinateur
- *M. Fabrizio DE VICO FALLANI*
  CR, Inria Paris, Directeur de thèse

Abstract

STATISTICAL GRAPH MODELS OF TEMPORAL BRAIN NETWORKS

by Catalina OBANDO

The emerging area of complex networks has led to a paradigm shift in neuroscience. Connectomes estimated from neuroimaging techniques such as electroencephalography (EEG), magnetoencephalography (MEG) and functional magnetic resonance imaging (fMRI) results in an abstract representation of the brain as a graph, which has allowed a major breakthrough in the understanding of topological and physiological properties of healthy brains in a compact and objective way.

However, state of the art approaches often ignore the uncertainty and temporal nature of functional connectivity data. Most of the available methods in the literature have been developed to characterize functional brain networks as static graphs composed of nodes (brain regions) and links (FC intensity) by network metrics. As a consequence, complex networks theory has been mainly applied to cross-sectional studies referring to a single point in time and the resulting characterization ultimately represents an average across spatiotemporal neural phenomena.

Here, we implemented statistical methods to model and simulate temporal brain networks. We used graph models that allow to simultaneously study how different network properties influence the emergent topology observed in functional connectivity brain networks. We successfully identified fundamental local connectivity mechanisms that govern properties of brain networks. We proposed a temporal adaptation of such fundamental connectivity mechanisms to model and simulate physiological brain network dynamic changes. Specifically, we exploited the temporal metrics to build informative temporal models of recovery of patients after stroke.

Contents

Abstract **3**

Scientific production **9**

Introduction **11**

1 Graph analysis of functional brain networks **15**
1.1 From time series to networks 17
1.1.1 Neuroimaging data 17
MRI and fMRI 17
EEG/MEG 17
1.1.2 Nodes and Links 18
1.1.3 Thresholding 20
1.2 Analyzing Brain Networks 22
1.2.1 Basic graph notions 22
1.2.2 Graph metrics 23
1.2.3 (Universal)Properties of Brain Networks 26
1.3 Temporal brain networks 30

2 Statistical graph models of brain networks **33**
2.1 Exponential Random Graph Models (ERGM) 34
2.1.1 Mathematical formulation 34
Alternative formulation 36
2.1.2 Classic examples 37
Properties 39
2.1.3 Estimation techniques 40
Pseudo-likelihood estimation 40
Markov chain Monte Carlo Maximum Likelihood Estimation (MCMC-MLE) 41
2.1.4 Model construction and considerations 42
Degeneracy 42
2.2 Temporal extension TERGM 44
2.2.1 Mathematical formulation 44
2.2.2 Temporal dependencies 44
2.2.3 Computational implementation 45

3 A statistical model for brain networks inferred from large-scale electrophysiological signals **47**
3.1 Synthetic networks 47
3.1.1 Validation 51

3.2 Resting state conditions 53
Model implementation 53
Validation 54

4 Temporal models of dynamic brain networks predict recovery after stroke 65
4.1 Temporal synthetic data 65
4.1.1 Temporal metrics 66
4.1.2 Model selection 67
4.2 Application to Stroke recovery 70
4.2.1 Time-varying brain network construction 71
4.2.2 Dynamic network mechanisms after stroke 73
Prediction of future outcome 76
4.2.3 Discussion 77
Modeling dynamic networks 77
Brain plasticity and stroke 78
Forecasting behavior and recovery 79
Limitations/perspectives 79
Conclusion 80

5 Discussion & Future Directions 83

Bibliography 85

List of Figures

1.1 Cortical surface parcellation generated by Gordon & Laumann and collegues Gordon et al., 2014 19
1.2 Illustration of an EEG cap comprising 74 electrodes. 19
1.3 Brain connectivity network constructed from EEG data before and after thresholding 21
1.4 Illustration of graph metrics 25
1.5 Illustration of time varying brain network 31

2.1 Sufficient statistic of the triad model: triangles and two paths 38
2.2 Sufficient statistic of the generalized random model: degree distribution 39

3.1 a) Two input network with random and lattice topology, b) Two simulated networks from ERGMs with hamiltonians $H(G) = \theta_1 E(G)$ (top) and $H(G) = \theta_1 D(G)$ (bottom), c) goodness of fit in terms of models over 100 simulated networks. 49
3.2 Sensitivity analysis of GW_K and GW_E and decay parameters τ in global and local efficiency values 50
3.3 The observed values of each input Watts-Strogatz network is shown in a solid point, and the boxplot shows the distribution of metrics GW_K, GW_E ,E_l, E_g over simulated networks from model 3.1 52
3.4 Area under the curves ROC and PR-C of models 3.1 (GW-solid yellow line) and TP (PERGM with triangles and two paths as metrics-blakc triangles). This plot has linear increment, to get more small-world and hopefully more smooth reduction. . . . 53

4.1 Time varying network generated from correlated Watts Strogatz 66
4.2 Count of temporal metrics of time varying network generated from correlated Watts Strogatz model 67
4.3 Goodness of fit of the model in terms of the area under the curve 68
4.4 Comparing different TERGM with temporal and static metrics 69
4.5 Comparing different (T)ERGM with temporal and static metrics in terms of AUC 69
4.6 a) Functional connectivity network b) Lesion occurrence over the population of cortical lesion patients c) Time varying brain networks d) Behaivoral scores changes over time 73
4.7 Statistical comparison of stroke connectivity mechanisms to controls 75
4.8 Weight parameters mapped in the cortex 76

4.9 Formation of interhemispheric short connections and intrahemispheric clustering connections predict language 77

Scientific production

PUBLICATIONS

- Obando, C., & De Vico Fallani, F. (2017). A statistical model for brain networks inferred from large-scale electrophysiological signals. Journal of The Royal Society Interface, 14(128), 20160940.
- Obando, C., & De Vico Fallani, F. Temporal models of dynamic brain networks predict recovery after stroke. In preparation

TALKS AND POSTERS

- Talk 20 min at ICCS, Cambridge, MA, USA *2018*
- Talk 20 min at NetSci: International School and Conference on Network Science, Paris *2018*
- Talk 20 min at Network Neuroscience Satellite, NetSci, Paris *2018*
- Talk 20 min at the 6th in the International Conference on Complex Networks and Their Applications, Lyon *2017*
- Talk 20 min at Complex networks: from socio-economic systems to biology and brain, Lipari, Italy *2017*
- Lightening talk and poster contribution in NetSci, Indianapolis, USA *2017*
- Talk 20 min at Workshop Dynamic Networks, INP-ENSEEIHT, Toulouse, France *2016*
- Poster contribution in the 22nd Annual Meeting of the Organization for Human Brain Mapping, Geneva, Switzerland *2016*

SCIENTIFIC VULGARISATION

- Salon de la culture et jeux mathématiques *2016*
- Féte de la science *2016*

Introduction

The emerging area of complex networks has led to a paradigm shift in neuroscience. Connectomes estimated from neuroimaging techniques such as electroencephalography (EEG), magnetoencephalography (MEG) and functional magnetic resonance imaging (fMRI) results in an abstract representation of the brain as a graph, which has allowed a major breakthrough in the understanding of topological and physiological properties of healthy brains in a compact and objective way (Bullmore and Sporns, 2009).

The nodes of these estimated connectomes, or brain networks, are established accordingly to the neuroimaging technique used to record brain connectivity data, and the links are defined by a functional connectivity (FC) measure of the temporal dependence between nodes. For example, when using an EEG, which is a sensor-base modality, to record electrical brain activity, then the brain nodes are commonly defined as the electrodes. If instead a voxel-base modality is used, such as fMRI, then the most common way to define brain nodes is to use a fixed anatomical atlas.

Brain networks, tend to exhibit similar organizational properties including small-worldness, cost-efficiency, modularity and node centrality (Bullmore and Sporns, 2009), as well as characteristic dependence from the anatomical backbone connectivity (Honey et al., 2009; Deco et al., 2013; Park and Friston, 2013) and genetic factors (Fornito et al., 2011). Furthermore, they show potentially clinical relevance as demonstrated by the recent development of network-based diagnostics of consciousness (Achard et al., 2012; Chennu et al., 2014), Alzheimer's disease (Tijms et al., 2013), stroke recovery (Grefkes and Fink, 2011), and schizophrenia (Lynall et al., 2010). In this sense, quantifying topological properties of intrinsic functional connectomes by means of graph theory has enriched our understanding of the structure of functional brain connectivity maps (Stam, 2004; Bullmore and Sporns, 2009; Rubinov and Sporns, 2010; Stam and Straaten, 2012).

The use of graph analysis in clinical neuroscience has also become essential to quantify brain dysfunctions in terms of the aberrant configuration of functional brain networks. Recent evidence from cross-sectional studies

(Grefkes and Fink, 2011) highlights that cerebrovascular damages to local areas of the brain (i.e. stroke) generally induce i) critical deviation from optimal (i.e. small-world) network topologies supporting both segregated and integrated information processing, ii) altered interhemispheric connectivity and modularity, iii) and abnormal region centrality in the ipsilesional hemisphere as well as in the contralesional hemisphere.

Nevertheless, these results refer to a descriptive analysis of the observed brain network, which is only one instance of several alternatives with similar structural features. This is especially true for functional networks inferred from empirically obtained data, where the edges (or links) are noisy estimates of the true connectivity and thresholding is often adopted to filter the relevant interactions between the system units (Tumminello et al., 2005; Vidal, Cusick, and Barabási, 2011; De Vico Fallani et al., 2014). Statistical models are therefore needed to reflect the uncertainty associated with a given observation, to permit inference about the relative occurrence of specific local structures, and to relate local-level processes to global-level properties (Goldenberg et al., 2009).

Furthermore, despite its evident impact, graph analysis of functional brain networks is not a simple toolbox that can be blindly applied to brain signals and many issues remain unaddressed (Bullmore and Sporns, 2009). Perhaps the most critical limitation is assuming that the way different brain regions are functionally connected is implicitly constant (stationarity hypothesis). Most of the available methods in the literature have been developed to characterize functional brain networks as static graphs composed of nodes (brain regions) and links (FC intensity), which do not change in time (De Vico Fallani et al., 2014). As a consequence, complex networks theory has been mainly applied to cross-sectional studies referring to a single point in time and the resulting characterization ultimately represented an average across spatiotemporal neural phenomena (Rubinov and Sporns, 2010).

However, recent evidence suggests that brain functional connectivity is highly variable across multiple time scales and that this non-stationary influences the emergence of global network properties and complex brain behavior (Hutchison et al., 2013). These aspects dramatically limit our ability to fully understand the brain organizational mechanisms after lesions and to probe the predictive power of possible network-based neuromarkers of recovery. The ability of the human brain to adapt to damages, for instance, to functionally reorganize after cerebrovascular “attacks” or stroke, and to restore lost functions is probably the most fascinating, yet unknown, process

characterized by a temporally dynamic reorganization (Grefkes and Fink, 2011). This dynamic skill, which is known in neuroscience as brain plasticity, is not only interesting from a network science perspective, but it also plays a crucial role in determining the motor/cognitive recovery of patients who survive a stroke.

The purpose of this Ph.D. thesis is to go beyond the descriptive analysis of brain networks to develop models that are capable to infer brain networks and that are a tool to understand brain network formation. Specifically, the objectives are:

- Develop statistical methods to model and simulate temporal brain networks
- Quantify network variability and isolate persistent network properties in the normal brain
- Model spatiotemporal network changes underlying plasticity after brain lesions.

The document is divided as follows, first chapter presents the state of the art of brain networks and graph theory tools relevant to its analysis; chapter two presents the general mathematical framework that we used to model brain networks; in chapter three we present the implantation and results of such models to statistical model resting state brain networks; in chapter four we apply the methodological framework to time-varying brain networks, specifically we look at stroke patients. Finally, in chapter five we conclude and discuss future directions.

Chapter 1

Graph analysis of functional brain networks

The representation of a system composed of agents and interactions among them with a complex network is an effective way to extract information on the nature and topology of such interactions. It allows us to abstract complex emergence behavior into a mathematical object that we can study with a set of tools coming from different disciplines such as statistical physics, dynamical systems, numerical simulations, graph theory among others.

In particular, the brain can be abstracted into a complex network. This idea has been supported since the nineteenth century by anatomical studies that mapped the brain's cytoarchitecture, cellular circuits and long-range fiber systems (Cajal, 1995; Sporns, 2013b). More recently, by high-quality neural data that allows studying the structure and function of the brain with more sophisticated methods.

Due to technological advancements we now have access to large and detail brain data. This constituted a paradigm shift in neuroscience as it allowed to study the brain in a more comprehensive and noninvasive manner. These data represent in general networks comprising the relations or interconnections that link the many elements of large-scale neurobiological systems (Bassett and Sporns, 2017), therefore the natural relation with complex networks.

Brain networks represent neurological systems and its interactions at different spatiotemporal levels. At the microscopic scale neurons and synaptic connections are taken as nodes and links. The C. elegans entire neurological system has been successfully mapped in this way (Li et al., 2004). At higher levels, units take different forms, e.g. cytoarchitectonically or functionally distinct volumes at the macroscale, or more arbitrary delineations, such as voxels (Bassett, Zurn, and Gold, 2018). Links can represent physical

or functional connections. These specifications depend on the neuroimaging technique employed to record data. In this work, we focus especially on functional brain networks, even though we will review some of the definitions and concepts of structural brain networks.

As with other complex networks, one is interested in studying the intrinsic dynamics and mechanisms that cause emergent behaviors and topologies. For example, in a social network, one could be interested in understanding how new friendships are formed and a plausible hypothesis could be that friendships among people who have a friend in common are more likely to happen. In a functional connectivity network, one is interested in study the statistical dependencies among remote neurophysiological events, how they occur and what can this tell us about specific brain states and/or populations. However, formulating a plausible hypothesis about brain connectivity mechanisms can be somewhat more complicated.

Network science is a discipline that offers tools to analyze the brain as a complex system of interactions. Briefly, a typical brain network study can be summarized by a pipeline starting with data acquisition, following by data processing, network construction and specifications, and finishing by analyzing the resulting brain network with quantitative techniques. Special care has to be taken in each of the steps aforementioned, each on its own are current subjects of active research and are discussed more in depth below. The work of this thesis focuses especially on the last step of analyzing brain networks.

The classic approach to analyze brain networks has been mainly a descriptive one. Essentially, brain networks are put under a graph metrics' lens to characterize many topological properties. These methods have had a prominent role in characterizing normal brain organization as well as alterations due to various brain disorders (Fox and Greicius, 2010).

In this chapter we present the general pipeline to build brain networks from neuroimaging data, then we discuss groundbreaking results on the field in the framework of graph theory, and we close examining the extension of these concepts into temporal brain networks.

1.1 From time series to networks

1.1.1 Neuroimaging data

Like any other real complex network, brain networks are built from real data, specifically from neuroimages. Neuroimages are noninvasive techniques that aim to capture the anatomical or functional structure of the brain by measuring proxies of brain activity in the nervous system. They have been used extensively in studies that have helped further our understanding of physical and cognitive properties of the brain (Aine, 1994; Casey et al., 2005). Here we focus on function of the brain, and we briefly discuss two categories of neuroimages techniques: magnetic resonance imaging (MRI) and electro/magneto-encephalogram (EEG/MEG) (see Rogers et al., 2007; Sakkalis, 2011 for reviews).

MRI and fMRI

MRI is a non-invasive medical imaging technique that generates detailed, cross-sectional images of organs and tissues. An MRI scanner uses a strong magnetic field to align the magnetic nucleus of hydrogen atoms, radio waves are applied at different timing and pulses to break this alignment, the nuclei then realign emitting a radio signal which is captured by the scanner and encodes information about the position and type of tissues in the body. MRI is used to reconstructed 3D shapes of the anatomical structure.

Functional magnetic resonance imaging (fMRI) uses the same technique but is design to capture brain activity by means of the BOLD (blood oxygen level-dependent) signal. The principle behind it is that as neuronal activity increases there is an increased demand for oxygen that causes a local increase of blood flow to the active regions. The BOLD contrast is measured in fMRI as an indirect measure of neural activity. One of the most exploited fMRI feature is its high spatial resolution to the level of millimeters (Heuvel et al., 2008; Salvador et al., 2005; Heuvel and Hulshoff Pol, 2010).

Another sophisticated use of magnetic resonance is diffusion-weighted imaging (DWI) which maps diffusion the diffusion of water molecules within the brain (Huisman, 2010).

EEG/MEG

Electroencephalogram or magnetoencephalography uses sensors attached to the scalp to measure electrical/magnetic neural activity. Electrical activity

of active neurons produces currents that spread in the head reaching the scalp. EEG records voltages difference on the brain electrical fields while MEG records brain magnetic field produced by those currents. EEG and MEG present a high temporal resolution and relatively poor spatial resolution as only a few hundred sensors are used. There are source reconstruction methods that try to project back the signal recorded in the scalp to the brain to increase spatial resolution, this is an active field of research (EEG Nunez and Srinivasan, 2006; Bonmassar et al., 2001; Casdagli et al., 1997; MEG Chen, 2001; Maldjian, Davenport, and Whitlow, 2014)

1.1.2 Nodes and Links

Nodes are defined according to the modality of data acquisition: voxel-based, e.g. fMRI; or sensor-based, e.g. EEG. We will see that in certain cases such definition are somewhat straightforward while in other cases uses other models to approximate a fair unite of analysis.

In voxel-based modality, the nodes can be defined directly as the voxels or as aggregates of voxels. The former was the first technique used, and we have seen a proliferation of the latter one (Stanley et al., 2013). The most common way to aggregate voxels is by using anatomical parcellations of the brain (Reus and Heuvel, 2013; Pereira et al., 2013). Parcellations of the brain divide its spatial domain into homogeneous parts in terms of cytoarchitecture, anatomical connectivity, functional connectivity or task-related activation. Such parcellation can be used in both structural and functional brain networks.

Figure **??** shows an example of a cortical surface parcellation of the brain. The parcellation is composed of 324 regions of interest (ROIs) each exhibiting homogeneous resting-state functional connectivity signal. In a higher level, we see the different ROIs group together to form subnetworks that activate in different motor and cognition tasks.

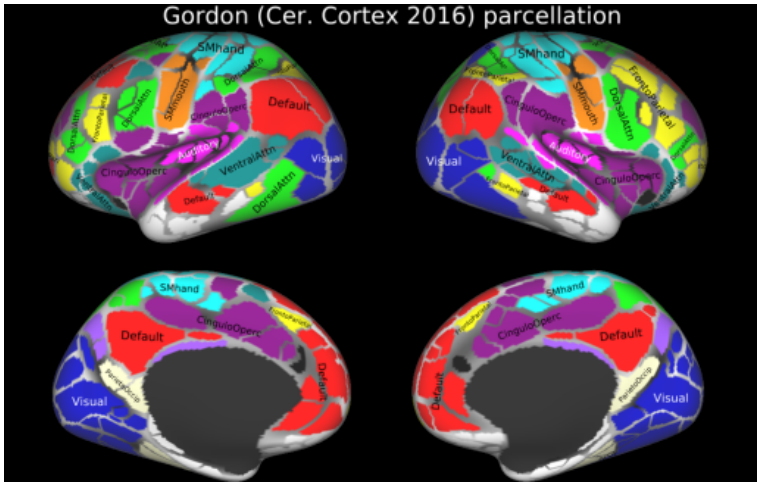

FIGURE 1.1: Cortical surface parcellation generated by Gordon & Laumann and collegues Gordon et al., 2014

In sensor-based modalities, the nodes can be directly assigned to the electrodes. However, the signal captured by each sensor of both EEG and MEG are a mixture of the signal emanating from the cortical surface. This effect can be either ignored, then special attention has to be taken in the interpretation of results, or addressed by techniques such as source reconstruction, where nodes are projected back onto the cortex, spatial filters or choosing specific functional connectivity measures (see section **??**).

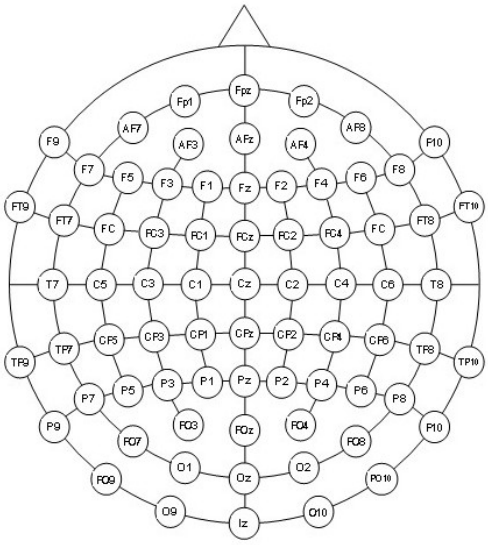

FIGURE 1.2: Illustration of an EEG cap comprising 74 electrodes.

After defining nodes the next natural step is to define links, or edges, among those nodes. Links can represent functional or anatomical connections. They are weighted, at least in a first instance, and can be directed or

undirected.

Functional links are in general defined as the statistical dependency of signals between each pair of nodes, which is measure through functional connectivity (FC) measures (Friston, 2011). FC measures range from simple correlations to more sophisticated methods that infer relations with informational meaning and can produce links that are directed, i.e. captures information propagation, or undirected, i.e. encodes information symmetry (Fingelkurts, Fingelkurts, and Kähkönen, 2005; Quiroga et al., 2002; David, Cosmelli, and Friston, 2004; Ansari-Asl et al., 2006). FC measures include synchronization, phase locking, coherence, and correlations. We give explicit formulas of the last two as those are used later in our work. Let X and Y be two signals coming from different nodes

Pearson correlation

$$\rho_{X,Y} = \frac{cov(X,Y)}{\sigma_X \sigma_Y}$$

Where cov is the covariance, $\sigma_{\cdot}$ is the standar deviation of X/Y.

Spectral coherence

$$w_{XY}(f) = \frac{\mid S_{XJ}(f) \mid^2}{S_{XX}(f) SYY(f)}$$

Where S_{XY} is the cross-spectrum between X and Y and S_{XX} and S_{YY} are the autospectra of X and Y, respectively. The imaginary coherence is given by the imaginary part of the coherence and is one of the FC measures that takes into account volume conduction effects.

One can also define structural links, which reflect anatomical connections and are typically based on synapses, white matter tracks or structural covariance. Diffusion tensor imaging (DTI), a special kind of DWI, maps tracks of water diffusion over the brain which are taken as anatomical connections.

1.1.3 Thresholding

Brain networks constructed via FC measures result in fully connected weighted networks. Many studies take these networks as the object of study, but it has been argued that very weak connections might be the results of noise in the acquisition step and thus they shouldn't be taken into account in further analysis. Filtering then is used to retain the strongest and therefore more significant functional links.

One common filtering or thresholding technique consists of keeping only the links whose FC measure is higher than a threshold value. The choice of

the threshold can follow different heuristics, e.g. that the resulting network is connected, or one can consider a range of threshold values and reproduce the analysis over each resulting network. Other methods have been proposed in the literature (Ginestet et al., 2011; Rubinov and Sporns, 2011; Achard et al., 2008; De Vico Fallani, Latora, and Chavez, 2016).

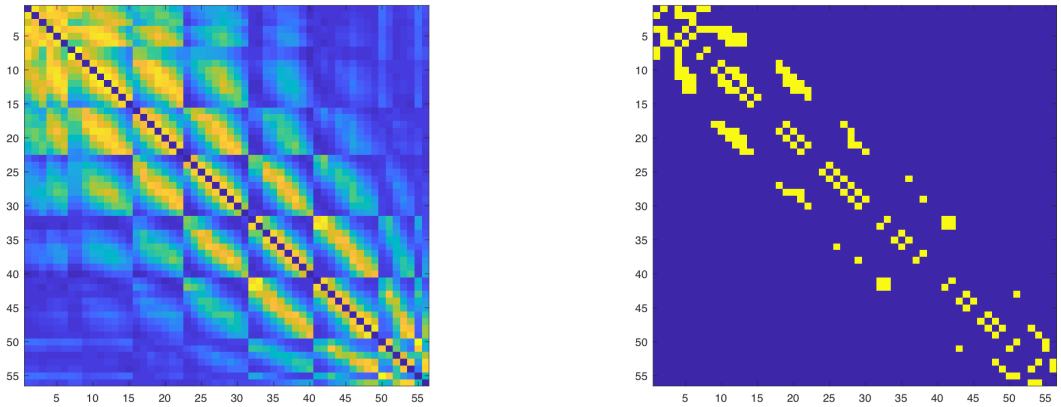

FIGURE 1.3: Brain connectivity network constructed from EEG data before and after thresholding

1.2 Analyzing Brain Networks

After constructing a brain network, one can use tools coming from graph theory to study how cognitive and behavior functionalities are supported by the synchronization patterns captured as a network. Here we give basic notions of graph theory, some important graph metrics widely used in the field of network neuroscience and finally specific properties that have been found consistently despite different network construction methodologies and in some cases across species.

1.2.1 Basic graph notions

Let $V = (v_1, v_2, ..., v_N)$ be a set of N vertices or nodes and a set of edges or links $E = \{(i,j)/i,j \in V\}$, a graph defined as an ordered pair $G = (V,E)$ [1]. A directed network is a network in which each edge has a direction, pointing from one vertex to another. By notation, the edge (i,j) points from vertex v_i to vertex v_j and is represented graphically by an arrow with this direction ($v_i \longrightarrow v_j$).

Vertices can also be joined by more than one edge, we refer to those edges as a multi-edge, the number of edges that joins a pair of vertices is called the multiplicity of the multi-edge. Edges can also join a single vertex, these edges are called self-edges. Weights $w_{ij} \in \mathbb{R}$ can be associated to links $(i,j) \in E$, which can represent some length, capacity or dependency on single links, and we say that a graph is unweighted if there are no multi-edges and $w_{ij} = 1, \forall (i,j) \in E$.

An undirected network without multi-edges or self-edges is called a *simple network*. From now on, we will consider simple undirected graphs unless stated otherwise. Most of the following notions and definitions have natural extensions to directed or weighted graphs.

A path between nodes i and j is an alternating sequence of nodes and edges that begins with i and ends in j. A shortest path or geodesic between two nodes i, j is a path of minimal length between nodes i and j. The distance d_{ij} between two nodes i and j is the length of the shortest path between them. If there exists no path connecting both nodes then $d_{ij} = \infty$. We say that a graph is connected if there exists a finite positive length path connecting each pair of nodes.

[1] We will denote a vertex by v_i or simply by the index, i.e. $V = (1, 2, ...n)$.

A graph G can be represented by an adjacency matrix $A \in \mathbb{R}^N \times \mathbb{R}^N$ with entries

$$A_{ij} = \begin{cases} 1 & \text{if there is an edge from j to i;} \\ 0 & \text{otherwise.} \end{cases}$$

Note that A is symmetric for undirected networks and that the number of links is given by $l = \sum_{i,j \in N} A_{ij}$. The number of links in a graph might be the first natural quantity to measure, however many other graph metrics have been proposed over the year responding to theoretical interests and prompt by its application to real-world complex networks.

1.2.2 Graph metrics

Different graph statistics can be computed from the adjacency matrix. Another simple measure is the degree $k_i = \sum_{j \in V} A_{ij}$ of a node. From it, one can build a distribution of degrees of the whole network. The cumulative distribution of the network is given by

$$P(k) = \sum_{k' \geq k} p(k')$$

where $p(k')$ is the probability of a node having degree k' (Barabasi and Albert, 1999).

These measures give information on the connectivity profile of individual nodes and can characterize classes of networks. For instance, most real networks exhibit degrees distributions that follow a power law.

We can also measure the density of a graph, which tell us the fraction of edges present in a graph with respect to a fully connected one as $\rho = \frac{2 \times l}{n \times (n-1)}$.

Characteristic path length L and global efficiency E_g are metrics that aim to measure how fast information in the network can travel across any arbitrarily chosen nodes (Watts and Strogatz, 1998; Latora and Marchiori, 2001).

$$L = \frac{1}{N} \sum_{i \in V} L_i = \frac{1}{N} \sum_{i \in V} \frac{\sum_{j \in V, j \neq i} d_{ij}}{N-1}$$

$$E_g = \frac{1}{N} \sum_{i \in V} E_i = \frac{1}{N} \sum_{i \in V} \frac{\sum_{i \in V, j \neq i} d_{ij}^{-1}}{N-1}$$

For example, in a connected random graph, where two nodes are connected with uniform probability p, L tends to be low and E_g high.

Clustering coefficient C, measures how well the set of near neighbors of a node is connected in proportion to the set being fully connected. Local efficiency E_l measures in average how the information travels locally (Watts and Strogatz, 1998; Latora and Marchiori, 2001).

$$C = \frac{1}{N}\sum_{i\in V} C_i = \frac{1}{N}\sum_{i\in v}\frac{\sum_{j,h\in V} A_{ij}A_{ih}A_{jh}}{k_i(k_i-1)}$$

$$E_l = \frac{1}{N}\sum_{i\in V} E_g(G_i)$$

where G_i is the subgraph formed by nodes connected to i.

Given a partition in modules $\{m_i\}$ of a graph, modularity Q measures to what extent those modules are more highly connected among them than to other modules. Over the year many different algorithms to detect modules or communities have been proposed and is currently an active topic of research. One simple and broadly used method is modularity maximization, i.e. the modules are taken as those that maximize Q (Newman, 2006)

$$Q = \frac{1}{l}\sum_{i,j\in V}\left(A_{ij} - \frac{k_i k_j}{l}\right)\delta_{m_i,m_j}$$

where m_i is the module containing node i, and $\delta_{m_i,m_j} = 1$ if $m_i = m_j$ and 0 otherwise.

Closeness centrality measures the average distance of a node i to all other nodes in a graph (Freeman, 1978).

$$L_i^{-1} = \frac{N-1}{\sum_{j\in V, j\neq i} d_{ij}}$$

Betweenness centrality measures how many shortest paths between all pair of nodes in a network passes though a node i (Freeman, 1978). Is one of the measures that attempts to quantify the importance of a node in the overall connectivity of the network. Nodes with high centrality are usually called hubs.

$$b_i = \frac{1}{(N-1)(N-2)}\sum_{\substack{h,j\in V\\ h\neq j, h\neq i, j\neq i}}\frac{\rho_{hj}(i)}{\rho_{hj}}$$

where ρ_{hj} is the number of shortest paths between h and j, and $\rho_{hj}(i)$ is the number of shortest paths between h and j that pass through i.

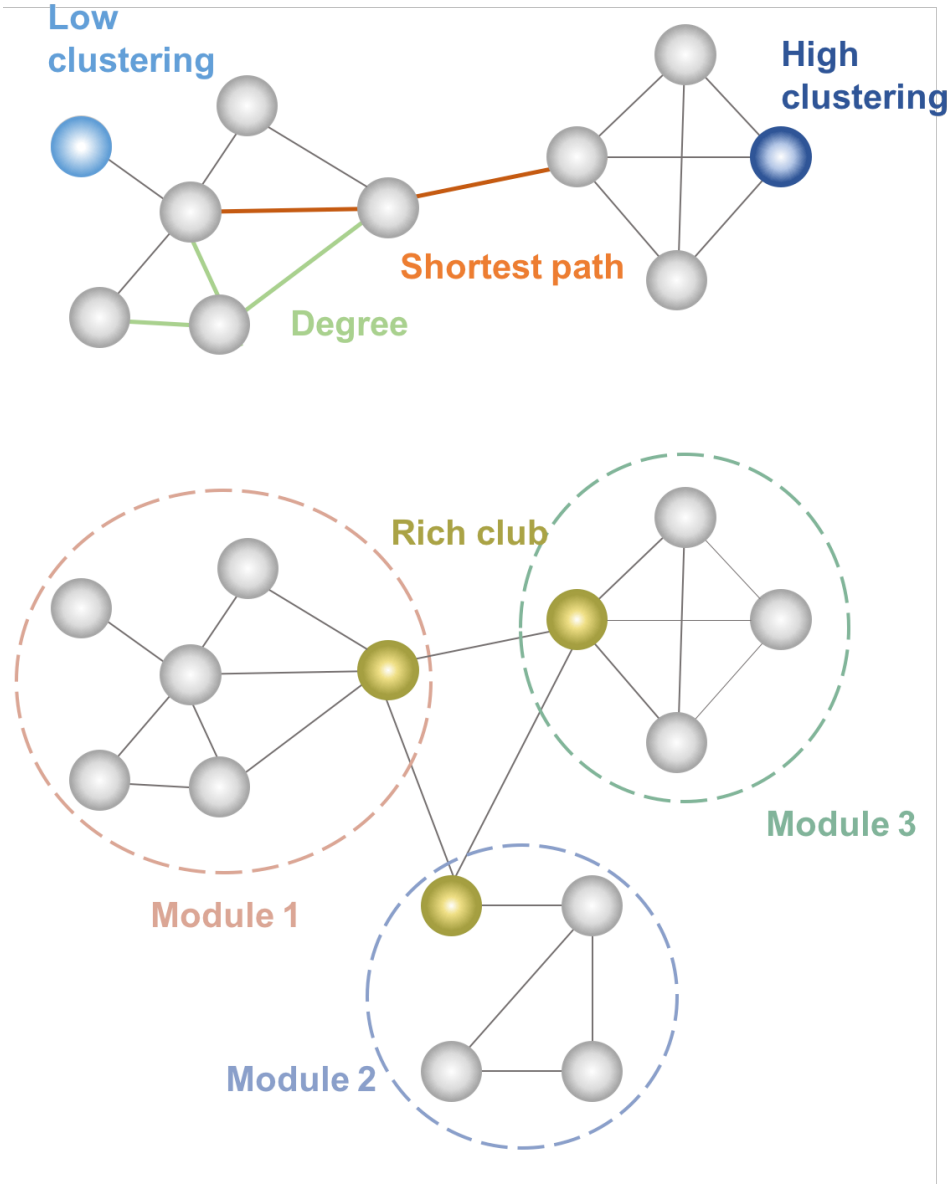

FIGURE 1.4: Illustration of graph metrics

1.2.3 (Universal)Properties of Brain Networks

Over the years graph metrics have been used to characterize brain networks of normal humans and other species, and to discriminate different population (e.g. healthy from diseased), or brain states (e.g. resting-state to activation tasks). Many of these properties are shared among other networks observed in nature and in this sense are regarded as universal, others are specific to network neuroscience and together have further our understanding of healthy and disease brain.

Here we summarize some of the main universal properties that have been found to be true across different neuroimaging modalities and even across species, and some important case studies that show the relevance of using graph tools in understanding normal and diseased brain states.

- Small-world
  The small-world property was first observed by Watts and Strogatz in its seminal paper Watts and Strogatz, 1998. They studied the topological properties of a lattice, (a network where each node is connected to its k nearest neighbors) and the resulted networks that occur from rewiring with increasing probability $p > 0$ its edges. When $p = 1$ networks are random. They observed that the values of clustering coefficient and characteristic path length are high and low, respectively, for a lattice and conversely for a random network. More interestingly, they noticed that at relatively low probability values (around $p = 0.01$) the resulting networks of rewiring the link of a lattice with such probabilities, exhibit both high clustering coefficient and characteristic path length, i.e. they displayed small-world property.

  They also showed in the same paper that several real-world networks have this property, including the neural network of the worm C. elegans. This property has been found across different species (e.g. cat and macaque Hilgetag and Kaiser, 2004; Sporns and Zwi, 2004) and both anatomical and functional brain networks (see for a review and further perspective on this topic Bassett and Bullmore, 2017). Although this model provoked a proliferation in the field of network science one critic that quickly came to light was that it didn't produce degree distributions that were realistic, i.e. found in nature.

- Scale-free
  Some studies have shown that brain networks exhibit exponential or

exponentially truncated power-law degree distributions, i.e few nodes exhibit a high degree (Sporns, 2013b; Achard et al., 2006). This is a property that has been observed in many other biological systems, however, is somewhat controversial in network neuroscience because of the brain networks' small size (Bassett and Bullmore, 2017).

- Communities
  Despite the heterogeneity on methods and data, numerous studies have shown that both structural and functional brain networks are organized in modules or communities that can be associated to cognitive functions by supporting the integration of information (Crossley et al., 2013).

  They have been also been identified as responsible for evolution (differentiation with other species), conservation of wiring cost and facilitating information and complex dynamics, see Sporns and Betzel, 2016 for a review. Furthermore, such modules exhibit a hierarchical organization, which means there are sub-modules within modules (Meunier, Lambiotte, and Bullmore, 2010; Bassett et al., 2008).

- Hubs/rich club
  Numerous studies have shown the existence of hubs in brain networks, these are nodes that are highly connected and play an important role in the integration of the information (Sporns, Honey, and Kötter, 2007). Moreover, is has been shown that hubs are organized in a "rich-club" architecture, i.e. hubs are densely connected among themselves than nodes with lower degree (Heuvel and Sporns, 2011).

- Integration and Segregation
  A widely accepted hypothesis is that brain networks, like many other spatially embedded complex networks, have evolved to optimize a balance between integration and segregation of information to support cognition and behavior (Bullmore and Sporns, 2009). Multiple strategies have been suggested to explain the actual mechanisms that the brain prioritizes to achieve this optimal balance.

One is related to the small-world property, as networks exhibiting this property balance global and local efficiency (Tononi, Sporns, and Edelman, 1994). It has also been suggested that integration and segregation are supported by communities and hubs respectively (Sporns, 2013a; Deco et al., 2015). Note that these structures do not necessarily appear in "simple" small-world networks, e.g. the ones observed in the Watts-Strogatz model.

- Cost efficient
  It has been shown that the brain aims at minimizing its wiring cost involved in both connecting neurons anatomically and functional connections (Achard and Bullmore, 2007; Bullmore and Sporns, 2012). However, it has been argued that the brain is not simply minimizing wiring cost but is balancing this against segregation and integration., i.e. there is a trade-off between high efficiency of information transfer and low-cost connections.

- Distortions in clinical populations
  These (universal) properties characterize the organization of normal structural and functional brain networks, and neurological disorders have been identified as deviations from "normal" properties. All of the properties listed above are broadly present in normal whole-brain networks characterizing its structural and functional organization. Deviations from these properties have been used to characterize neurological and psychiatric disorders (Stam and Reijneveld, 2007; Stam, 2014). Example of such studies are: schizophrenia (Liu et al., 2008; Wang et al., 2010b); autism (Barttfeld et al., 2011); stroke (Wang et al., 2010a); spinal cord injure (De Vico Fallani et al., 2007); Alzheimer's disease (Supekar et al., 2008).

The identification and understanding of the aforementioned properties have expanded our understanding of brain organization and the promise of further advancements is still latent. Nevertheless, these results refer to a descriptive analysis of brain networks. Essentially, it describes by means of graph metrics an observed topology but it does not explain the underlying network mechanisms that are into play in the emergence of the observed complexity.

For example, different studies of Alzheimer's disease (AD) patients have reported contrary results when looking at the change in path length over disease progression. In general, such results can be sensitive to the brain network construction methodology, e.g. the type of neuroimage or FC measure used, but even in somewhat homogeneous fMRI studies, both increased and decreased average path length has been observed (Stam, 2014). One of the challenges then is to find consistent features or biomarkers to identify network changes due to certain disease and to ultimately improve early diagnosis and guide treatment.

Another important point illustrated in the former example is the temporality of brain networks. Brains are intrinsically dynamic yet a large bulk of literature in network neuroscience looks at static brain networks. Looked with a historical perspective it could be argued that this responds to the natural steps a new field undertakes. Indeed, we have seen a growing interest and necessity to pursue studies that take into account the dynamic nature of the brain.

1.3 Temporal brain networks

The brain is a dynamic system that is in constant activity, even at rest, it changes across time on both long-time (Wang et al., 2010a) and short-time scales (Bassett et al., 2011), therefore is undeniable not only the interest but the need to study it as such. However, as Holme and Saramäki, 2012 puts it "the literature on static graphs is many times larger than that on temporal graphs, for a natural reason: it is usually much easier to analyze static graphs, especially analytically", which is an idea also applicable to the literature on brain networks. It is also true that in a new field, such as network neuroscience, there should be a natural evolution of studying "simple" static brain networks to dynamic ones. This idea is also embodied in this thesis by following a bottom up approach.

Interesting questions are, but not limited to: how does brain network topology changes over time in normal or injured brains? What are the connectivity mechanisms that supports dynamically behavioral or cognitive process?

There are different temporal scales one might consider to study as they encode diverse neurological processes. At small or rapid scales, one can be interested in studying flows of neural activity that occur at the level of milliseconds. Then at the level of seconds, one could observe motor task brain mechanisms or schizophrenia episodes, at scales of days or months processes such as learning or plasticity can be tracked, and at the level of years or decades, normal aging or progression or neurodegenerative diseases such as Alzheimer's disease becomes visible.

Such type of dynamics can be capture into temporal or time-varying networks. There exist different kinds of possible mathematical representations: aggregating over time periods(Holme, 2003; Rosvall and Bergstrom, 2010), reachability graphs (Moody, 2002), line graphs (Liljeros, Edling, and Amaral, 2003), transmission graphs (Riolo, Koopman, and Chick, 2001), stream graphs (Latapy, Viard, and Magnien, 2017), multi-layer networks (Kivela et al., 2014; Muldoon and Bassett, 2016). Many of the graph metrics describe in Section 1.2.2 can be extended to temporal networks and we refer to Holme and Saramäki, 2012 for details.

Here we focus on aggregate over time period temporal brain networks,

that is a sequence of time-order networks each of which is the accumulation or average of connections for a specific interval of time. For low temporal scales the aggregation can be done with a sliding window and for larger scales, the aggregation is done per unit of time.

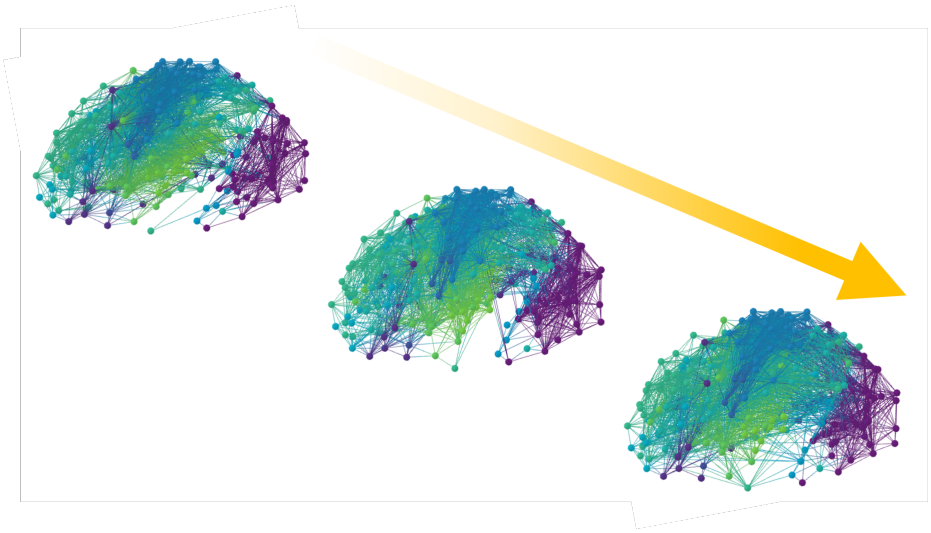

FIGURE 1.5: Illustration of time varying brain network

A similar descriptive approach to that of static brain networks can be performed by investigating the evolution of graph metrics computed time-wise (see for example De Vico Fallani et al., 2007; Valencia et al., 2008).

However, as neuroimaging recordings suffer from noise it is necessary to go beyond descriptive and characterization analysis to models that accounts for the statistical importance of connectivity mechanisms in healthy and diseased brain. We want to model and simulate the emergent behavior that neurological system exhibit in order to better understand the organizational mechanisms of the brain.

Chapter 2

Statistical graph models of brain networks

Complex networks are data representations of systems and therefore a particular instance or observation of such systems. Statistical inference of relational data is then a crucial tool to understand, control and ultimately predict the behavior of many real complex systems.

In particular, in the field of network neuroscience, the term network model can bring some confusion as they can be regarded as biological or animal models. Consider the three dimensions of models types proposed by Bassett, Zurn, and Gold, 2018: "The first dimension is a continuum that extends from data representation to pure (or 'first- principles') theory. The second dimension is a continuum that extends from biophysical realism to phenomenological estimates of functional capacity ('functional phenomenology'). The third dimension is a continuum that extends from elementary descriptions to coarse-grained approximations".

Here we are interested in first-principle theory informed by functional phenomenology data of coarse-grained approximations. In other words, statistical models over brain networks constructed from functional connectivity data.

A flexible yet powerful family of models is the exponential-family of random graphs which models the probability of edge existence in a graph G by fitting the probability mass function of G as a function of a $r-$vector of network statistics.

This chapter presents the general theory of exponential random graph models, its properties, computational implementation, and general model formulation. In the second part, the extension to temporal exponential random graphs is presented.

2.1 Exponential Random Graph Models (ERGM)

One of the first models for networks is the so-called Bernoulli model first proposed by Gilbert, 1959. This model assumed that the probability of an edge existing between two nodes was equal to some value $\pi \in [0,1]$, i.e. edges were assumed to be independent. Exponential random graph models (ERGMs) are an extension of Markov random graphs models proposed by Holland and Leinhardt, 1981 and (Frank and Strauss, 1986) which first proposed a family of distributions for undirected and directed graphs where the probability of the existence of edges had non-trivial dependence assumptions but considered conditional independence properties.

This work was extended by Frank, 1991 and Wasserman and Pattison, 1996 to include more arbitrary independence conditions focusing on directed graphs, which led to a family of probability functions called the p^* model. Further developments were made by Pattison and Wasserman, 1999 and Robins, Pattison, and Wasserman, 1999 regarding valued and multivariate relations.

2.1.1 Mathematical formulation

Let $\mathcal{G}$ be a set of possible network realizations with n nodes, an exponential random graph model assumes that the probability of observing a particular network $g \in \mathcal{G}$ is a function sufficient statistics vector $\boldsymbol{x} = \{x_1, x_2, ..., x_r\}$ such that he probability distribution $P(G)$ over $\mathcal{G}$ is given by

$$P_\theta(G = g) = exp\{\sum_{i=1}^{r} \theta_i x_i(g) - Z(\theta)\} \tag{2.1}$$

where $\theta \in \mathbb{R}^r$ denotes the statistical parameter governing the probabilistic formation of the network and $Z(\theta)$ is a normalizing constant

The aim is to choose a probability distribution P_θ over $\mathcal{G}$ such that conditions 2.2 and 2.3 are satisfied.

$$\sum_{G \in \mathcal{G}} P(G) = 1 \tag{2.2}$$

$$\langle x_i \rangle = \sum_{G \in \mathcal{G}} x_i(G) P(G) = x_i^* \tag{2.3}$$

where $\langle x_i \rangle$ is the expected values of the $i-$th graph metric over $G \in \mathcal{G}$ and $x_i|_{G=g} = x_i^*, \forall i$.

This problem can be translated into a maximization problem where the *best choice* of probability distribution P_θ is the one that maximizes the Shannon/Gibbs entropy (equation 2.4) subject to the constraints 2.2, 2.3, where the *best choice* refers to the one that makes the minimum assumptions about the distribution (Newman, 2010)

$$S = -\sum_{G\in\mathcal{G}} P(G) ln P(G) \tag{2.4}$$

Using the method of Lagrange multipliers, the maximization problem of equation 2.4 subject to the constraints 2.2 and 2.3 takes the form

$$\frac{\partial}{\partial P(G)}\left[S - \alpha\left(1 - \sum_{G\in\mathcal{G}} P(G)\right) - \sum_{i=1}^{r}\theta_i\left(x_i^* - \sum_{G\in\mathcal{G}} x_i(G)P(G)\right)\right] = 0$$

$$\Rightarrow -ln(P(G)) - 1 + \alpha + \sum_{i=1}^{r}\theta_i x_i(G) = 0$$

$$\Rightarrow P(G) = exp\left[\alpha - 1 + \sum_{i=1}^{r}\theta_i x_i(G)\right]$$

$$\Rightarrow P(G) = \frac{e^{H(G)}}{Z} \tag{2.5}$$

where α and $\{\theta_i\}$ are lagrange multipliers, $H(G) = \sum_{i=1}^{r}\theta_i x_i(G)$ is the graph Hamiltonian, θ_i is the ith model parameter to be estimated and $Z = \sum_{G\in\mathcal{G}} e^{H(G)}$ is the so called partition function.

The model parameters vector $\boldsymbol{\theta} = [\theta_1, \theta_2, ..., \theta_r]$ quantifies the relative significance of the network graph metrics to explain the topology of the network while taking into account the contribution of all the other graph metrics in the model. More specifically, the estimated value of a parameter θ_i indicates the change in the (log-odds) likelihood of an edge for a unit change in graph metric x_i. If the estimated value of θ_i is large and positive, the associated graph metric x_i plays an important role in explaining the topology of G more than would be expected by chance. Note that here chance corresponds to randomly choosing a network from the space $\mathcal{G}$. If instead the estimated value of θ_i is negative and large, then x_i still plays an important role in explaining the topology of G but it is less prevalent than expected by chance (Robins et al., 2007).

The constant Z ensures that the function P_θ is indeed a probability function, i.e. that condition 2.3 is satisfied. In general, the fact that the space $\mathcal{G}$ can be very large even for relatively small n, as well as the inclusion of graph metrics that are not simple linear combinations of G_{ij}, in practice make it impossible to derive analytically the model parameters vector $\boldsymbol{\theta}$ (Frank and Strauss, 1986; Hunter and Handcock, 2006). Numerical methods, such as Markov chain Monte Carlo (MCMC) approximations of the maximum-likelihood estimators (MLEs) of the model parameters vector $\boldsymbol{\theta}$, are typically adopted to circumvent this issue (Snijders TAB, 2006).

This model formulation is a very flexible one, allowing many kinds of graph metrics, which in turn induces different dependency assumptions. Graph statistics are in general functions of G, i.e. structural terms measuring from local to global properties, nevertheless it is also possible to incorporate covariates and node-level effects into the model. See Morris, Handcock, and Hunter, 2008 for a non-exhaustive list of possible terms that can be included in an ERGM.

The dependency assumptions among dyads will be given by the type of graph metrics included. It can be assumed that edges are independent, or that disjoint edges are independent conditional on the rest of the graph (Markovian dependence), or less restrictive assumptions proposed by Pattison and Robins, 2002 and that we discuss in section 3.1.

Alternative formulation

Alternatively, equation 2.1 can be formulated in terms of what has been called the *change statistic* by exploiting the dichotomous nature of the random variable G_{ij}.

We consider the conditional probability that a link between i and j is present condition on the complement G_{ij}^c of G_{ij}, that is the rest of the network G except G_{ij}.

First, note that

$$P_{\boldsymbol{\theta}}(G = g) = \frac{exp\{\boldsymbol{\theta}^{'}\boldsymbol{x}(g)\}}{Z} \iff P_{\boldsymbol{\theta}}(G = g) \propto exp\{\boldsymbol{\theta}^{'}\boldsymbol{x}(g)\} \tag{2.6}$$

then

$$Pr(G_{ij} = 1 \mid G_{ij}^c) = \frac{Pr(G = g_{ij}^+)}{Pr(G = g_{ij}^+) + Pr(G = g_{ij}^-)} = \frac{exp\{\boldsymbol{\theta}' \boldsymbol{x}(g_{ij}^+)\}}{exp\{\boldsymbol{\theta}' \boldsymbol{x}(g_{ij}^+)\} + exp\{\boldsymbol{\theta}' \boldsymbol{x}(g_{ij}^-)\}} \tag{2.7}$$

where the g_{ij}^+, g_{ij}^- are networks such that

$$g_{ij}^+ = \begin{cases} 1 & \text{for entry } (i,j)\ ; \\ G_{kl} & \text{for entries } (k,l) \neq (i,j) \end{cases} \qquad g_{ij}^- = \begin{cases} 0 & \text{for entry } (i,j)\ ; \\ G_{kl} & \text{for entries } (k,l) \neq (i,j) \end{cases}$$

Note that the expression does not depend on the normalization constant Z. By considering the odds ratio of the presence of a link between i and j in expression 2.7 we have

$$\frac{Pr(G_{ij} = 1 \mid G_{ij}^c)}{Pr(G_{ij} = 0 \mid G_{ij}^c)} = \frac{exp\{\boldsymbol{\theta}' \boldsymbol{x}(g_{ij}^+)\}}{exp\{\boldsymbol{\theta}' \boldsymbol{x}(g_{ij}^-)\}} = exp\{\boldsymbol{\theta}' \left[\boldsymbol{x}(g_{ij}^+) - \boldsymbol{x}(g_{ij}^-)\right]\} \tag{2.8}$$

Finally, the log odds ration takes the following form

$$log\left\{\frac{Pr(G_{ij} = 1 \mid G_{ij}^c)}{Pr(G_{ij} = 0 \mid G_{ij}^c)}\right\} = \boldsymbol{\theta}' \left[\boldsymbol{x}(g_{ij}^+) - \boldsymbol{x}(g_{ij}^-)\right] \tag{2.9}$$

The change statistic δ_x of graph metric $\boldsymbol{x}$ is define as $\delta_{\boldsymbol{x}}(G) = \boldsymbol{x}(g_{ij}^+) - \boldsymbol{x}(g_{ij}^-)$, i.e. the change in graph metric $\boldsymbol{x}$ when toggling dyad (i,j) from 0 to 1.

This formulation eased the computation implementation of estimation methods as is pointed out in section 2.1.3.

This formulation represents a great improvement in the speed of the computational implementation of estimation methods but it also shed light on some issues of degeneracy for certain classes of models. We will discuss this in more depth below but first, we give some example of classical ERGMs.

2.1.2 Classic examples

The exponential-family of random graphs generalizes well-known networks models, such as the Erdos-Renyi (Erd6s and Rényi, 1960). Below we present

other spacial cases of classical network models.

- Triad Model (Frank and Strauss, 1986)

$$H(G) = \theta_1 E(G) + \theta_2 V(G) + \theta_3 T(G)$$

Where E measures the number of edges, V the number of two stars and T the number of triangles. This model reduces to the Bernoulli if $\theta_2 = \theta_3 = 0$, to the two-stars model is $\theta_3 = 0$ and to the Strauss's Model if $\theta_2 = 0$.

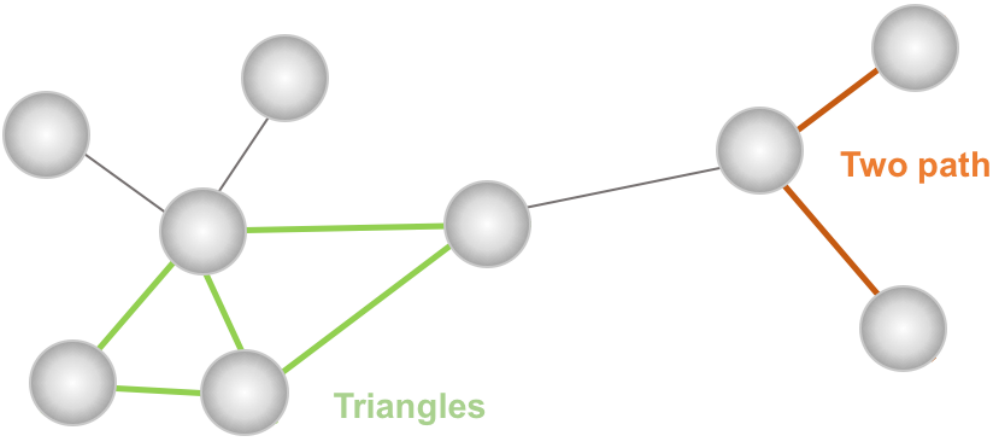

FIGURE 2.1: Sufficient statistic of the triad model: triangles and two paths

- Generalized Random Graphs (Newman, Strogatz, and Watts, 2001)

$$H(G) = \sum_{i=1}^{N} \theta_i k_i(G)$$

where $\{k_i\} = \{k_1, k_2, ..., k_N\}$ is the node degree sequence. Assuming a sparse network and using the handshaking lemma, the connection probability can be written as

$$p_{ij} \approx \frac{\langle k_i \rangle \langle k_j \rangle}{\langle k \rangle N}$$

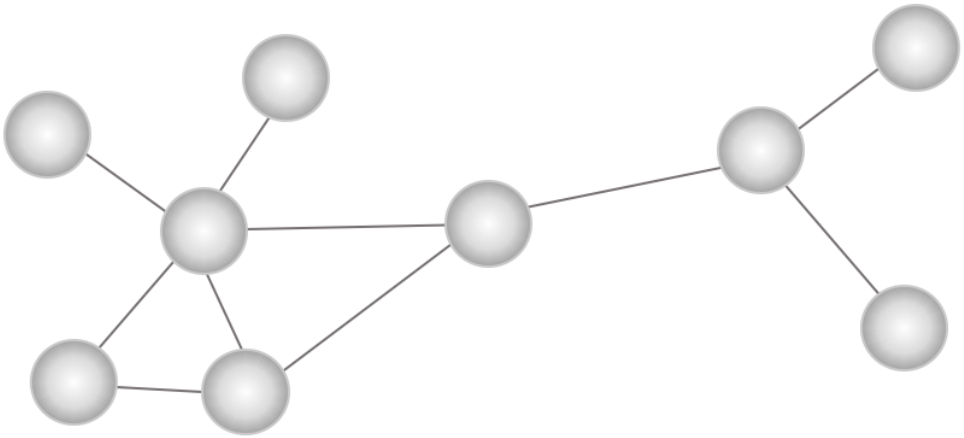

FIGURE 2.2: Sufficient statistic of the generalized random model: degree distribution

The latter example can be solved analytically. We refer to Fronczak, 2012 for the exact calculations. However, when other metrics that are not simple linear combinations of G_{ij} are included, such as triangles and two stars, the model has no closed form solution. This together with the fact that the space $\mathcal{G}$ can be very large even for relatively small n, in practice makes it impossible to derive analytically the model parameters vector $\boldsymbol{\theta} = [\theta_1, \theta_2, ..., \theta_r]$ (Frank and Strauss, 1986; Hunter and Handcock, 2006). Numerical methods, such as Markov chain Monte Carlo (MCMC) approximations of the maximum-likelihood estimators (MLEs) of the model parameters vector $\boldsymbol{\theta}$, are typically adopted to circumvent this issue (see Section 2.1.3).

Properties

The probability distribution $P(G)$ can be used to calculate estimates of other quantities of interest y over the space $\mathcal{G}$

$$\langle y \rangle = \sum_{G \in \mathcal{G}} y(G) P(G) = \frac{1}{Z} \sum_{G \in \mathcal{G}} y(G) e^{H(G)} \tag{2.10}$$

In particular

$$\begin{aligned}\langle x_j \rangle &= \frac{1}{Z} \sum_{G \in \mathcal{G}} x_j(G) e^{\sum_{i=1}^{r} \theta_i x_i(G)} = \frac{1}{Z} \frac{\partial}{\partial \theta_j} \sum_{G \in \mathcal{G}} e^{\sum_{i=1}^{r} \theta_i x_i(G)} \\ &= \frac{1}{Z} \frac{\partial Z}{\partial \theta_j} = \frac{\partial F}{\partial \theta_j} \end{aligned} \tag{2.11}$$

where $F = ln(Z)$ is called the free energy.
Similarly as in equation 2.11 one can show that the second derivative of the free energy with respect to θ_j gives the mean square fluctuation of x_j, known as the fluctuation-response relation (Fronczak, 2012)

$$\langle x_j^2 \rangle - \langle x_j \rangle^2 = \frac{\partial \langle x_j \rangle}{\partial \theta_j} = \frac{\partial^2 F}{\partial \theta_j^2} \tag{2.12}$$

2.1.3 Estimation techniques

Parameter estimation has been an active topic of research since the early proposals of simple ERGMs. As pointed out before, models become quickly too complicated to solve analytically. Techniques first started to exploit maximum likelihood maximization methods but later with new computational power, the preferred methods became computational driven. Below general review of the principal ideas of such methods, for interested readers we refer to Snijders, 2002 and Robins et al., 2003.

Pseudo-likelihood estimation

Is the first and most simplest method used to estimate the parameters in an ERGM (Strauss and Ikeda, 1990). It consists in approximating the likelihood by the so-called pseudolikelihood

$$l(\theta) := \sum_{ij} ln(P_\theta \left\{ G_{ij} = g_{ij} \mid G_{hk} = g_{hk} \quad \forall (h,k) \neq (i,j) \right\})$$

Then one can maximize the pseudolikelihood, using logistic regression methods, to obtain an estimator (MPLE). Despite the practicality of its implementation, the MPLE's statistical properties are not well understood for ERGMs, which has been reported extensively in the literature.

Markov chain Monte Carlo Maximum Likelihood Estimation (MCMC-MLE)

Driven by difficulty of evaluating Z, stochastic methods to approximate the maximum-likelihood where developed from the early nineties (Geyer and Thompson, 1992; Dahmstrum and Dahmstrum, 1993; Corander, Dahmström, and Dahmström, 1998).

The general idea of this method is to use Markov chain Monte Carlo algorithms, whose stationary distribution is given by equation 2.1 with a particular parameter value, to draw a sample of graphs which are in turn used to update the value of parameters. Hence, there are two recursive steps, the simulation, and the estimation algorithms, that iterates in a loop until the parameter value satisfies some criteria of convergence.

For a fixed value of parameters, simulation algorithms such as Gibbs sampler and Metropolis-Hasting algorithm are used to simulate random draws of the stationary distribution P_θ. Loosely, it consists on visiting each dyad (i, j) and setting the value of $G_{i,j}$ to one or zero with some probability π that will in general depend on the change statistic (see section 2.1.1). For example, the Gibbs Sampler method samples the value of G_{ij} from the following conditional probability.

$$\frac{P(G_{ij} = 1 \mid G_{ij}^c = g_{ij}^c)}{P(G_{ij} = 0 \mid G_{ij}^c = g_{ij}^c)} = exp\{\boldsymbol{\theta}\delta_{\boldsymbol{x}}(G)\}$$

These algorithms produce a Markov chain whose distribution is ensured to converge to the exponential random graph distribution by detailed balance. There are many mixing techniques, for instance, dyad can be visit sequentially or at random, or by more sophisticated schemes that have been proposed, see some examples in Snijders, 2002.

Now, to estimate the parameters, repeatedly MCMC simulations are used to update its value. Again, many different methods have been proposed over the years mostly driven by the type of ERGM parameterization. In general, such algorithms set the initial values of the model parameters $\theta_{(0)}$ by means of a maximum pseudo-likelihood estimation (MPLE) and update $\theta_{(t)}$ to $\theta_{(t+1)}$ by using approximations of moments of the distribution computed from the MCMC simulations. Examples of such algorithms adaptations are Robbins-Monro or Newton-Raphson or Geyer-Thompson. This process is repeated iterative until the parameter values stabilizes or condition 2.3 is satisfied.

Here we outline a pseudocode for this methodology in general.

let m be MCMC sample size
initialize $\boldsymbol{\theta}^{[0]}$
for $i = 1$ up until convergence **do**
  sample $\hat{G_1}, \hat{G_2}, ..., \hat{G_m} \sim P(G, \boldsymbol{\theta}^{[i-1]})$
  $C(\hat{\theta}) = ln\left(\sum_{j=1}^{m} exp\left[(\boldsymbol{\theta} - \boldsymbol{\theta}^{[i-1]})\boldsymbol{x}(\hat{G_j})\right]\right)$
  $\boldsymbol{\theta}^{[i]} = argmax_\theta\left[\sum_{t=1}^{n} \boldsymbol{\theta} x(G^t) - C(\hat{\theta})\right]$
end for

2.1.4 Model construction and considerations

Here we summarize the general framework of model formulation and estimation when applying it to real data, as in the case of brain networks.

For a particular complex network G, each network link is regarded as a random variable and the aim is to define a probability distribution P on the edge existence. An ERGM assumes that P is completely determined by a set of sufficient statistics which in turn impose a specific dependency assumption on the links of G.

Such metrics have to be chosen by the researcher based on priors that motivate scientific hypothesis on the network edge formation process and that can be tested in an ERGM. The model can be further specified by imposing parameters homogeneity or other constraints, for example fixing the density of the network.

The model is then estimated with MCMC computational methods. After checking for possible degeneracy issues and refining the model formulation to one with good convergence properties, one can asses the goodness of fit of the model by comparing topological properties of synthetic networks simulated from the model to the observed network.

Finally, parameter interpretation can give insight in the direction and magnitude of different network metrics affecting edge formation for a particular system. Parameters can also be used to discriminate different networks populations.

Degeneracy

The use of stochastic simulations to estimate the parameters revealed that for certain specifications the models displayed ill distributions in the sense that they sample graphs that were topological far from real observed networks.

For instance, the model including two stars and triangles would sample either empty or full graphs, which are both very unlike to observe in nature or man-made systems.

This triggered research on the properties of parameter spaces of ERGMs finding that, depending on the form of the model and algorithm used, MCMC for the probability distribution P_θ converges to degenerate graphs (Robins et al., 2003). There is two main type of degeneracy: near degeneracy property and bimodal. The former refers to models formulation that implies that only a few simulated graphs had other than very low probability, and the latter refers to models that have a probability distribution with a binomial shape.

Degeneracy has been consistently reported when triangles and two paths are included as sufficient statistics in an ERGM, nevertheless, these two metrics are intuitively important building blocks of many real complex networks. In particular, in the field of social networks, that has driven many of the recent ERGMs developments, these metrics are regarded as omnipresent. To overcome degeneracy issue new specifications of triangles and two paths have been defined. See section 3.1 and Hunter, 2007 for more details.

2.2 Temporal extension TERGM

To go beyond modeling one instance of a dynamic complex system we want to develop a coherent framework to properly characterize dynamic brain networks. We use Temporal exponential random graph models (TERGM) which is a natural extension of ERGM to model time-varying networks first proposed by Hanneke, Fu, and Xing, 2010 following ideas in Robins and Pattison, 2001. A TERGM defines the probability of a network at time step t as a function of graph metrics and the observed graph up to time step $t-K$ and which has an ERGM form

2.2.1 Mathematical formulation

Let $G^t = \{G^1, ..., G^T\}$ be a time-varying network where each graph G^t lays in a set $\mathcal{G}$ of possible network realizations with a fix number of nodes N and edges might change from one time point to another representing the evolution of some underlying process. Then the conditional probability of observing the time series of networks is given by

$$P(G^t|G^{t-K}, ..., G^{t-1}, \boldsymbol{\theta}) = \frac{exp(\boldsymbol{\theta}'\boldsymbol{x}(G^t, G^{t-1}, ..., G^{t-K}))}{Z(\boldsymbol{\theta}, G^{t-K}, ..., G^{t-1})} \tag{2.13}$$

In a second step, one computes the product over all time periods in order to determine the probability of the time series of networks.

$$P(G^{K+1}, ..., G^T|G^1, ..., G^K, \boldsymbol{\theta}) = \prod_{t=K+1}^{T} P(G^t|G^{t-K}, ..., G^{t-1}, \boldsymbol{\theta}) \tag{2.14}$$

In other words, the probability of observing a graph G^t given the previous times $t-1, t-2, ...t-K$ is model by an ERGM which allows statistics that depend both in time t and in the past.

2.2.2 Temporal dependencies

This model allows two levels of temporal dependencies: one is given by the joint probability distribution which gives us a set of parameters for a time-order graph sequence, and the other is given by the metrics $\boldsymbol{x}$ that can be on their own temporal.

The time lag K is the interval of dependency between graphs in the time-varying network, i.e. network G^l for $l < t - K$ are independent of G^t. It is important to define it accordingly to the time dependencies of the underlying time evolving process. This process is governed by one single vector parameter $\boldsymbol{\theta}$ that weight the relative importance of each graph metric x_i in explaining the observed topology and its evolution over time.

In a TERGM the sufficient statistics $\boldsymbol{x}$ can be temporal, in the sense that are graph metrics that depend both in time t and in the past $t - K$ steps. This is an important future as it allows to study temporal or dynamic connectivity mechanisms and goes beyond looking at the evolution of graph metrics applied time-wise.

Below we list some example of possible networks that can be considered as sufficient statistics, both static and temporal:

Exogenous covariates

- With no temporal dependencies: $h_X(G^t, X^t) = \sum_{i \neq j} G^t_{ij} X^t_{ij}$

Endogenous dependencies:
With no temporal dependencies the metrics take the form as in an ERGM.
With temporal dependencies the general form is $h(G^t, G^{t-1}, ..., G^{t-K}) = \sum_{ij} h_{ij}(G^t, G^{t-1}, ..., G^{t-K})$

- Stability:

$$h_S(G^t_{ij}, G^{t-1}_{ij}) = \sum_{ij} G^t_{ij} G^{t-1}_{ij} + (1 - G^t_{ij})(1 - G^{t-1}_{ij})$$

- Auto-regression:

$$h_A(G^t_{ij}, G^{t-1}_{ij}) = \sum_{ij} G^t_{ij} G^{t-1}_{ij}$$

- Loss:

$$h_L(G^t_{ij}, G^{t-1}_{ij}) = \sum_{ij} (1 - G^t_{ij}) G^{t-1}_{ij}$$

- Innovation:

$$h_I(G^t_{ij}, G^{t-1}_{ij}) \sum_{ij} G^t_{ij} G^{t-1}_{ij}$$

2.2.3 Computational implementation

As the core of a TERGM is still an ERGM many of the challenges prevail. Notably, the fact that it is not possible to derive analytically the model's parameters vector except for very small networks or simple graph metrics $\boldsymbol{x}$.

Therefore computational methods are used to estimate the model parameter vector $\boldsymbol{\theta}$

However, in terms of computational methods, some advantages have been exploited by the fact of having more networks as input. In an ERGM the input network is regarded as a single multivariate observation, in a TERGM the input network is a time-varying network, essentially a time-order sequence of networks.

Here we consider two existing computational methods: MCMCM-MLE (see 2.1.3 and bootstrap methods with estimation via maximum pseudolikelihood (BMPLE). The BMPLE takes advantage of the practical MPLE implementation and it ensures a consistent estimator $\hat{\boldsymbol{\theta}}$ (Leifeld, Cranmer, and Desmarais, 2015). It also decreases the occurrence of degeneracy in the models.

The choice between one method or another will depend in general on the number of time points and size of the time-varying network. Bootstrap MPLE does not require simulation which represents a substantial advantage over MCMC-MLE that is more computationally demanding but can be more robust when few time points are provided.

Chapter 3

A statistical model for brain networks inferred from large-scale electrophysiological signals

As presented in chapter 1 the study of the brain as a static network provides an insightful characterization of brain connectivity patterns. By using graph theory tools we can measure different topological signatures which encodes biological principles. To disentangle those principles we propose to use a graph model to test which of topological signatures are essential in the underlying network formation process.

First, we will identify candidates of topological signatures by looking at the existent literature of brain networks and more in general complex networks. Then, we use ERG models to test which of those signatures are statistically sufficient to generate observed network topologies. We consider synthetic generated networks to study the capabilities and behavior of the model under known network generation processes and then we apply such model to brain networks of normal subjects in resting-state.

Resting-state provides a setting to study the spontaneous activity of the brain. Even though there is evidence that suggests that those signals exhibit fluctuations and nonstationary (Betzel et al., 2012), collapsing the time recordings to an average network is reasonable when one wants to study prevailing topological properties.

3.1 Synthetic networks

Consider a space of topology network types bounded by three different types: lattice, random and scale-free. In one extreme of this triangle lays a lattice which exhibits high clustering and local rewiring cost, in the other, random

topologies are characterized by high global integration and scale-free networks are distinguished by power-law degree distributions. Normal brain network's topology share combine attributes in the space formed by these extremes (Bullmore and Sporns, 2012; Stam, 2014). Some of the more interesting and consistently reported are related to lattice and random, i.e. the trad-off between segregation and integration balance and low wiring cost (see section 1.2.3).

The Watts-Strogatz model provides a process to generate networks with changing topology from regular to random. This simple yet powerful model was first presented in the seminal paper Watts and Strogatz, 1998, and to a large extent gave rise to modern network science. The paper sought to explain how synchronization was accomplished among cricket chirps. The model and its applications put in evidence the importance of the small-world property. It not only explained how information can be efficiently transmitted both locally and globally but it is one that is found in real complex networks across all sort of disciplines from ecology, epidemiology to transportation or social science.

Here, we use this model to generate synthetic network data. We start with N nodes each connected to its k neighbors and let p be the probability of rewiring a randomly chosen link with initial value $p = 0$. The network generative process consists in taking each time a lattice and rewire its links with probability p. When $p = 1$ the resulting network is random.

This network topology transition is characterized by local E_l and global E_g efficiency. Lattice networks have a high local efficiency and low global efficiency. Information traveling between two nodes that are physically far away must travel an average of $\frac{1}{2}\left(\frac{n}{2}+1\right)$ steps, however, locally all neighbors are connected. Random networks, on the other hand, have low local efficiency but high global efficiency. As links are rewired, they serve to bridge non-neighboring nodes.

These two apparently opposed properties are supported by triangles and the tendency of short paths and are balanced for small probabilities $p > 0$. Accordingly, we use these two metrics to model the networks in an ERGM. As shown in section 2.1.2, the Erdos Renyi is a special case of an ERGM where the Hamiltonian is given by $H(G) = \theta_1 E(G)$ where E is the number of edges in the network and therefore such model will generate networks as the ones obtained by rewiring links with $p = 1$. If we then take the model defined by the Hamiltonian $H(G) = \theta_1 D(G)$, where $D(G) = G_1, G_2, ...$ is the degree distribution of a network–D_k is equal to the number of nodes with degree

k–we can simulate lattice-like networks.

Figure 3.1 shows the goodness of fit of such models fitted over a random and a lattice network respectively. The goodness of fit measures how well the model can reproduce networks with similar topological properties to the observed ones. We see that the degree, edge-wise shared pattern and geodesic distance for each model (box-plots) fit very well the observed distributions (solid line).

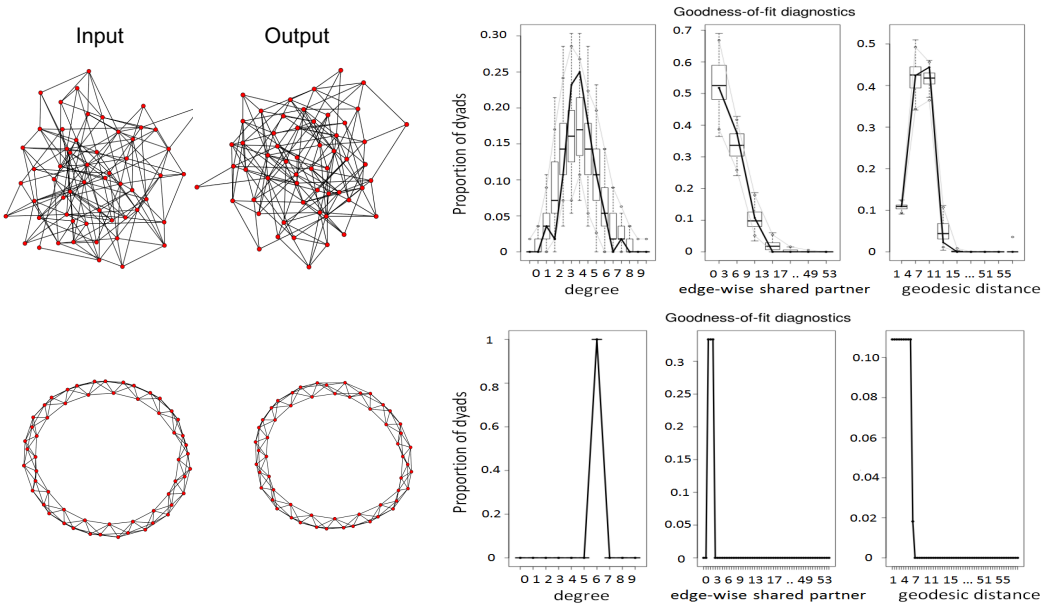

FIGURE 3.1: a) Two input network with random and lattice topology, b) Two simulated networks from ERGMs with hamiltonians $H(G) = \theta_1 E(G)$ (top) and $H(G) = \theta_1 D(G)$ (bottom), c) goodness of fit in terms of models over 100 simulated networks.

Real life complex networks are rarely, if not never, regular or random. Therefore we would like to define one single simple model that can at the same time model lattice and random topologies and in between small-world topologies. A flexible model that can capture different topologies in this space.

We notice that triangles and two paths are two metrics that are signatures of such topology changes. However, it has been shown extensively, especially in computational social science, that those metrics incur in serious degeneracy issues (see section 2.1.4). The triangles metrics is especially problematic as it leads to degenerate mass probability functions which generates either complete or empty networks. To overcome this issues curved exponential family models are somewhat preferred, these are model that include

parameterized graph metrics and that mitigates degeneracy by giving less weight to high order structures.

Therefore we consider the ERGM with Hamiltonian

$$H(G) = \theta_1 GW_K(G) + \theta_2 GW_E(G) \tag{3.1}$$

where GW_K is the geometrically weighted degree distribution and GW_E is the geometrically weighted edgewise shared partner distribution, both curved metrics first proposed by Hunter, 2007. The metrics sought to capture clustering effect, such as triangles, and integration, such a tendency to form two paths without suffering from degeneracy issues. By weighting high order structures with decaying parameter τ the two extreme states of complete and empty graphs are avoided with a high probability, and the resulted fitted ERGMs can model non-trivial network topologies.

Sensitive analysis of metrics GW_K, GW_E and its associated decay parameters τ on the values of global and local efficiency reveals that high values of global and local efficiency can be achieved for a large part of the parameter space (Fig3.2). Curved metrics GW_K, GW_E are not exactly measuring local or global efficiency yet promote small-world topology, this supports the idea that efficiency in a network is not necessarily a result of high local and global efficiency but there might be other mechanisms such as hubs and communities which promotes the balance of integration and segregation of information.

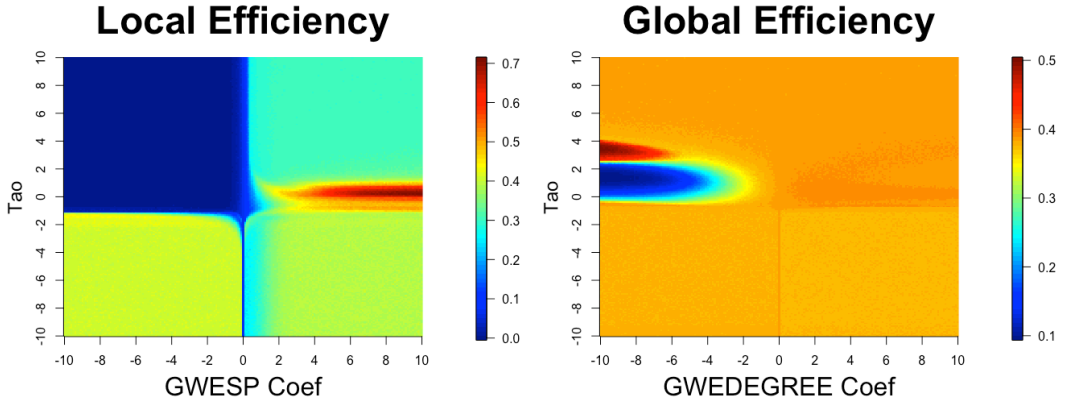

FIGURE 3.2: Sensitivity analysis of GW_K and GW_E and decay parameters τ in global and local efficiency values

3.1.1 Validation

Consider three networks from the Watts-Strogatz model: lattice ($p = 0$), small-world ($p = 0.1$) and random ($p = 1$) and fit ERGM 3.1.

One of the first things to check is if condition 2.3 is satisfied by network simulated form the model. Failing to do so would indicate either that the model is not well defined, i.e. the graph metrics specifying the model are not sufficient statistics for the probability distribution, or the model exhibits degeneracy. In either case, no relevant conclusions could be drawn from such a model as the assumptions are not satisfied.

Then one can cross-validate the fit, this is to check if simulated networks from the model have the same topology as the observed one. There is not an unequivocal way of doing this, as there is no one single metric that can define the entire topology of a network. One could look at, among others, the distance of simulated to the graph or a profile of different metrics. Thus this rest at the discretion of the researcher and is strongly dependent on the type of system under study.

Here we decide to look at E_g, E_l as these are truly characteristic of the Watts-Strogatz model. We compare the value of local and global efficiency of network generated by the Watts-Strogatz model to networks simulated by model 3.1.

Figure 3.3 shows both the values of sufficient statistics GW_K, GW_E and graph metrics E_l, E_g. One can see that the model recovers strikingly well those graph metrics, suggesting good convergence properties and no-degeneration. It shows as well that we can recover network with varying topologies ranging from lattice to random.

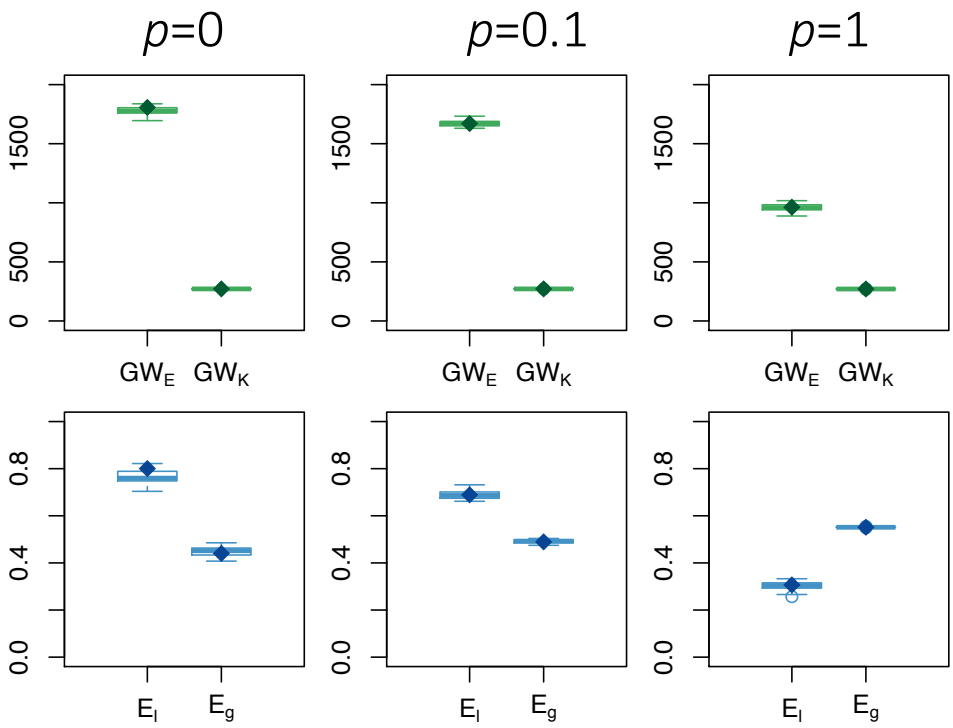

FIGURE 3.3: The observed values of each input Watts-Strogatz network is shown in a solid point, and the boxplot shows the distribution of metrics GW_K, GW_E ,E_l, E_g over simulated networks from model 3.1

We can also look at link prediction capacity by computing the receiver operating characteristic (ROC) and the precision-recall (PR) curves of the out-of-sample prediction of network links. The area under the curves quantifies the how well edges are predicted with respect to input networks.

Notably, if we were to try to fit a model, call it TP, with triangles and two paths as metrics, the convergence of the model would be hindered by the input network. Consider a longer sequence from Watts-Strogatz model, i.e take a longer probability vector p. If we look at the area under the ROC and PR curves of model 3.1 we see that the values start high (> 0.8) and then stabilize around 0.5 3.4.

On the other hand, model TP almost never converges for low probabilities p (evidenced by the lack of triangles in Figure 3.1). For higher probabilities, the two models behave similar, as expected.

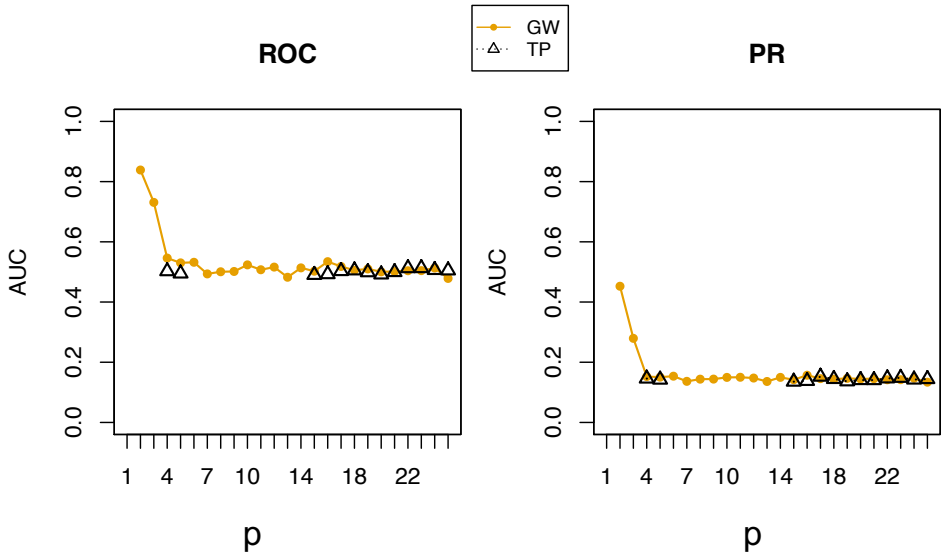

FIGURE 3.4: Area under the curves ROC and PR-C of models 3.1 (GW-solid yellow line) and TP (PERGM with triangles and two paths as metrics-blakc triangles). This plot has linear increment, to get more small-world and hopefully more smooth reduction.

3.2 Resting state conditions

To study functional brain connectivity networks we propose to implement ERGMs that allow us to statistically test which connectivity mechanisms support the emergence of such synchronization patterns. We use EEG resting state data because it provides a non-invasive setting to study spontaneous brain activity at rest.

With these models, we expect to be able to simulate networks that are topologically very close to observed brain networks and retrieve key discriminating principles. For example, we know that in resting state EEG signals the α frequency band is discriminant of eyes open and eyes closed resting state conditions.

Model implementation

We take model 3.1 as a reference one, hypothesizing that the curved metrics will promote balance in integration and segregation, however since the intrinsic connectivity mechanisms are unknown we fit the data to other models, using also curved terms metrics that have been successfully used in the social science community.

Validation

We found that indeed ERGM 3.1 ranks very well across different measures. We proceed to further validate the model by looking at its goodness of fit and to cross-validate with other graph metrics that were not included either in the model nor in the ranking score.

We conclude that the model reproduces the most important topological properties of observed resting state brain networks. Furthermore, it captures important group differences that have been reported in the literature. Taken together, these findings support the current view of the functional segregation and integration of the brain in terms of modules and hubs and provide a statistical approach to extract new information on the (re)organizational mechanisms in healthy and diseased brains.

Below we present the complete version of the published article that presents our findings Obando and De Vico Fallani, 2017.

INTERFACE

rsif.royalsocietypublishing.org

Research

Cite this article: Obando C, De Vico Fallani F. 2017 A statistical model for brain networks inferred from large-scale electrophysiological signals. *J. R. Soc. Interface* **14**: 20160940. http://dx.doi.org/10.1098/rsif.2016.0940

Received: 23 November 2016
Accepted: 10 February 2017

Subject Category:
Life Sciences–Physics interface

Subject Areas:
computational biology, biomedical engineering

Keywords:
exponential random graph models, brain connectivity, graph theory, electroencephalography, resting states

Author for correspondence:
Fabrizio De Vico Fallani
e-mail: fabrizio.devicofallani@gmail.com

Electronic supplementary material is available online at https://dx.doi.org/10.6084/m9.figshare.c.3695518.

THE ROYAL SOCIETY PUBLISHING

A statistical model for brain networks inferred from large-scale electrophysiological signals

Catalina Obando[1,2] and Fabrizio De Vico Fallani[1,2]

[1]Inria Paris, Aramis Project Team, 75013 Paris, France
[2]Sorbonne Universites, UPMC Univ. Paris 06, Inserm, CNRS, Institut du Cerveau et la Moelle (ICM), Hôpital Pitié-Salpêtrière, 75013 Paris, France

FDVF, 0000-0001-8035-7883

Network science has been extensively developed to characterize the structural properties of complex systems, including brain networks inferred from neuroimaging data. As a result of the inference process, networks estimated from experimentally obtained biological data represent one instance of a larger number of realizations with similar intrinsic topology. A modelling approach is therefore needed to support statistical inference on the bottom-up local connectivity mechanisms influencing the formation of the estimated brain networks. Here, we adopted a statistical model based on exponential random graph models (ERGMs) to reproduce brain networks, or connectomes, estimated by spectral coherence between high-density electroencephalographic (EEG) signals. ERGMs are made up by different local graph metrics, whereas the parameters weight the respective contribution in explaining the observed network. We validated this approach in a dataset of $N = 108$ healthy subjects during eyes-open (EO) and eyes-closed (EC) resting-state conditions. Results showed that the tendency to form triangles and stars, reflecting clustering and node centrality, better explained the global properties of the EEG connectomes than other combinations of graph metrics. In particular, the synthetic networks generated by this model configuration replicated the characteristic differences found in real brain networks, with EO eliciting significantly higher segregation in the *alpha* frequency band (8–13 Hz) than EC. Furthermore, the fitted ERGM parameter values provided complementary information showing that clustering connections are significantly more represented from EC to EO in the *alpha* range, but also in the *beta* band (14–29 Hz), which is known to play a crucial role in cortical processing of visual input and externally oriented attention. Taken together, these findings support the current view of the functional segregation and integration of the brain in terms of modules and hubs, and provide a statistical approach to extract new information on the (re)organizational mechanisms in healthy and diseased brains.

1. Introduction

The study of the human brain at rest provides precious information that is predictive of intrinsic functioning, cognition, as well as pathology [1]. In the last decade, graph theoretic approaches have described the topological structure of resting-state connectomes derived from different neuroimaging techniques, such as functional magnetic resonance imaging (fMRI) or magneto- (MEG) and electroencephalography (EEG).

These estimated connectomes, or brain networks, tend to exhibit similar organizational properties, including small-worldness, cost-efficiency, modularity and node centrality [2], as well as characteristic dependence from the anatomical backbone connectivity [3–5] and genetic factors [6]. Furthermore, they potentially show clinical relevance, as demonstrated by the recent

development of network-based diagnostics of consciousness [7,8], Alzheimer's disease [9], stroke recovery [10] and schizophrenia [11]. In this sense, quantifying the topological properties of intrinsic functional connectomes by means of graph theory has enriched our understanding of the structure of functional brain connectivity maps [2,12–14]. Nevertheless, these results refer to a descriptive analysis of the observed brain network, which is only one instance of several alternatives with similar structural features. This is especially true for functional networks inferred from empirically obtained data, where the edges (or links) are noisy estimates of the true connectivity and thresholding is often adopted to filter the relevant interactions between the system units [15–17].

Statistical models are, therefore, needed to reflect the uncertainty associated with a given observation, to permit inference about the relative occurrence of specific local structures and to relate local-level processes to global-level properties [18]. A first approach consists in generating synthetic random networks that preserve some observed properties, such as the degree distribution or the random walk distribution, and then contrasting the values of the graph indices obtained in these synthetic networks with those extracted from the estimated connectomes [13]. While these methods often provide appropriate null models, and can improve the identification of relevant network properties [19–21], they do not inform on the organizational mechanisms modelling the whole network formation [22,23]. Alternative approaches consider probabilistic growth models such as those based on spatial distances between nodes [24]. Interesting results have been achieved in identifying some basic connectivity rules reproducing both structural and functional brain networks [25,26]. However, these methods suffer from the rough approximation (e.g. Euclidean) of the actual spatial distance between nodes, and, moreover, they do not indicate whether the identified local mechanisms are either necessary or sufficient as descriptors of the global network structure.

To support inference on the processes influencing the formation of network structure, statistical models have been conceived to consider the set of all possible alternative networks weighted on their similarity to the observed one [18]. Among others, exponential random graph models (ERGMs) represent a flexible category that allows the simultaneous assessment of the role of specific graph features in the formation of the entire network. These models were first proposed as an extension of the triad model defined in [27] to characterize Markov graphs [28,29] and have been widely developed to understand how simple interaction rules, such as transitivity, could give rise to the complex network of social contacts [30–38].

Recently, the use of ERGMs has been proved to successfully model imaging connectomes derived respectively from spontaneous fMRI activity [39] and diffusion tensor imaging (DTI) [40]. Despite its potential, the use of ERGMs in network neuroscience is still in its infancy and more evidence is needed to better elucidate its applicability to connectomes inferred from other types of neuroimaging data and across different experimental conditions. In addition, many methodological issues remain unanswered, such as the relationships between the graph metrics included in the ERGM and the graph indices used to describe the topology of the observed connectomes.

To address the above issues, we proposed and evaluated several ERGM configurations based on the combination of different local connectivity structures (i.e. graph metrics). Specifically, we modelled brain networks estimated from high-density EEG signals in a group of healthy individuals during eyes-open (EO) and eyes-closed (EC) resting states. Our goal was to identify the best ERGM configuration reproducing EEG-derived connectomes in terms of functional integration and segregation, and to evaluate the ability of the estimated ERGM parameters in providing new information discriminating between EO and EC conditions.

2. Material and methods

2.1. Electroencephalographic data and brain network construction

We used high-density EEG signals freely available from the online PhysioNet BCI database [41,42]. EEG data consisted of 1 min resting state with EO and 1 min resting state with EC recorded from 56 electrodes in 108 healthy subjects. EEG signals were recorded with an original sampling rate of 160 Hz. All the EEG signals were referenced to the mean signal gathered from electrodes on the ear lobes. We subsequently downsampled the EEG signals to 100 Hz after applying a proper anti-aliasing low-pass filter. The electrode positions on the scalp followed the standard 10–10 montage.

We used the spectral coherence [43] to measure functional connectivity (FC) between EEG signals of sensors i and j at a specific frequency band f as follows:

$$w_{ij}(f) = \frac{|S_{ij}(f)|^2}{S_{ii}(f)S_{jj}(f)}, \tag{2.1}$$

where S_{ij} is the cross-spectrum between i and j, and S_{ii} and S_{jj} are the autospectra of i and j, respectively. Specifically, we computed cross- and auto-spectra by means of Welch's averaged modified periodogram with a sliding Hanning window of 1 s and 0.5 s of overlap. The number of fast Fourier transform points was set to 100 for a frequency resolution of 1 Hz. As a result, we obtained for each subject a connectivity matrix $W(f)$ of size 56×56 where the entry $w_{ij}(f)$ contains the value of the spectral coherence between the EEG signals of sensors i and j at the frequency f.

We then averaged the connectivity matrices within the characteristic frequency bands *theta* (4–7 Hz), *alpha* (8–13 Hz), *beta* (14–29 Hz) and *gamma* (30–40 Hz). These matrices constituted our raw brain networks whose nodes corresponded to the EEG sensors ($n = 56$) and links corresponded to the w_{ij} values. Finally, we thresholded the values in the connectivity matrices to retain the strongest links in each brain network. Specifically, we adopted an objective criterion, i.e. the efficiency cost optimization (ECO), to filter and binarize a number of links such that the final average node degree $k = 3$ [44]. We also considered $k = 1$, 2, 4, 5 to evaluate the main brain network properties around the representative threshold $k = 3$. The resulting sparse brain networks, or graphs, were represented by adjacency matrices A, where each entry indicates the presence $a_{ij} = 1$ or the absence $a_{ij} = 0$ of a link between nodes i and j.

2.2. Graph indices

We evaluated the global structure of brain networks by measuring graph indices at large-scale topological scales. We focused on well-known properties of brain networks such as optimal balance between integration and segregation of information [2,45,46]. Integration is the tendency of the network to favour distributed connectivity among remote brain areas; conversely,

segregation is the tendency of the network to maintain connectivity within specialized groups of brain areas [47].

In graph theory, integration has been typically quantified by the global-efficiency E_g and by the characteristic path length L,

$$\left.\begin{aligned} E_g &= \frac{1}{n(n-1)} \sum_{i,\, j=1,\, i\neq j}^{n} \frac{1}{d_{ij}} \\ \text{and} \qquad L &= \frac{1}{n(n-1)} \sum_{i,\, j=1,\, i\neq j}^{n} d_{ij}, \end{aligned}\right\} \tag{2.2}$$

where d_{ij} is the distance, or the length of the shortest path, between nodes i and j [48,49].

Segregation is typically measured by means of the local-efficiency E_l and by the clustering coefficient C:

$$\left.\begin{aligned} E_l &= \frac{1}{n} \sum_{i=1}^{n} E_g(G_i) \\ \text{and} \qquad C &= \frac{1}{n} \sum_{i=1}^{n} \frac{2t_i}{k_i(k_i-1)}, \end{aligned}\right\} \tag{2.3}$$

where G_i is the subgraph formed by the nodes connected to i; t_i is the number of triangles around node i; and k_i is the degree of node i [48,49].

In addition, we evaluated the strength of division of a network into modules by measuring the modularity Q:

$$Q = \frac{1}{l} \sum_{i,\, j=1}^{n} \left(A_{ij} - \frac{k_i k_j}{l} \right) \delta_{m_i, m_j}, \tag{2.4}$$

where $l = \sum_{i,j=1}^{n} A_{ij}$ is the number of edges, m_i is the module containing node i and $\delta_{m_i, m_j} = 1$ if $m_i = m_j$ and 0 otherwise. We used the Walktrap algorithm to generate a sequence of community partitions [50] and we selected the one that maximized Q according to the standard algorithm proposed in [51]. Modularity can be seen as a compact measure of the integration and segregation of a network, as it measures the propensity to form dense connections between nodes within modules (i.e. segregation) but sparse connections between nodes in different modules (i.e. inverse of integration).

2.3. Exponential random graph model

Let G be a graph in a set $\mathcal{G}$ of possible network realizations, $g = [g_1, g_2, \ldots, g_r]$ be a vector of graph statistics, or metrics, and $g^* = [g_1^*, g_2^*, \ldots, g_r^*]$ be the values of these metrics measured over G. Then, we can statistically model G by defining a probability distribution $P(G)$ over $\mathcal{G}$ such that the following conditions are satisfied:

$$\sum_{G \in \mathcal{G}} P(G) = 1 \tag{2.5}$$

and

$$\langle g_i \rangle = \sum_{G \in \mathcal{G}} g_i(G) P(G) = g_i^*, \quad i = \{1, 2, \ldots, r\}, \tag{2.6}$$

where $\langle g_i \rangle$ is the expected value of the ith graph metric over $\mathcal{G}$.

By maximizing the Gibbs entropy of $P(G)$ constrained to the above conditions, the probability distribution reads as:

$$P(G) = \frac{e^{H(G)}}{Z}, \tag{2.7}$$

where $H(G) = \sum_{i=1}^{r} \theta_i g_i(G)$ is the graph Hamiltonian, θ_i is the ith model parameter to be estimated and $Z = \sum_{G \in \mathcal{G}} e^{H(G)}$ is the so-called partition function [52]. The estimated value of a parameter θ_i indicates the change in the (log-odds) likelihood of an edge for a unit change in graph metric g_i. If the estimated value of θ_i is large and positive, the associated graph metric g_i plays an important role in explaining the topology of G more than would be expected by chance. Note that here chance corresponds to randomly choosing a network from the space $\mathcal{G}$. If instead the estimated value of θ_i is negative and large, then g_i still plays an important role in explaining the topology of G but it is less prevalent than expected by chance [53].

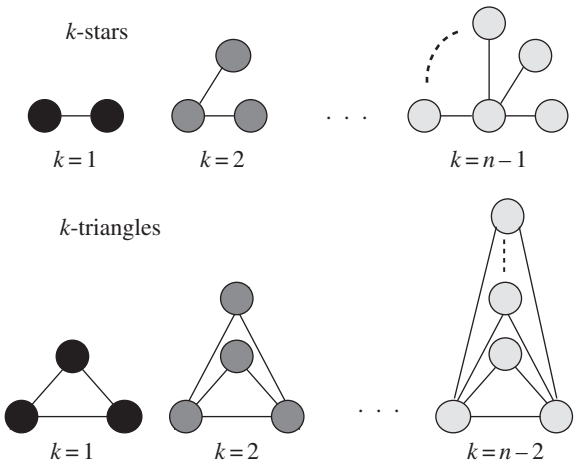

Figure 1. Graphical representation of k-stars and k-triangles.

In general, the fact that the space $\mathcal{G}$ can be very large even for relatively small n, as well as the inclusion of graph metrics that are not simple linear combinations of G_{ij}, in practice make it impossible to derive analytically the model parameters vector $\boldsymbol{\theta} = [\theta_1, \theta_2, \ldots, \theta_r]$ [27,31].

Numerical methods, such as Markov chain Monte Carlo (MCMC) approximations of the maximum-likelihood estimators (MLEs) of the model parameters vector $\boldsymbol{\theta}$, are typically adopted to circumvent this issue [54].

2.3.1. Model construction and implementation

We considered graph metrics reflecting the basic properties of complex systems such as hub propensity and transitivity in the network [46,55,56]. Specifically, we focused on k-stars to model highly connected nodes (hubs) and k-triangles to model transitivity, where k refers to the order of the structures as illustrated in figure 1.

In general, this leads to a large number of model parameters to be estimated, i.e. $n - 1$ for k-stars and $n - 2$ for k-triangles. To avoid consequent degeneracy issues in the ERGM estimation, we adopted a compact specification for these metrics that combines them in an alternating geometric sequence [31,57].

Because k-stars are related to the node degree distribution D [33], we used the *geometrically weighted degree distribution* $\mathrm{GW_K}$ as a graph metric to characterize hub propensity:

$$\mathrm{GW_K} = e^{2\tau} \sum_{i=1}^{n-1} \left((1 - e^{-\tau})^i - 1 + i e^{-\tau} \right) D_i, \tag{2.8}$$

where $\tau > 0$ is a *ratio parameter* to penalize nodes with extremely high node degrees.

Similarly, because k-triangles are related to the *shared pattern distribution* S, we used the *geometrically weighted edgewise shared partner distribution* to characterize transitivity:

$$\mathrm{GW_E} = e^{\tau} \sum_{i=1}^{n-2} \left(1 - (1 - e^{-\tau})^i \right) S_i, \tag{2.9}$$

where the element S_i is the number of dyads that are directly connected and that have exactly i neighbours in common.

In addition, complementary metrics have been defined based on the *shared partner distribution*:

$\mathrm{GW_N}$: *geometrically weighted non-edgewise shared partner distribution* given by equation (2.9), with S_i considering exclusively dyads that are not connected.

$\mathrm{GW_D}$: *geometrically weighted dyadwise shared partner distribution* given by equation (2.9), with S_i considering any dyad, connected or not.

Table 1. Set of model configurations. Models M_1-M_{10} include at most two of the four considered graph metrics, i.e. GW_K, GW_E, GW_N, GW_D. The metric 'edges' is fixed and equal to the actual number of edges in the observed brain networks in all the configurations but M_{11} model. *Metrics that are fixed. ✓Metrics that are variable.

models	edges	GW_K	GW_E	GW_N	GW_D
M_1	*	✓	✓	–	—
M_2	*	—	✓	—	✓
M_3	*	—	—	✓	✓
M_4	*	—	✓	✓	—
M_5	*	—	✓	—	—
M_6	*	—	—	✓	—
M_7	*	✓	—	✓	—
M_8	*	✓	—	—	✓
M_9	*	✓	—	—	—
M_{10}	*	—	—	—	✓
M_{11}	✓	—	✓	✓	—

The above specifications yield particular ERGMs that belong to the so-called curved exponential family [33] and that have been extensively used in social science [32,58,59].

We constructed different ERGM configurations by including these graph metrics as illustrated in table 1. For the sake of simplicity, we only considered combinations of two graph metrics at most, except in one case where we also included the number of edges as a further metric [39,40].

We tested the different configurations by fitting the ERGM to brain networks in each single subject ($N = 108$), frequency band (*theta*, *alpha*, *beta*, *gamma*) and condition (EO, EC). To fit ERGMs, we used an MCMC algorithm (Gibbs sampler) that samples networks from an exponential graph distribution. Specifically, we set the initial values of the model parameters $\boldsymbol{\theta}^0$ by means of a maximum pseudo-likelihood estimation (MPLE) [54,60]. Then, we adopted Fisher's scoring method to update the model parameters $\boldsymbol{\theta}$ until they converged to the approximated MLEs $\hat{\theta}$ [31]. As we used curved ERGMs, the ratio parameters τ were not fixed but were estimated.

Eventually, for each fitted ERGM configuration we generated 100 synthetic networks in order to obtain appropriate confidence intervals.

2.3.2. Goodness of fit

First, we used the Akaike information criterion (AIC) to evaluate the relative quality of the ERGMs' fit by taking into account the maximum value of the likelihood function and the number of model parameters [61].

We also adopted a different approach to assess the absolute quality of the fit by comparing the synthetic networks generated by the estimated ERGMs and the observed brain networks. Specifically, we defined the following score based on the integration and segregation properties of networks:

$$\delta(E_g, E_l) = \max(|\eta_{E_g}|, |\eta_{E_l}|), \tag{2.10}$$

where η_{E_g}, η_{E_l} are the relative errors between the mean values of the global/local efficiency of the simulated networks and the value of the observed brain network. By selecting the maximum absolute error, we were considering the worst case, similar to what was proposed in [26]. Based on the above criteria, we selected the best model, which minimizes the AIC and δ mean values. To validate the model adequacy (equation (2.6)), we computed the *Z*-scores between the graph metrics' values of brain networks and synthetic networks.

Furthermore, we cross-validated the best model configuration by evaluating the synthetic networks' fit to graph indices that were explicitly not included in either the ERGM or the model selection criteria. We computed Pearson's correlation coefficient between the values of the characteristic path length (L), clustering coefficient (C) and modularity (Q) extracted from the observed brain networks and the mean values obtained from the corresponding simulated networks. In addition, we used the Mirkin index (MI) [62] to evaluate the similarity between the community partitions of the observed networks and the consensus partitions of the corresponding synthetic networks.

2.4. Statistical group analysis

We assessed the statistical differences between the values of the graph indices extracted from the brain networks in the EO and EC resting-state conditions. We also computed between-condition differences using the synthetic networks fitted by the best ERGM. In this case, we considered the mean values of the graph indices in order to have one value corresponding to one brain network. Eventually, we computed the statistical differences between the values of the best ERGM parameters in the EO and EC conditions in order to assess their potential to provide complementary information to that provided by standard graph analysis. For each comparison, we used a non-parametric permutation *t*-test and we fixed a statistical threshold of $\alpha = 0.001$ and 100 000 permutations.

3. Results

3.1. Characteristic functional segregation of electroencephalographic resting-state networks

The group analysis revealed a significant increase in the local-efficiency in EO, compared with that in EC, for the *alpha* band ($T = 3.529$, $p = 0.0007$, figure 2). We also reported a significant increment ($T = 3.557$, $p = 0.0007$) for the modularity in the *alpha* band, while no other statistically significant differences were observed in the other frequency bands, graph indices or metrics (electronic supplementary material, table S3).

These differences were obtained for brain networks thresholded with an average node degree $k = 3$ according to the ECO criterion [44]. We reported a similar increase in functional segregation (local-efficiency) in the *alpha* band for $k = 5$ (electronic supplementary material, figure S1). More details on the analysis for $k = 5$ can be found in the electronic supplementary material (Supp_text.pdf).

In terms of existing relationships between graph indices and ERGM metrics, we could not establish univocal associations between E_g and E_l values and the metrics' values used in the ERGMs (electronic supplementary material, table S1). This was especially true for the global-efficiency, which exhibited significantly high correlations with all the other graph metrics (Spearman's $|R| > 0.43$, $p < 10^{-39}$).

3.2. Triangles and stars as fundamental constituents of functional brain networks

All the proposed ERGM configurations exhibited a relatively good fitting in terms of AIC, except for M_{11} (electronic supplementary material, figure S2). Notably, the latter was the only configuration where the number of edges was considered

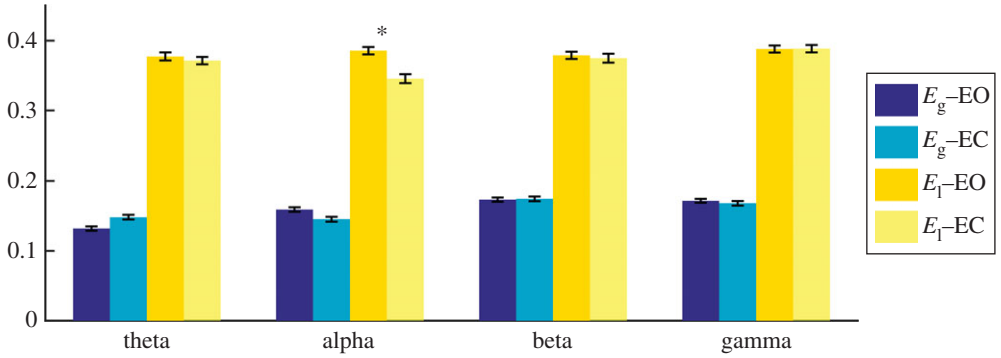

Figure 2. Median values and standard errors of global- and local-efficiency measured from EEG brain networks across 108 subjects in eyes-open (EO) and eyes-closed (EC) resting states. *p-value < 0.001.

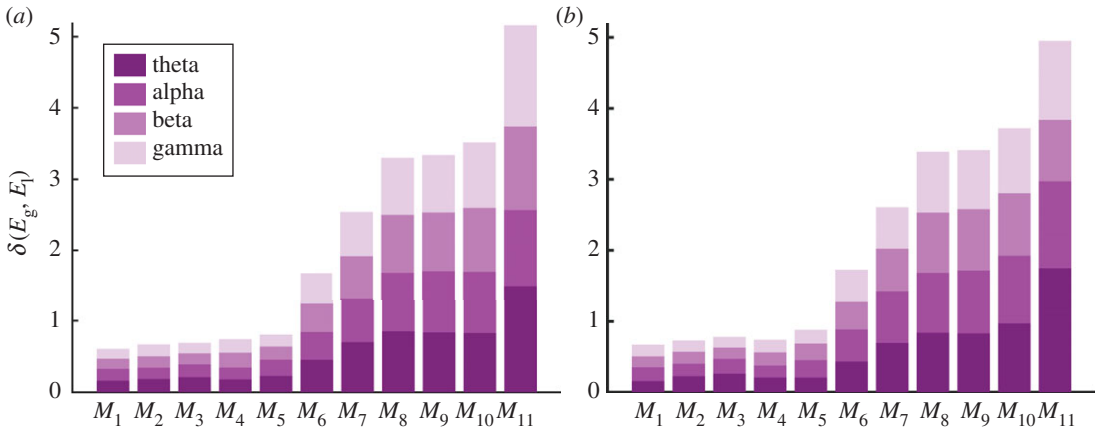

Figure 3. Absolute quality of the fit of ERGMs. Coloured bars show the group-averaged cumulative errors $\delta(E_g, E_l)$ in terms of the relative of global- and local-efficiency across frequency bands. Model configurations are listed on the x-axis. (*a*) Values for the eyes-open resting state (EO); (*b*) the error values for the eyes-closed resting state (EC). (Online version in colour.)

as a model parameter and not as a constraint. M_1 gave the lowest $\delta(E_g, E_l)$ scores compared with the other configurations in both the EO and EC conditions (figure 3). Notably, the configurations giving lower $\delta(E_g, E_l)$ scores included, directly or indirectly, the metric GW_E, with the exception of M_{11}.

We selected M_1 as a potentially good candidate to model EEG-derived brain networks. According to this model configuration the mass probability density reads $P(G) = Z^{-1} \exp\{\theta_1 GW_E + \theta_2 GW_K\}$. The group-median values of the estimated parameters (θ_1 and θ_2) were all positive and larger than 1 in each band and condition (table 2). This means that the likelihood of an edge existing in a simulated network is larger if that edge is part of a triangle (GW_E) or of a star (GW_K), and that these connectivity structures are statistically relevant for the brain network formation.

Overall, the GW_E and GW_K values of the synthetic networks generated by M_1 were not significantly different from those of the observed brain networks (figure 4). This was true in every subject for GW_E ($Z < 2.58$, $p > 0.01$) and in at least 94% of the subjects for GW_E ($Z < 2.58$, $p > 0.01$). Furthermore, the values of the characteristic path length (L), clustering coefficient (C) and modularity (Q) extracted from synthetic networks were significantly correlated (Pearson's $R > 0.44$, $p < 10^{-6}$) with those of the brain networks in each frequency band (figure 5; electronic supplementary material, table S2). In addition, synthetic networks exhibited a similar community partition to individual brain networks, as revealed by the low MI values (MI < 0.21) (electronic supplementary material, figure S3). These results confirmed that M_1 adequately models the obtained EEG brain networks.

3.3. Simulating network differences between absence and presence of visual input

Figure 6 illustrates the brain networks for a representative subject in the *alpha* band along with the corresponding synthetic networks generated by M_1. In both the EO and EC conditions, simulated networks and brain networks share similar topological structures characterized by diffused regularity and more concentrated connectivity in parietal and occipital regions.

The group analysis over the synthetic networks revealed the ability of M_1 to capture not only the individual properties of brain networks but also the main observed difference between the EC and EO resting states, reflecting, respectively, the absence and presence of visual input. Similarly to observed brain networks, we obtained, for simulated networks, a marginally significant increase in the local-efficiency from EC to EO, in the *alpha* band ($T = 3.168$, $p = 0.002$). No other significant differences were reported in any other band or graph index/metric (electronic supplementary material, table S3).

Finally, by looking at the values of the estimated parameters, we observed that θ_1 values were significantly larger in EO than in EC for both the *alpha* ($T = 3.746$, $p =$

Table 2. Statistics for the estimated parameters of the model configuration M_1. Median values and standard errors (within parentheses) are reported for the two resting-state conditions EO and EC. *t*-values and *p*-values (within parentheses) from non-parametric permutation-based *t*-tests between EO and EC are shown in the third column of each subsection marked with the heading EO − EC.

	θ_1			θ_2		
	EO	EC	EO − EC	EO	EC	EO − EC
theta	1.528 (0.045)	1.531 (0.039)	−0.281 (0.7804)	1.502 (0.169)	1.443 (0.159)	−0.406 (0.690)
alpha	1.449 (0.041)	1.297 (0.039)	3.746 (0.0002)	1.327 (0.123)	1.317 (0.532)	−1.084 (0.347)
beta	1.487 (0.457)	1.326 (0.046)	1.514 (0.0009)	1.062 (0.149)	1.303 (0.169)	−0.890 (0.371)
gamma	1.552 (0.046)	1.509 (8.266)	−0.992 (0.8521)	0.878 (0.125)	1.140 (3.002)	−1.064 (0.135)

0.0002) and *beta* ($Z = 1.514$, $p = 0.0009$) frequency bands, while no significant differences were found for θ_2 values (table 2).

4. Discussion

In recent years, the use of statistical methods to infer the structure of complex systems has gained increasing interest [39,64–66]. Beyond the descriptive characterization of networks, statistical network models aim to statistically assess the local connectivity processes involved in the global structure formation [18]. This is a crucial advance with respect to standard descriptive approaches because imaging connectomes, as with other biological networks, is often inferred from experimentally obtained data and therefore the estimated edges can suffer from statistical noise and uncertainty [67].

In our study, we used ERGMs to identify the local connectivity structures that statistically form the intrinsic synchronization of large-scale electrophysiological activities. This model formulation has the advantage of statistically inferring the probability of edge formation accounting for highly dependent configurations, such as transitivity structures, something that is lacking in, for example, the Bernoulli model. Furthermore, it is possible to include, in theory, graph metrics measuring global and local properties and discriminating node and edges attributes, such as homophily effects. In addition, it generalizes well-known network models such as the stochastic block model, where a block structure is imposed by including the count of edges between groups of nodes as a model metric [68].

Here, the results showed that the tendency to form triangles (GW_E) and stars (GW_K) was sufficient to statistically reproduce the main properties of the EEG brain networks, such as functional integration and segregation, measured by means of global-efficiency E_g and local-efficiency E_l (electronic supplementary material, table S3). Our findings partially deviate from previous studies, which have used ERGMs to model fMRI and DTI brain networks, where GW_E and the geometrically weighted non-edgewise shared partner GW_N were selected under the assumption that these could be related, respectively, to local- and global-efficiency [39,40]. However, here we showed that a univocal relationship between the ERGM graph indices and the metrics used to describe the EEG connectomes could not be statistically established (electronic supplementary material, table S1). While the propensity to form triangles (GW_E) can lead to cohesive clustering in the network (E_l), the propensity to form redundant paths of length 2 (i.e. GW_N) is not clearly related to the formation of short paths between nodes (E_g) [57]. Thus, while in general a good fit can be achieved by including GW_N in the ERGM, the subsequent interpretation in terms of brain functional integration appears less straightforward. Here, we showed that GW_E together with the tendency to form stars (GW_K) gave the best fit in terms of local- and global efficiency. Triangles and stars, giving rise to clustering and hubs, are fundamental building blocks of complex systems reflecting important mechanisms such as transitivity [48] and preferential attachment [69]. Notably, the existence of highly connected nodes is compatible with the presence of short paths (e.g. in a star graph the characteristic path length $L = 2$). This supports the recent view of brain functional integration where segregated modules exchange information through central hubs and not necessarily through the shortest paths [70,71].

In the cross-validation phase, the selected model configuration captured other important brain network properties as measured by the clustering coefficient C, the characteristic path length L and the modularity Q (figure 5). In terms of the differences between conditions, the simulated networks gave a marginally significant increase ($p = 0.002$) in E_l in the *alpha* band during EO as compared with EC, while, differently from observed brain networks, no significant differences were reported for the modularity Q (electronic supplementary material, table S3). The latter could be, in part, ascribed to the absence of specific metrics in the ERGM accounting for modularity. In this respect, stochastic block models, which explicitly force modular structures, could represent an interesting alternative to explore in the future [72,73]. Here, the increased *alpha* local-efficiency suggests a modulation of augmented specialized information processing, from EC to EO, that is consistent with typical global power reduction and increased regional activity [74]. Possible neural mechanisms explaining this effect have been associated with the automatic gathering of non-specific information resulting from more interactions within the visual system [75] and with shifts from interoceptive towards exteroceptive states [76–78].

As a crucial result, we provided complementary information by inspecting the fitted ERGM parameters. The positive $\theta_1 > 1$ and $\theta_2 > 1$ values indicated that both GW_E and GW_K are fundamental connectivity features that emerge in brain networks more than expected by chance (table 2). However, only θ_1 values showed a significant difference (EO > EC) in the *alpha* band, as well as in the *beta* band (table 2), suggesting that the tendency to form triangles,

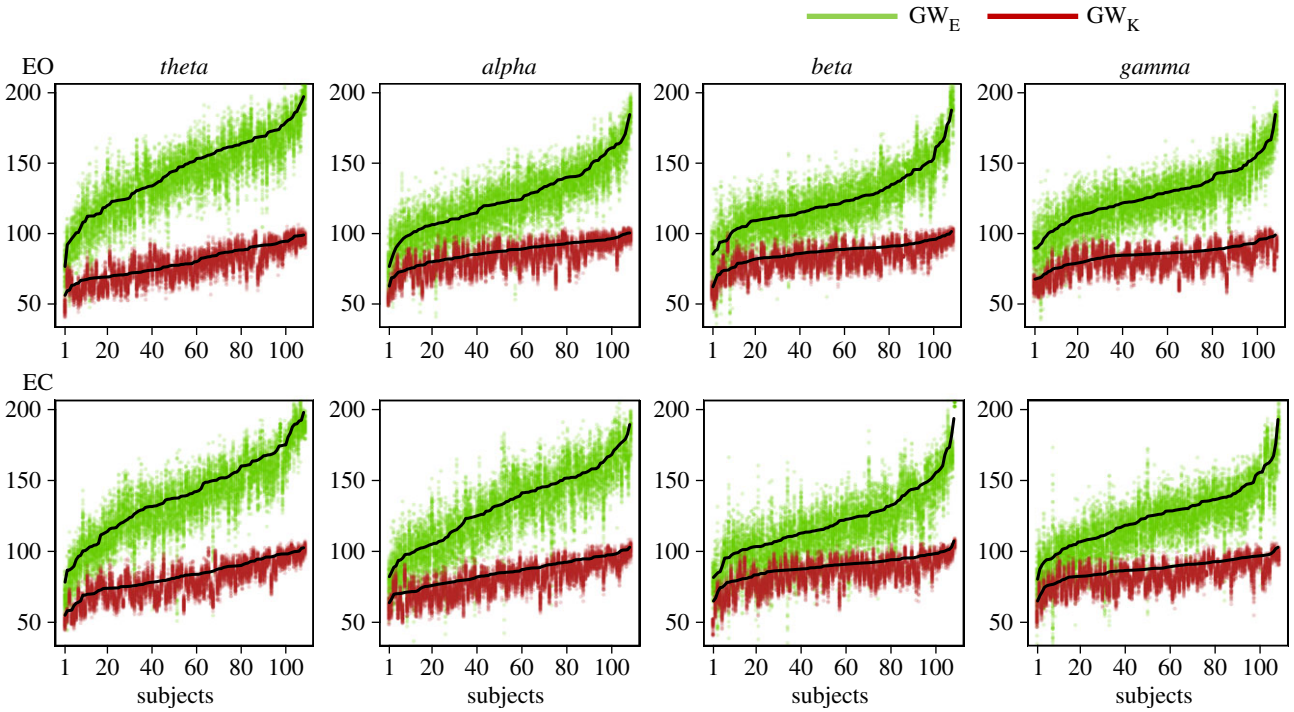

Figure 4. Adequacy of the model configuration M_1. Green and red dots represent, respectively, the values of the *geometrically weighted edgewise shared pattern distribution* (GW_E) and the *geometrically weighted degree distribution* (GW_K) measured in simulated networks. Black dot lines indicate the values measured in the observed brain networks.

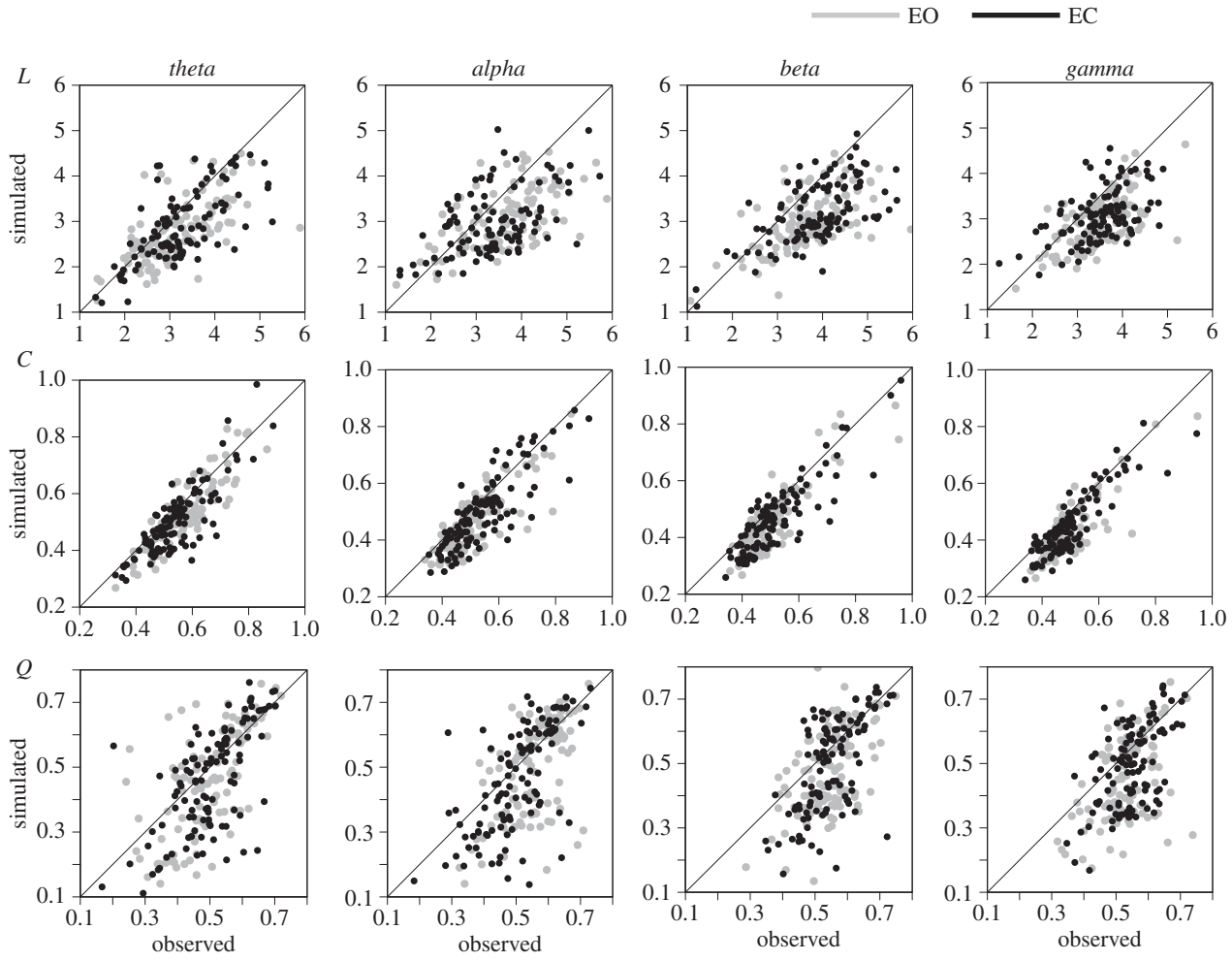

Figure 5. Cross-validation for the model configuration M_1. Scatter plots show the values of the graph indices measured in the observed brain networks (*x*-axis) against the mean values obtained from synthetic networks (*y*-axis). Three graph indices were considered: characteristic path length (*L*), clustering coefficient (*C*) and modularity (*Q*). Grey dots correspond to eyes-open resting states (EO); black dots correspond to eyes-closed resting states (EC).

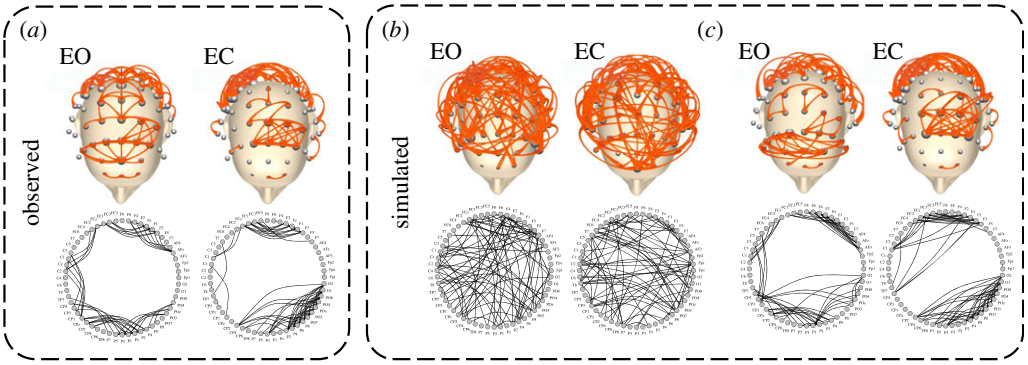

Figure 6. Brain networks and synthetic networks for a representative subject. (*a*) Brain network in the *alpha* band for the eyes-open (EO) and eyes-closed (EC) resting state. (*b*) One instance of the corresponding synthetic networks generated by the model configuration M_1. (*c*) Because node labels are not preserved in the simulated networks, we re-assigned them virtually by using the Frank–Wolfe algorithm [63], which optimizes the graph matching with the observed brain network. In the upper part of the figure, nodes correspond to EEG electrodes, whose position follows a standard 10–10 montage. In the bottom part, the nodes are arranged into a circle. (Online version in colour.)

rather than the tendency to form stars, is a discriminating feature of EO and EC modes. More concentrated EEG activity among parieto-occipital areas has been largely documented in the *alpha* and also in the *beta* bands, the latter reflecting either cortical processing of visual input or externally oriented attention [74,79]. Notably, the role of the *beta* band could not be found when analysing either brain networks or synthetic networks (figure 2; electronic supplementary material, table S3) and we speculate that this result specifically stems from the inherent ability of ERGMs to account for potential interaction between different graph metrics [57].

4.1. Methodological considerations

We estimated EEG connectomes by means of spectral coherence. While this measure is known to suffer from possible volume conduction effects [80], it has also been demonstrated that, probably due to this effect, it has the advantage of generating connectivity matrices that are highly consistent within and between subjects [81]. In addition, spectral coherence is still one of the most used measures to infer FC in the electrophysiological literature on resting states because of its simplicity and relatively intuitive interpretation. Thus, constructing EEG connectomes by means of spectral coherence allowed us to better contextualize the results obtained with ERGM from a neurophysiological perspective. Future studies will have to assess if and how different connectivity estimators affect the choice of the model parameters.

We used a density-based thresholding procedure to filter information in the EEG raw networks by retaining and binarizing the strongest edges. Despite the consequent information loss, thresholding is often adopted to mitigate the uncertainty of the weakest edges, reduce the false positives and facilitate the interpretation of the inferred network topology [13,17].

Selecting a binarizing threshold does have an impact on the topological structure of brain networks [82]. Based on the optimization of fundamental properties of complex systems, i.e. efficiency and economy, the adopted thresholding criterion (ECO) leads to sparse networks, with an average node degree $k = 3$, causing possible nodes to be disconnected. However, it has demonstrated empirically that the size of the resulting largest component typically contains more than 60% of the brain nodes, thus ensuring a sparse but meaningful network structure [44]. In a separate analysis, we verified that the validity of the model and the characteristic between-condition differences observed in the *alpha* band were also globally preserved for $k = 5$ (electronic supplementary material, Supp_text.pdf).

Authors' contributions. C.O. and F.D.V.F. both designed the study; C.O. performed the analysis and wrote the paper; and F.D.V.F. wrote the paper.

Competing interests. We declare we have no competing interests.

Funding. This work has been partially supported by the Agence Nationale de la Recherche (French programme) ANR-10-IAIHU-06 and ANR-15-NEUC-0006-02.

Acknowledgements. We are grateful to M. Chavez and J. Guillon for their useful comments and suggestions.

References

1. Raichle ME, MacLeod AM, Snyder AZ, Powers WJ, Gusnard DA, Shulman GL. 2001 A default mode of brain function. *Proc. Natl Acad. Sci. USA* **98**, 676–682. (doi:10.1073/pnas.98.2.676)
2. Bullmore E, Bullmore E, Sporns O, Sporns O. 2009 Complex brain networks: graph theoretical analysis of structural and functional systems. *Nat. Rev. Neurosci.* **10**, 186–198. (doi:10.1038/nrn2575)
3. Honey CJ, Sporns O, Cammoun L, Gigandet X, Thiran JP, Meuli R, Hagmann P. 2009 Predicting human resting-state functional connectivity from structural connectivity. *Proc. Natl Acad. Sci. USA* **106**, 2035–2040. (doi:10.1073/pnas.0811168106)
4. Deco G, Ponce-Alvarez A, Mantini D, Romani GL, Hagmann P, Corbetta M. 2013 Resting-state functional connectivity emerges from structurally and dynamically shaped slow linear fluctuations. *J. Neurosci.* **33**, 11239–11252. (doi:10.1523/JNEUROSCI.1091-13.2013)
5. Park H-J, Friston K. 2013 Structural and functional brain networks: from connections to cognition. *Science* **342**, 1238411. (doi:10.1126/science.1238411)
6. Fornito A *et al*. 2011 Genetic influences on cost-efficient organization of human cortical functional networks. *J. Neurosci.* **31**, 3261–3270. (doi:10.1523/JNEUROSCI.4858-10.2011)

7. Achard S, Delon-Martin C, Vértes PE, Renard F, Schenck M, Schneider F, Heinrich C, Kremer S, Bullmore ET. 2012 Hubs of brain functional networks are radically reorganized in comatose patients. *Proc. Natl Acad. Sci. USA* **109**, 20 608–20 613. (doi:10.1073/pnas.1208933109)
8. Chennu S *et al.* 2014 Spectral signatures of reorganised brain networks in disorders of consciousness. *PLoS Comput. Biol.* **10**, e1003887. (doi:10.1371/journal.pcbi.1003887)
9. Tijms BM, Wink AM, de Haan W, van der Flier WM, Stam CJ, Scheltens P, Barkhof F. 2013 Alzheimer's disease: connecting findings from graph theoretical studies of brain networks. *Neurobiol. Aging* **34**, 2023–2036. (doi:10.1016/j.neurobiolaging.2013.02.020)
10. Grefkes C, Fink GR. 2011 Reorganization of cerebral networks after stroke: new insights from neuroimaging with connectivity approaches. *Brain* **134**, 1264–1276. (doi:10.1093/brain/awr033)
11. Lynall M-E, Bassett DS, Kerwin R, McKenna PJ, Kitzbichler M, Muller U, Bullmore E. 2010 Functional connectivity and brain networks in schizophrenia. *J. Neurosci.* **30**, 9477–9487. (doi:10.1523/JNEUROSCI.0333-10.2010)
12. Stam C. 2004 Functional connectivity patterns of human magnetoencephalographic recordings: a 'small-world' network? *Neurosci. Lett.* **355**, 25–28. (doi:10.1016/j.neulet.2003.10.063)
13. Rubinov M, Sporns O. 2010 Complex network measures of brain connectivity: uses and interpretations. *NeuroImage* **52**, 1059–1069. (doi:10.1016/j.neuroimage.2009.10.003)
14. Stam CJ, van Straaten ECW. 2012 The organization of physiological brain networks. *Clin. Neurophysiol.* **123**, 1067–1087. (doi:10.1016/j.clinph.2012.01.011)
15. Tumminello M, Aste T, Matteo TD, Mantegna RN. 2005 A tool for filtering information in complex systems. *Proc. Natl Acad. Sci. USA* **102**, 10 421–10 426. (doi:10.1073/pnas.0500298102)
16. Vidal M, Cusick M, Barabási A-L. 2011 Interactome networks and human disease. *Cell* **144**, 986–998. (doi:10.1016/j.cell.2011.02.016)
17. De Vico Fallani F, Richiardi J, Chavez M, Achard S. 2014 Graph analysis of functional brain networks: practical issues in translational neuroscience. *Phil. Trans. R. Soc. B* **369**, 20130521. (doi:10.1098/rstb.2013.0521)
18. Goldenberg A, Zheng AX, Fienberg SE, Airoldi EM. A survey of statistical network models. (http://arxiv.org/abs/0912.5410)
19. Milo R, Shen-Orr S, Itzkovitz S, Kashtan N, Chklovskii D, Alon U. 2002 Network motifs: simple building blocks of complex networks. *Science* **298**, 824–827. (doi:10.1126/science.298.5594.824)
20. Garlaschelli D, Loffredo MI. Patterns of link reciprocity in directed networks. *Phys. Rev. Lett.* **93**, 268701. (doi:10.1103/PhysRevLett.93.268701)
21. Humphries MD, Gurney K. 2008 Network 'small-world-ness': a quantitative method for determining canonical network equivalence. *PLoS ONE* **3**, e0002051. (doi:10.1371/journal.pone.0002051)
22. Barabasi A-L, Jeong H, Néda Z, Ravasz E, Schubert A, Vicsek T. 2002 Evolution of the social network of scientific collaborations. *Physica A* **311**, 590–614. (doi:10.1016/S0378-4371(02)00736-7)
23. Newman MEJ, Watts DJ, Strogatz SH. 2002 Random graph models of social networks. *Proc. Natl Acad. Sci. USA* **99**, 2566–2572. (doi:10.1073/pnas.012582999)
24. Barthélemy M. 2011 Spatial networks. *Phys. Rep.* **499**, 1–101. (doi:10.1016/j.physrep.2010.11.002)
25. Vertes PE, Alexander-Bloch AF, Gogtay N, Giedd JN, Rapoport JL, Bullmore ET. 2012 Simple models of human brain functional networks. *Proc. Natl Acad. Sci. USA* **109**, 5868–5873. (doi:10.1073/pnas.1111738109)
26. Betzel RF, *et al*. 2016 Generative models of the human connectome. *NeuroImage A* **124**, 1054–1064. (doi:10.1016/j.neuroimage.2015.09.041)
27. Frank O, Strauss D. 1986 Markov graphs. *J. Am. Stat.* **81**, 832–842. (doi:10.2307/2289017)
28. Frank O. 1991 Statistical analysis of change in networks. *Stat. Neerland.* **45**, 283–293. (doi:10.1111/j.1467-9574.1991.tb01310.x)
29. Wasserman S, Pattison P. 1996 Logit models and logistic regressions for social networks: I. An introduction to Markov graphs and *p. Psychometrika* **61**, 401–425. (doi:10.1007/BF02294547)
30. Handcock MS. 2002 Statistical models for social networks: inference and degeneracy. In *Dynamic social network modeling and analysis* (eds R Breiger, K Corley, P Pattison), pp. 229–240. Washington, DC: National Academies Press.
31. Hunter DR, Handcock MS. 2006 Inference in curved exponential family models for networks. *J. Comput. Graph. Stat.* **15**, 565–583. (doi:10.1198/106186006X133069)
32. Goodreau SM. 2007 Advances in exponential random graph (p^*) models applied to a large social network. *Soc. Netw.* **29**, 231–248. (doi:10.1016/j.socnet.2006.08.001)
33. Hunter DR. 2007 Curved exponential family models for social networks. *Soc. Netw.* **29**, 216–230. (doi:10.1016/j.socnet.2006.08.005)
34. Rinaldo A, Fienberg SE, Zhou Y. 2009 On the geometry of discrete exponential families with application to exponential random graph models. *Electron. J. Stat.* **3**, 446–484. (doi:10.1214/08-EJS350)
35. Robins G, Pattison P, Wang P. 2009 Closure, connectivity and degree distributions: exponential random graph (p^*) models for directed social networks. *Soc. Netw.* **31**, 105–117. (doi:10.1016/j.socnet.2008.10.006)
36. Goodreau SM, Kitts JA, Morris M. 2009 Birds of a feather, or friend of a friend? Using exponential random graph models to investigate adolescent social networks. *Demography* **46**, 103–125. (doi:10.1353/dem.0.0045)
37. Wang P, Pattison P, Robins G. 2013 Exponential random graph model specifications for bipartite networks: a dependence hierarchy. *Soc. Netw.* **35**, 211–222. (doi:10.1016/j.socnet.2011.12.004)
38. Niekamp AM, Mercken LAG, Hoebe CJPA, Dukers-Muijrers NHTM. 2013 A sexual affiliation network of swingers, heterosexuals practicing risk behaviours that potentiate the spread of sexually transmitted infections: a two-mode approach. *Soc. Netw.* **35**, 223–236. (doi:10.1016/j.socnet.2013.02.006)
39. Simpson SL, Hayasaka S, Laurienti PJ. 2011 Exponential random graph modeling for complex brain networks. *PLoS ONE* **6**, e20039. (doi:10.1371/journal.pone.0020039)
40. Sinke MRT, Dijkhuizen RM, Caimo A, Stam CJ, Otte WM. 2016 Bayesian exponential random graph modeling of whole-brain structural networks across lifespan. *NeuroImage* **135**, 79–91. (doi:10.1016/j.neuroimage.2016.04.066)
41. Goldberger AL *et al*. 2000 PhysioBank, PhysioToolkit, and PhysioNet: components of a new research resource for complex physiologic signals. *Circulation* **101**, e215–e220. (doi:10.1161/01.CIR.101.23.e215)
42. Schalk G, McFarland DJ, Hinterberger T, Birbaumer N, Wolpaw JR. 2004 BCI2000: a general-purpose brain-computer interface (BCI) system. *IEEE Trans. Biomed. Eng.* **51**, 1034–1043. (doi:10.1109/TBME.2004.827072)
43. Carter GC. 1987 Coherence and time delay estimation. *Proc. IEEE* **75**, 236–255. (doi:10.1109/PROC.1987.13723)
44. De Vico Fallani F, Latora V, Chavez M. 2017 A topological criterion for filtering information in complex brain networks. *PLoS Comput. Biol.* **13**, e1005305. (doi:10.1371/journal.pcbi.1005305)
45. Tononi G, Sporns O, Edelman GM. 1994 A measure for brain complexity: relating functional segregation and integration in the nervous system. *Proc. Natl Acad. Sci. USA* **91**, 5033–5037. (doi:10.1073/pnas.91.11.5033)
46. Bassett DS, Bullmore E. 2006 Small-world brain networks. *Neuroscientist* **12**, 512–523. (doi:10.1177/1073858406293182)
47. Friston KJ. 2011 Functional and effective connectivity: a review. *Brain Connect.* **1**, 13–36. (doi:10.1089/brain.2011.0008)
48. Watts DJ, Strogatz SH. 1998 Collective dynamics of 'small-world' networks. *Nature* **393**, 440–442. (doi:10.1038/30918)
49. Latora V, Marchiori M. 2001 Efficient behavior of small-world networks. *Phys. Rev. Lett.* **87**, 198701. (doi:10.1103/PhysRevLett.87.198701)
50. Pons P, Latapy M. 2005 Computing communities in large networks using random walks. In *Computer and information sciences—ISCIS 2005*, pp. 284–293. Berlin, Germany: Springer. (doi:10.1007/11569596_31).
51. Newman MEJ. 2006 Modularity and community structure in networks. *Proc. Natl Acad. Sci. USA* **103**, 8577–8582. (doi:10.1073/pnas.0601602103)
52. Newman M. 2010 *Networks: an introduction*. Oxford, UK: Oxford University Press.
53. Robins G, Pattison P, Kalish Y, Lusher D. 2007 An introduction to exponential random graph (p^*) models for social networks. *Soc. Netw.* **29**, 173–191. (doi:10.1016/j.socnet.2006.08.002)

54. Snijders TAB. 2002 Markov Chain Monte Carlo estimation of exponential random graph models. *J. Soc. Struct.* **3**, 1–40.
55. Amaral LAN, Scala A, Barthélémy M, Stanley HE. 2000 Classes of small-world networks. *Proc. Natl Acad. Sci. USA* **97**, 11 149–11 152. (doi:10.1073/pnas.200327197)
56. Wang XF, Chen G. 2003 Complex networks: small-world, scale-free and beyond. *IEEE Circuits Syst. Mag.* **3**, 6–20. (doi:10.1109/MCAS.2003.1228503)
57. Snijders PP, Robins GL, Handcock MS. 2006 New specifications for exponential random graph models. *Sociol. Methodol.* **36**, 99–153. (doi:10.1111/j.1467-9531.2006.00176.x)
58. Robins G, Snijders T, Wang P, Handcock M, Pattison P. 2007 Recent developments in exponential random graph (p^*) models for social networks. *Soc. Netw.* **29**, 192–215. (doi:10.1016/j.socnet.2006.08.003)
59. Lusher D, Koskinen J, Robins G. 2012 *Exponential random graph models for social networks: theory, methods, and applications*. Cambridge, UK: Cambridge University Press.
60. van Duijn MAJ, Gile KJ, Handcock MS. 2009 A framework for the comparison of maximum pseudo-likelihood and maximum likelihood estimation of exponential family random graph models. *Soc. Netw.* **31**, 52–62. (doi:10.1016/j.socnet.2008.10.003)
61. Akaike H. 1998 Information theory and an extension of the maximum likelihood principle. In *Selected papers of Hirotugu Akaike* (eds E Parzen, K Tanabe, G Kitagawa), pp. 199–213. Springer Series in Statistics. New York, NY: Springer.
62. Meilă M. 2007 Comparing clusterings–an information based distance. *J. Multivar. Anal.* **98**, 873–895. (doi:10.1016/j.jmva.2006.11.013)
63. Vogelstein JT, Conroy JM, Lyzinski V, Podrazik LJ, Kratzer SG, Harley ET, Fishkind DE, Vogelstein RJ, Priebe CE. Fast approximate quadratic programming for large (brain) graph matching. (http://arxiv.org/abs/1112.5507)
64. Guimerà R, Sales-Pardo M. 2013 A network inference method for large-scale unsupervised identification of novel drug-drug interactions. *PLoS Comput. Biol.* **9**, e1003374. (doi:10.1371/journal.pcbi.1003374)
65. Martin T, Ball B, Newman MEJ. 2016 Structural inference for uncertain networks. *Phys. Rev. E* **93**, 012306. (doi:10.1103/PhysRevE.93.012306)
66. Hric D, Peixoto TP, Fortunato S. 2016 Network structure, metadata and the prediction of missing nodes and annotations. *Phys. Rev. X* **6**, 031038. (doi:10.1103/PhysRevX.6.031038)
67. Craddock RC *et al*. 2013 Imaging human connectomes at the macroscale. *Nat. Methods* **10**, 524–539. (doi:10.1038/nmeth.2482)
68. Holland PW, Laskey KB, Leinhardt S. 1983 Stochastic blockmodels: first steps. *Soc. Netw.* **5**, 109–137. (doi:10.1016/0378-8733(83)90021-7)
69. Barabasi A-L, Albert R. 1999 Emergence of scaling in random networks. *Science* **286**, 509–512. (doi:10.1126/science.286.5439.509)
70. Sporns O. 2013 Network attributes for segregation and integration in the human brain. *Curr. Opin. Neurobiol.* **23**, 162–171. (doi:10.1016/j.conb.2012.11.015)
71. Deco G, Tononi G, Boly M, Kringelbach ML. 2015 Rethinking segregation and integration: contributions of whole-brain modelling. *Nat. Rev. Neurosci.* **16**, 430–439. (doi:10.1038/nrn3963)
72. Karrer B, Newman MEJ. 2011 Stochastic blockmodels and community structure in networks. *Phys. Rev. E* **83**, 016107. (doi:10.1103/PhysRevE.83.016107)
73. Pavlovic DM, Vértes PE, Bullmore ET, Schafer WR, Nichols TE. 2014 Stochastic blockmodeling of the modules and core of the *Caenorhabditis elegans* connectome. *PLoS ONE* **9**, e97584. (doi:10.1371/journal.pone.0097584)
74. Barry RJ, Clarke AR, Johnstone SJ, Magee CA, Rushby JA. 2007 EEG differences between eyes-closed and eyes-open resting conditions. *Clin. Neurophysiol.* **118**, 2765–2773. (doi:10.1016/j.clinph.2007.07.028)
75. Yan C, Liu D, He Y, Zou Q, Zhu C, Zuo X, Long X, Zang Y. 2009 Spontaneous brain activity in the default mode network is sensitive to different resting-state conditions with limited cognitive load. *PLoS ONE* **4**, e5743. (doi:10.1371/journal.pone.0005743)
76. Marx E, Deutschländer A, Stephan T, Dieterich M, Wiesmann M, Brandt T. 2004 Eyes open and eyes closed as rest conditions: impact on brain activation patterns. *NeuroImage* **21**, 1818–1824. (doi:10.1016/j.neuroimage.2003.12.026)
77. Bianciardi M, Fukunaga M, van Gelderen P, Horovitz SG, de Zwart JA, Duyn JH. 2009 Modulation of spontaneous fMRI activity in human visual cortex by behavioral state. *NeuroImage* **45**, 160–168. (doi:10.1016/j.neuroimage.2008.10.034)
78. Xu P *et al*. 2014 Different topological organization of human brain functional networks with eyes open versus eyes closed. *NeuroImage* **90**, 246–255. (doi:10.1016/j.neuroimage.2013.12.060)
79. Boytsova YA, Danko SG. 2010 EEG differences between resting states with eyes open and closed in darkness. *Hum. Physiol.* **36**, 367–369. (doi:10.1134/S0362119710030199)
80. Srinivasan R, Winter WR, Ding J, Nunez PL. 2007 EEG and MEG coherence: measures of functional connectivity at distinct spatial scales of neocortical dynamics. *J. Neurosci. Methods* **166**, 41–52. (doi:10.1016/j.jneumeth.2007.06.026)
81. Colclough GL, Woolrich MW, Tewarie PK, Brookes MJ, Quinn AJ, Smith SM. 2016 How reliable are MEG resting-state connectivity metrics? *NeuroImage* **138**, 284–293. (doi:10.1016/j.neuroimage.2016.05.070)
82. Garrison KA, Scheinost D, Finn ES, Shen X, Constable RT. 2015 The (in)stability of functional brain network measures across thresholds. *NeuroImage* **118**, 651–661. (doi:10.1016/j.neuroimage.2015.05.046)

Chapter 4

Temporal models of dynamic brain networks predict recovery after stroke

Brain networks are constructed from temporal recordings that encode dynamic neural activity which is captured at different scales. Regardless of the scale, we can always observe changes in the brain that withholds precious information in its normal functioning and pathologies.

In this chapter, we embark in modeling time-varying brain networks. Brian dynamics are abstracted into a time-order sequence of networks and we sought to model connectivity changes over time. To do so we implement temporal exponential random graph models with temporal metrics. We study the capabilities of temporal metrics over synthetic temporal data and then we study brain plasticity over a population of stroke patients using TERGMs to statistically test which connectivity mechanisms support a good recovery of lost brain functions.

4.1 Temporal synthetic data

Most real complex systems are dynamic by nature and exhibit some degree of dependency over time. Here we propose a simple extension of the Watts-Strogatz model to generate time-dependent networks. The resulting time-varying network can be regarded as a correlated Watts-Strogatz temporal network.

Take the first network G^1 to be a lattice with N nodes and mean degree k, then we rewire each link with some small probability p and take the resulting network as G^2, next we increase p and take the resulting network

as the following graph in the time-varying network. We repeat this procedure sequentially until we reach $p = 1$. Note that in this model each network G^t (for $t > 2$) is constructed from the previous network G^{t-1} and not from a lattice as is the case in the classical Watts-Strogatz model. Therefore this model results in a time-varying network which exhibits time dependencies rather than an independent sequence of networks given by the classical Watts-Strogatz. This property is desirable as most real time-varying networks will exhibit time dependencies.

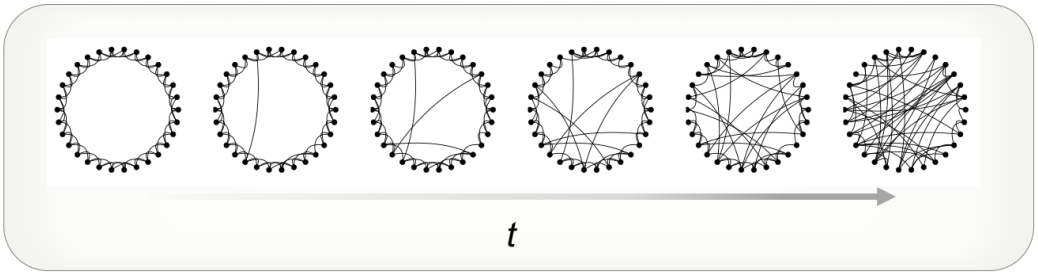

FIGURE 4.1: Time varying network generated from correlated Watts Strogatz

4.1.1 Temporal metrics

Over the years one common method to study temporal brain networks is looking at the progression of different graph metrics over time, i.e. to compute at each time point a vector of certain network metrics and report its evolution. However, this approach disregards temporal information such as connectivity that occur over time and not necessarily at a specific time point.

Moreover, the connectivity of a node does influence the connectivity of the nodes to which it is connected, and in general the overall network structure. This evidence naturally introduces dependence between graph indexes at different topological scales. To tackle this we propose to incorporate the following temporal metrics

Temporal triangles $\mathbf{T_t}$

$$T_t(G^t, G^{t-1}) = \sum_{ijk} G^{t-1}_{ik} G^{t-1}_{kj} G^t_{ij} \tag{4.1}$$

Temporal two-path $\mathbf{P_t}$

$$P_t(G^t, G^{t-1}) = \sum_{ijk} G^{t-1}_{ik}(1 - G^{t-1}_{ij})G^t_{kj}(1 - G^t_{ij}) \tag{4.2}$$

Note that both metrics count the persistence and formation of triangles and two paths respectively. Persistence refers to triangles or two paths that exist in both times $t-1$ and t and the formation to triangles or two paths that do not exist at any specific time but over time steps. Figure 4.2 show the count of temporal metrics over a time-varying network generated with the correlated Watts-Strogatz model.

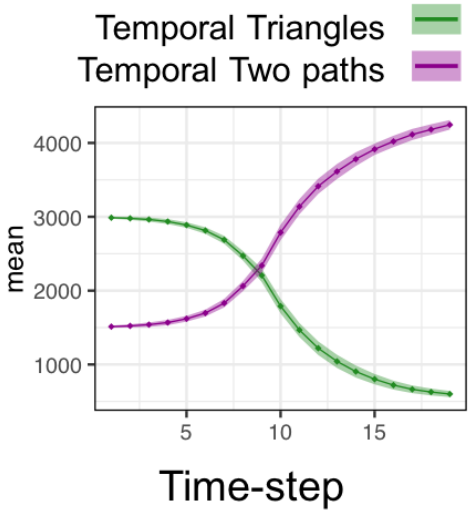

FIGURE 4.2: Count of temporal metrics of time varying network generated from correlated Watts Strogatz model

4.1.2 Model selection

We fit a TERGM with temporal metrics T_t, P_t over a correlated Watts Strogatz sequence. The corresponding Hamiltonian is given by

$$H(G^{t-1}, G^t) = \theta_1 T_t(G^{t-1}, G^t) + \theta_2 P_t(G^{t-1}, G^t) \tag{4.3}$$

The probability of observing the entire series of networks was controlled by two parameters - $theta_T$ and $theta_P$ - which weighted the relative contribution of T_t and P_t

From the fitted probability mass function we can generate synthetic time-varying networks and compared them to the correlated Watts-Strogatz sequence. By looking at the area under the ROC and PR curve we confirmed good convergence and goodness-of-fit (Fig. 4.3). The model is capable of reproducing correlated Watts Strogatz sequences.

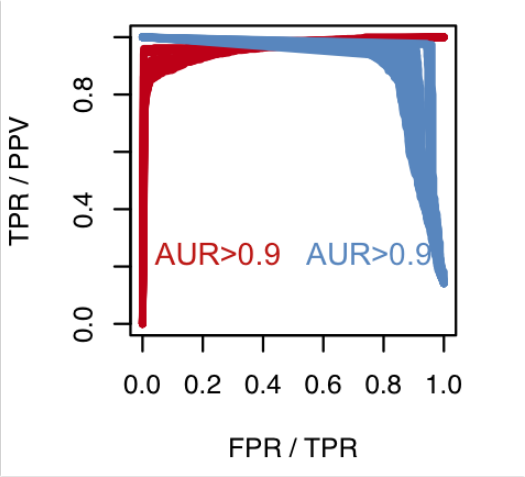

FIGURE 4.3: Goodness of fit of the model in terms of the area under the curve

Furthermore, we showed that the networks sampled with the fitted TERGM also recovered integration and segregation properties - here quantified by global- and local-efficiency respectively - that were not directly included in the model but that were intrinsically representative of the temporal Watts-Strogatz sequence. Notably, this cross-validation completely failed when we substituted the temporal graph metrics in the TERGM with static graph metrics which simply account for the presence of triangles and short paths in each time stamp (Fig. 4.4) .

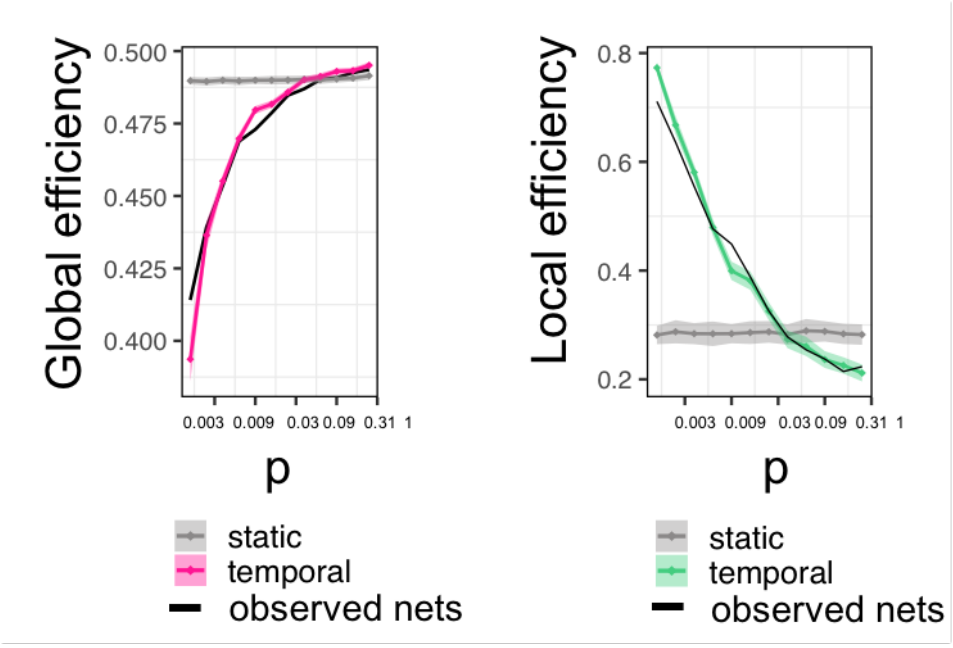

FIGURE 4.4: Comparing different TERGM with temporal and static metrics

An interesting point is to compare model 4.3 to other TERGMs with static metrics (Fig. 4.4) and to ERGM fitted at each time point. Figure 4.5 shows the are under the ROC and PR curve for models: model 4.5 ($M1$); model with static triangle and two-path counts ($M2$), and ERGM fitted at each time stamp with static triangle and two paths counts ($M3$).

Notable neither recovers the topological changes as the first model, showing that both levels of temporalities are important when modeling time-varying networks, i.e. the temporal model but as well temporal metrics.

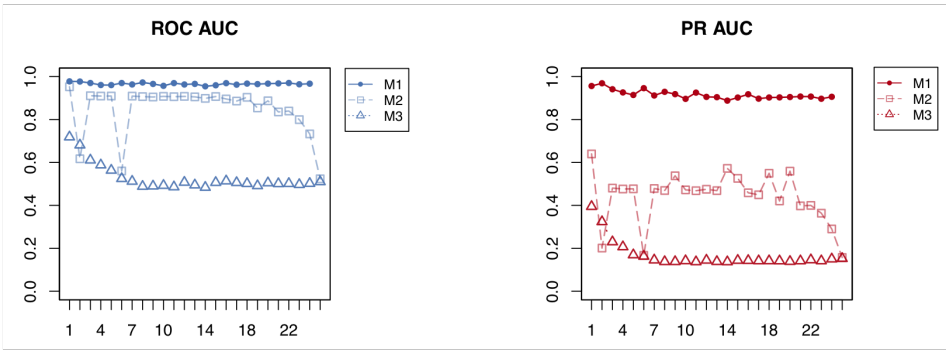

FIGURE 4.5: Comparing different (T)ERGM with temporal and static metrics in terms of AUC

4.2 Application to Stroke recovery

The brain is a networked system whose parts dynamically interact over multiple temporal and spatial scales. Such network properties are at the basis of neuroplasticity allowing for the acquisition of new skills (e.g., learning) as well as for the functional recovery after brain injuries (e.g., stroke). When locally damaged, the brain tends to spontaneously adapt by recruiting new resources through the network to compensate for the loss of the neuronal tissue and recover the associated motor or cognitive functions. At small spatial scales, dendritic remodeling, axonal sprouting, and synapse formation have been best demonstrated in the peri-lesional tissue of animal models during the first weeks after stroke (Mostany and Portera-Cailliau, 2011; Brown, Wong, and Murphy, 2008; Carmichael et al., 2001). At larger scales, it is well known that post-stroke plasticity also involves regions outside the peri-infarct cortex - including the contralesional hemisphere - and that the associated brain activity and connectivity changes can last several months in an effort to return to a normal condition (Carrera and Tononi, 2014; Siegel et al., 2016; Weiller et al., 1992; Dancause et al., 2005; Van Meer et al., 2010; He et al., 2007).

Recovery after stroke is a temporally dynamic network phenomenon, but only recent longitudinal studies have allowed to demonstrate a direct association between changes in time-varying brain networks and spontaneous recovery in humans (Ramsey et al., 2016). Both increased interhemispheric homotopic integration and intrahemispheric segregation appear to be fundamental principles for recovery of associative/higher cognitive functions (e.g. attention, memory), as quantified by the return to a normal modular organization (Siegel et al., 2018). Indeed, the role of time in complex networks has been recently revised as a fundamental variable to model and analyze real-world connection phenomena (Li et al., 2017; Holme and Saramäki, 2012). By introducing time, new higher-order properties emerge that cannot be captured by a static network, or graph, approaches and that are related to purely temporal concepts such as formation and persistence of specific connectivity patterns. Interestingly, the inherent ability of temporal connection mechanisms to characterize dynamic brain networks, as well as to predict future behavior, have been increasingly demonstrated in the context of human neuroscience (Bassett et al., 2011; Tang et al., 2009; Thompson, Brantefors, and Fransson, 2017; Braun et al., 2016; Cole et al., 2013; Ekman et al., 2012).

To date, however, the existence of dynamic brain network signatures in

stroke and their ability to predict functional recovery in individual patients has not been proved directly. Based on these theoretical and empirical grounds, we hypothesized that temporal connection mechanisms are fundamental principles of recovery after stroke. More specifically, based on the current evidence relating changes in functional integration and segregation after the injury, we expected that the formation of interhemispheric short connections and intrahemispheric clustering connections would characterize the subacute phases of recovery. Furthermore, we hypothesized that these temporal properties would allow to predict their functional outcome in the subsequent chronic phase.

To test these hypotheses, we considered longitudinal brain networks derived from resting-state fMRI BOLD activity recorded in a group of patients at 2 weeks, 3 months and 1 year after their first-ever unilateral stroke. Neurological impairments were described using multidomain behavioral measurements at each time point. We evaluated the significance of the hypothesized temporal connection mechanisms through a rigorous statistical network modeling approach and we tested their relationship with the functional recovery of single patients.

4.2.1 Time-varying brain network construction

High-resolution functional MRI data from 51 first time human stroke patients with clinical evidence of motor, language, attention, visual, or memory deficits based on neurological examination were used to map functional brain networks at several time points (2 weeks, 3 months and 1 year after stroke onset). Data were collected at the Washington University School of Medicine (WUSM). Resting-state functional scans were acquired with gradient echo EPI sequence (TR = 200 msec, TE = 2 msec, 32 contiguous 4 mm slices,4 $\times$ 4 mm in-plane resolution). The acquisitions were six to eight resting state fMRI runs, each including 128 volumes (30 min total). For more information in the full MRI protocol and fMRI preprocessing and processing see Siegel et al., 2016.

For each patient, lesions were manually segmented using structural MRI images (T1-weighted MP-RAGE, T2-weighted spin echo images, and FLAIR images obtained 1-3 weeks post-stroke) using the Analyze biomedical imaging software system (Robb and Hanson, 1991). The cortical surface was parcellated by Gordon & Laumann atlas (Gordon et al., 2014) which includes

324 regions of interest (ROI). Functional connectivity (FC) was computed between each parcel time series using Fisher z-transformed Pearson correlation (include equation?). As a result, we obtained for each patient a weighted connectivity matrix $W(t)$ of size 324×324 where the entry $w_{ij}(t)$ contains the value of FC between signals in parcel i and j and time t.

All vertices that fell within the lesion were masked out, and parcels with greater than 50% lesion overlap were excluded from the analysis. We also excluded nodes that felt in an unassigned brain system. This produced connectivity matrices of different sizes (mean=275.6, sd= 6.8). Finally, we thresholded the values in the connectivity matrices to retain the strongest links in each brain network. Specifically, we considered edge densities ranging from 5% to 20% as Siegel et al., 2018 and here we show results for networks with density 10%.

The resulting sparse time-varying brain networks were represented by adjacency matrices G^t, where each entry indicated the presence $G^t_{ij} = 1$ or the absence $G^t_{ij} = 0$ of a link between nodes i and j and time t and where the number of nodes N can vary across patients.

Damaged areas involved both subcortical and cortical ROIs, with unilateral cortical lesions mainly covering cingulo-opercular, auditory, ventral-attention, and default mode network systems. We differentiate patients into two groups those with cortical lesions, i.e the lesion affected directly one of the brain systems and, those with no cortical lesions, i.e the lesion is either in the brainstem, the cerebellar, only in the white matter or subcortical. For the cortical lesioned patients we take the subnetwork consisting of only the brain systems that were affected by the lesion (mean network size $= 81.13, sd = 47.78$) to capture more accurately the biological hypothesis.

Static descriptive approaches demonstrated a progressive restoration of modularity in the large-scale functional brain network that was associated with the recovery of multidomain functions (Siegel et al., 2018). These changes were more evident in the sub-acute phases (2 weeks and 3 months).

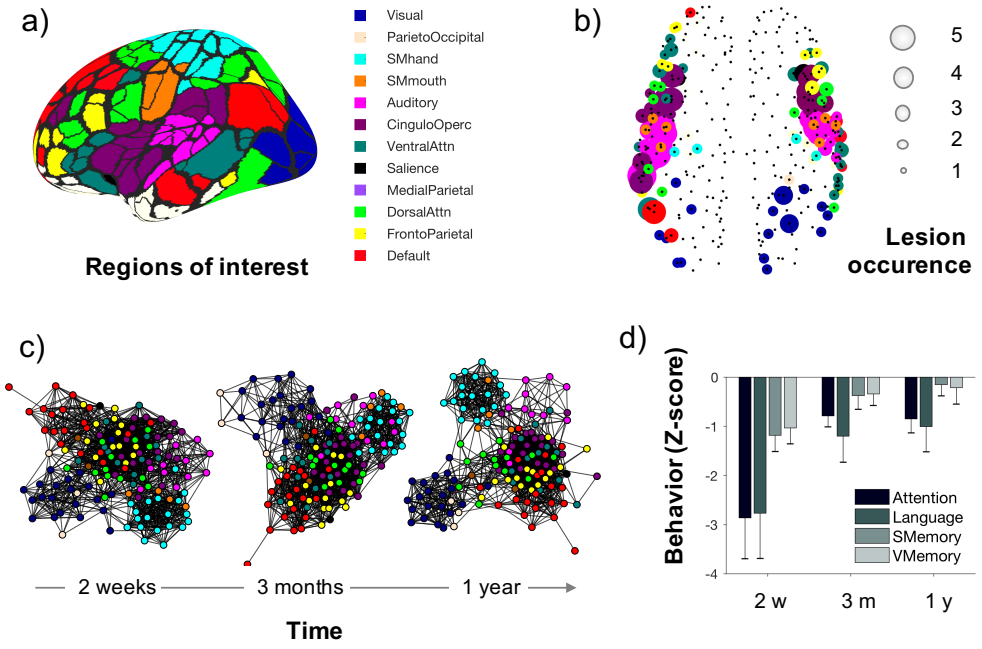

FIGURE 4.6: a) Functional connectivity network b) Lesion occurrence over the population of cortical lesion patients c) Time varying brain networks d) Behaivoral scores changes over time

4.2.2 Dynamic network mechanisms after stroke

It has been theoretically hypothesized and recently empirically observed that functional recovery after stroke is supported by the emergence and consolidation of intra-hemispheric segregation and inter-hemispheric integration. To quantify the formation of interhemispheric short connections and intra-hemispheric clustering connections we introduce two temporal metrics temporal triangles T_t and temporal interhemispheric connection Ih_t that take into account the spatial nature of brain networks and the specificity of the recovery process

$$T_t(G^t, G^{t-1}) = \sum_{ijk} G^{t-1}_{ik} G^{t-1}_{kj} G^t_{ij} \cdot L_{ij} \tag{4.4}$$

Where $L_{ij} = 1$ if i and j belongs to the same ipsi-lesional module.

$$Ih_t(G^t, G^{t-1}) = \sum_{ij} (1 - G^{t-1}_{ij}) G^t_{ij} \cdot H_{ij} \tag{4.5}$$

Where $H_{ij} = 1$ if i and j belongs to the same module in different hemispheres.

Temporal triangles quantify the temporal formation of cluster connections whereas temporal interhemispheric connections quantify the temporal

formation of long-range connections. Note that T_t, Ih_t are counting temporal formation, i.e. configurations that might not be present in either $t-1$ and t but that are observed over time. Further, the count of T_t, Ih_t between $t-1$ and t are not equivalent to the count of static triangles and connections in the collapsed network $(G^{t-1}+G^t)/2$, as the latter would also count triangles that are observed only at one time point and the former only counts the persistence of connections.

We adopted a TERGM modeling approach to identify the temporal mechanisms underlying such recovery and the extent to which they could predict future recovery in each patient. To evaluate the evolution of connectivity after stroke, we implemented a temporal exponential random graph model

$$P(G^t|G^{t-1},\boldsymbol{\theta}) = \frac{exp(\theta_T T_t(G^t,G^{t-1}) + \theta_{Ih} Ih_t(G^t,G^{t-1}))}{Z(\boldsymbol{\theta},G^{t-1})} \tag{4.6}$$

To assess how well our models fit the empirical data, we followed a generative model evaluation framework (Betzel et al., 2016). We generated synthetic data using the inferred edge-existence parameters of the TERG model. To asses the adequacy of the model we look at the area under the receiver operating characteristic (ROC) curve and the precision-recall (PR) curve of the out-of-sample prediction of network ties. We found a general high goodness-of-fit in terms of link prediction capacity regardless of the observation period (i.e. 3 months or 1 year) and location of the lesion (i.e. subcortical/cortical).

AUC	Patients		Controls	
	mean	sd	mean	sd
ROC	0.80	0.05	0.83	0.02
PRC	0.53	0.12	0.67	0.05

TABLE 4.1: Link prediction capacity of model 4.6

To test if our hypothesized network mechanisms are indeed representative of stroke recovery and not only of normal evolution of the brain over time, we fit the same model to a group of controls with matched characteristics. To make a fair comparison we only look at no cortical subjects versus controls, as these subjects have the same network sizes and in this way, we

avoid a size/variability effect. We look at parameters θ_T, θ_{Ih} for no-cortical lesion patient model and controls model.

At a global scale, the values of the fitted TERGM parameters were significantly larger from those obtained in a group of age-matched healthy controls. This indicated that the formation of triangles and interhemispheric connections are peculiar mechanisms of brain network reconfiguration after stroke.

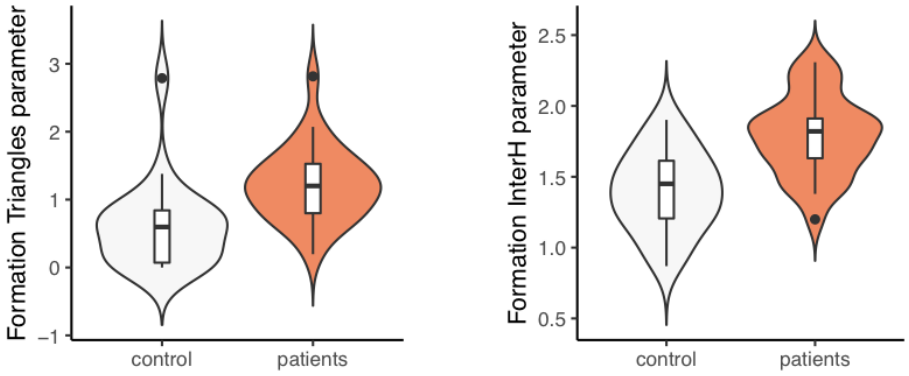

FIGURE 4.7: Statistical comparison of stroke connectivity mechanisms to controls

By analyzing the brain networks of patients affected by cortical lesions, we also found that these dynamic features were more or less prevalent depending on which system is damaged. Larger values of $theta_T$ and $theta_{Ih}$ were observed when the stroke lesion implicated ROIs in the visual and sensorimotor systems, and to a minor extent in the cingulo-opercular system (Fig 4.8).

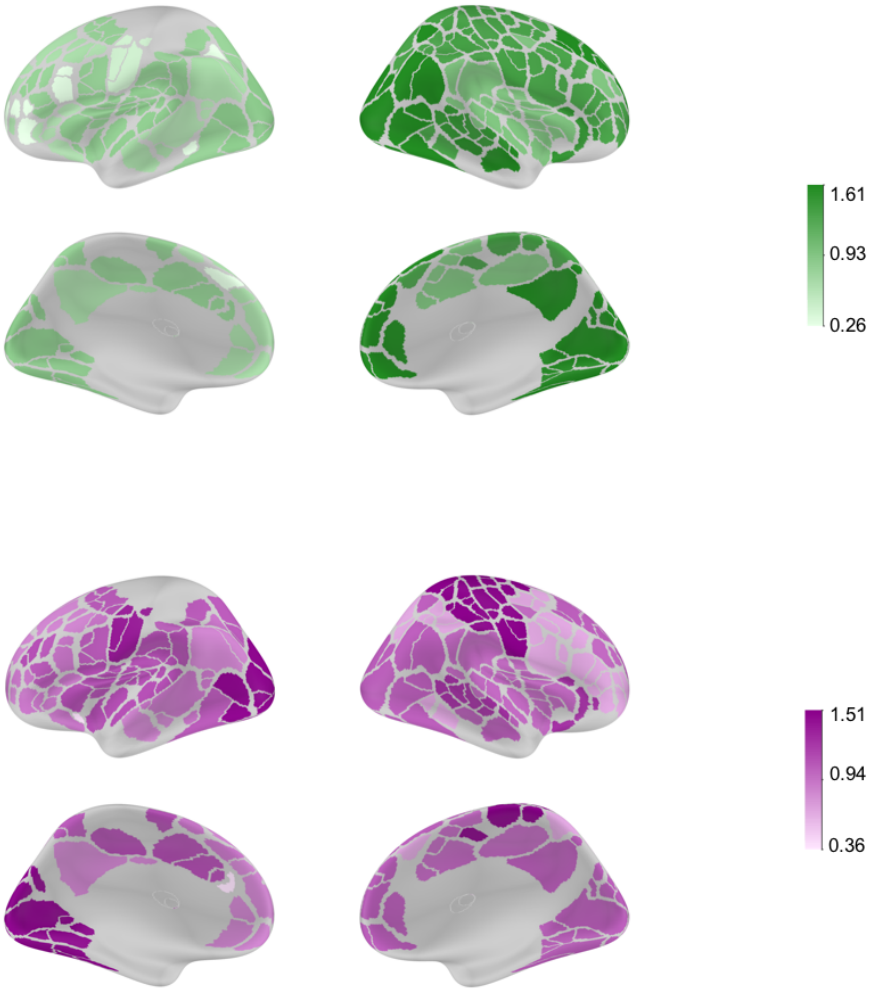

FIGURE 4.8: Weight parameters mapped in the cortex

Prediction of future outcome

Given the dynamic nature of brain connectivity after stroke, we finally asked whether such temporal network properties could be predictive of the future outcome of patients. To do so, we correlated the values of the TERGM parameters fitted over the dynamic brain networks in the subacute phase (i.e. 2 weeks and 3 months) with the multi-domain behavioral scores gathered in the chronic phase (i.e. 1 year).

We found that intrahemispheric temporal triangles and interhemispheric connections significantly predicted language for the patients with subcortical lesion ($p < 0.01$).

For patients with cortical lesions with found a significant correlation with visual levels. However, we didn't find many counts of temporal triangles for

subjects with small size networks therefore the parameter T_t was not meaningful.

No other significant correlations were found with the other behavioral scores. Notably, we found no significant correlations with static network properties such as modularity, or when we considered static connectivity metrics within the TERGM.

We finally showed that simply measuring the values of temporal graph metrics outside the TERGM did not lead to significant correlation with the behavior suggesting that the model parameters $theta_T$ and $theta_{Ih}$, which evaluate statistically the relevance of T_t and Ih_t, are indeed carrying more robust information for the prediction of stroke recovery.

Our results indicate that the use of purely temporal connection mechanisms, such as the formation and persistence of triangles and long-range connections - here reflecting within-hemisphere segregation and interhemispheric homotopic integration - hold a predictive power that cannot be achieved by simply looking at static network properties over time.

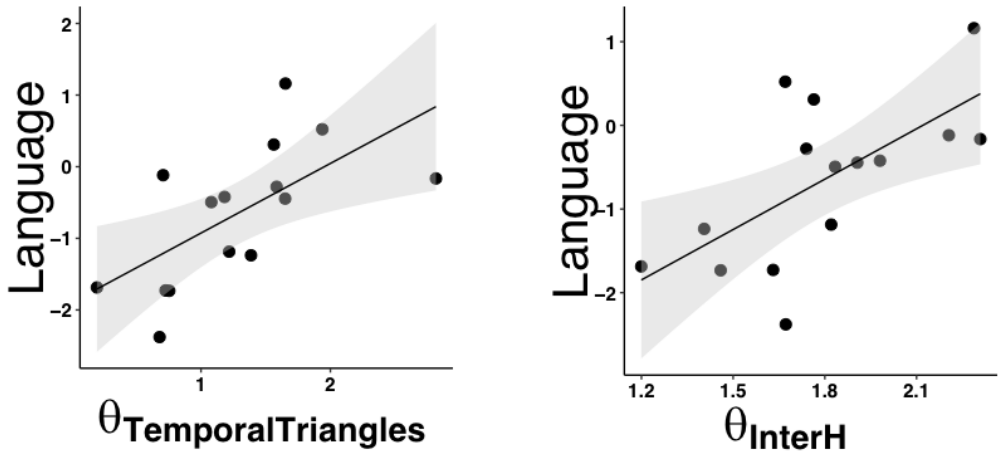

FIGURE 4.9: Formation of interhemispheric short connections and intrahemispheric clustering connections predict language

4.2.3 Discussion

Modeling dynamic networks

Most natural and social interconnected systems are characterized by time-varying interactions so that the network's structure changes over time. Such temporality has been shown to affect many dynamical processes on the network such as slowing down synchronization and diffusion of information,

impeding exploration and accessibility, as well as favoring system control (Li et al., 2017).

More pertinent to this paper, recent evidence suggests that brain functional connectivity is inherently dynamic exhibiting relatively fast fluctuations that support normal cognitive abilities - such as learning - as well as slower changes associated to neurodegenerative diseases or recovery after brain injuries (Vergara et al., 2018; Córdova-Palomera et al., 2017).

Despite the ubiquity of temporality, brain connectivity networks have been mostly studied with cross-sectional experiments and static graph approaches. Furthermore, the statistical relevance of the extracted network properties remain largely unknown and group-level analysis are typically used to determine the confidence intervals, thus leading to a critical loss of individual specificity (De Vico Fallani et al., 2014).

To address these limitations we adopted a model-based statistical framework to test the significance of specific local connection rules to generate an observed time series of temporal networks. We showed that the temporal formation of clustering connections and short-range connections - i.e. basic components of global segregation and integration - are sufficient to capture and statistically reproduce dynamic brain networks in single stroke patients.

Brain plasticity and stroke

Although stroke represents a focal damage, it is well known that consequences involve areas that are also outside the peri-lesional tissue Siegel et al., 2018; Li et al., 2014. Efforts to characterize brain network reorganization after stroke has focused almost exclusively on the static representation of underlying connectivity patterns (Siegel et al., 2018). However, both scientific intuition and recent evidence suggest that temporal network properties might also contain important information about the mechanisms of brain plasticity.

Our exploration of temporal network properties provides new insights into the brain organizational principles after stroke. We found that the formation of triangles within the perilesional area, as well as of long-range connections with the homotopic region in the contralesional hemisphere, constitute fundamental building blocks of cortical plasticity after stroke.

Biologically, these temporal connection processes quantify respectively dynamic within hemisphere segregation and between hemisphere integration, which have been hypothesized to underlie the subacute phase of stroke recovery and are in line with recent evidence showing a progressive return to a normal modular organization (Siegel et al., 2018).

Such reorganizational mechanisms were particularly evident in the visual and motor systems. Vulnerability and modeling analyses indicated that attacking such systems will have relatively little effect in terms of widespread connectivity disruption as compared, for example, to midline and fronto-temporal cortices (Alstott et al., 2009). Thus, even when damaged, the visual and motor system would exhibit a high neural plasticity potential and our results indicate that dynamic network reorganization after stroke is indeed taking place in these cortical systems.

Forecasting behavior and recovery

Forecasting behavior is one of the main challenges in many real-life situations from econometry to epidemiology. In clinical neuroscience, a correct prognosis will have a concrete impact on the life of people allowing to identify the appropriate therapeutic or strategy to slow down the progression of disease or promote effective recovery.

Our results show that the intrinsic temporal brain network signatures in the subacute phase after a stroke (between 2 weeks and 3 months) can predict the future clinical outcome of patients in the chronic phase (1-year post-stroke), whereas static network approaches failed to do so. In particular, temporal triangles could predict visual levels while short paths predicted the recovery of language. We found no correlations with more specific related scores, such as motor or visual behavior.

It has been shown that lesions of specific brain regions are often associated with specific cognitive and behavioral disturbances, and lesions of some areas tend to have more severe effects than others Damasio, 1989; Mesulam, 2000; Caplan and Van Gijn, 2012. Because of the heterogeneity of the studied population, we could not assess if it is the case. By looking at the correlation plot we could not observe a clear pattern.

Limitations/perspectives

The studied dynamic brain networks consisted of three-time points - two for the subacute phase and one for the chronic phase -allowing to have a partial understanding of the reorganizational mechanisms taking place after stroke. While from a methodological perspective TERGMs are relatively robust with respect to the length of the network time series, a higher frequency sampling would have provided more detailed dynamics. However, due to the difficulty of recruiting stroke patients over long periods the large parts

of the studies are cross-sectional or only consider two-time points. Although the dataset used here is one of the most complete currently available, more longitudinal studies will be important to assess dynamic neural mechanisms after a stroke at a finer temporal resolution.

Temporal triangles were not found to be significantly present for some cortical lesion patients with small network size and this presents a problem in the model fit. However, this could be addressed by considering parcellations with higher resolutions or other functional connectivity networks with higher spatial resolution.

The temporal graph metrics implemented in our TERGMs were designed to capture monotonic network changes over time, such as the formation of specific connectivity motifs. This means that in general, these models cannot capture inverse trends - e.g. pattern dissolution - or more complex dynamics. While this is not a major issue in the case of neural recovery and neurodegeneration, the study of functional brain networks at shorter time scales might need more sophisticated approaches that also model connectivity fluctuations. More research is needed in this direction and possible solutions may arrive from the development of network models with time-varying parameters (Lee, Li, and Wilson, 2017).

The cohort of stroke patients was heterogeneous in terms of stroke lesion type and location (Siegel et al., 2018). Because patients suffered from unilateral lesions - except for brainstem damages - we only considered the corresponding cortical hemisphere as the affected one. However, unilateral lesions of subcortical structures - including white matter and cerebellum - could result in a more complex pattern which partly involving both cortical hemispheres. In a separate analysis, we showed that consideringboth the hemispheres as affected decrease the relevance of TERGM parameters as well as their predictive ability, suggesting that there were not major reorganizational processes taking place in the unaffected hemisphere.

Conclusion

Consistent with our hypothesis, we have identified two significant temporal network mechanisms that characterize dynamic brain networks after stroke. Formation of clustering connections within the perilesional tissue and of short pathways between the perilesional area and the homotopic regions in the contralesional hemisphere are significantly abundant in stroke patients

as compared to healthy controls. These temporal signatures, which are respectively related to intrahemispheric segregation and interhemispheric integration, varied over individuals during the acute phases after stroke and were significant predictors of attention and memory deficit in the subsequent chronic phase. Furthermore, we reported a general framework for the statistical validation of temporal network metrics in arbitrary interconnected systems. Taken together, our results offer new insights into the crucial role of temporal connection mechanisms in the prediction of the dynamic system performance.

Chapter 5

Discussion & Future Directions

Network neuroscience has proven to be a leading field in advancing our understanding of the brain. As many relatively new fields, it is normal to see plenty reviews presenting current challenges and possible solutions to redirect the focus and efforts of the field in an effective way. There are two aspects that almost always pop and those are: the need for more theory-based models and, the interest in the temporal nature of brain networks, both of which are the focus of this thesis.

We looked at fundamental properties consistently found in brain networks studies and used the modelization framework of exponential random graph family to statistically test to what extent different connectivity mechanisms impact the emergent topology of functional patterns in the brain. The main objective was to account for statistical and temporal properties of functional connectivity mechanisms in the study of brain networks. To achieve this aim, we carefully built (T)ERG models to model and simulate temporal brain networks.

ERGMs have been extensively used in the field of social networks with great proliferation and although this is not the first application to network neuroscience, it is somewhat unusual. One of our contributions has been to carefully translate this framework into models with biological meaning and do extensive validation from synthetic data to static and temporal brain networks.

By following a bottom-up approach, we first studied and validated ERGMs in normal brain. By identifying persistent network properties, we were able to successfully define a model which reproduced brain connectivity networks at rest and that accounted for the uncertainty associated to each observation. The model not only recovered key topological properties but it was also capable of discriminating between eyes open and eyes closed resting state conditions.

From this study, by thoroughly testing which connectivity mechanisms were important we identified the tendency to form triangles and two paths as key ones, as expected. Then later, we adapted these two connectivity mechanisms into temporal attributes to study changes in the brain, in particularly plasticity.

We constructed TERGMs informed by biological hypothesis to study global network changes occurring during stroke recovery. We validated the temporal metrics and model over synthetic data. We successfully applied the model over real data showing the crucial role of temporal connection mechanisms in the prediction of the dynamic system performance.

Special care was taken in the goodness of fit aspect of the models. It is a very fundamental scientific question in that it tests its validity. There are many sensitive steps that will impact this, from the construction of brain networks to the model definition. Brain networks were constructed following state of the art methods that were taken into account also when interpreting the results. The bottom-up approach that we follow allowed us to construct models with a clear interpretation.

Although we reproduced with high accuracy resting state brain networks we did not exploit the natural spatial embedding of the brain. We used graph matching algorithms to evidence the similarity between observed and simulated networks. We explored the inclusion of metrics encoding spatial information such as distance matrices of nodes without success. The inclusion of spatial information is potentially crucial into modeling brain networks and more research should be done in the future.

Another common limitation is the amount of available data. It would be interesting to reproduced this study over other data sets. From data sets with more patients to other kind of neurodegenerative disease. The parameters of the model could be used into feeding machine learning algorithms to improve classification of diagnosis or as biomarkers.

This thesis served a proof of concept to show how to model temporal brain network accounting for the uncertainty associated with the data. We sought to use simple statistical models to explain as much as the complexity observed in temporal brain networks. However, (T)ERGMs are flexible enough to allow the inclusion of different statistics, therefore the design of graph metrics, informed by biological hypothesis and spatiotemporal information, could be crucial to test specific connectivity mechanisms across different brain states and conditions and with a meaningful interpretation and applicability.

Bibliography

Achard, Sophie and Ed Bullmore (2007). "Efficiency and Cost of Economical Brain Functional Networks". en. In: *PLOS Computational Biology* 3.2, e17. ISSN: 1553-7358. DOI: 10.1371/journal.pcbi.0030017. URL: https://journals.plos.org/ploscompbiol/article?id=10.1371/journal.pcbi.0030017 (visited on 09/25/2018).

Achard, Sophie et al. (2006). "A Resilient, Low-Frequency, Small-World Human Brain Functional Network with Highly Connected Association Cortical Hubs". en. In: *Journal of Neuroscience* 26.1, pp. 63–72. ISSN: 0270-6474, 1529-2401. DOI: 10.1523/JNEUROSCI.3874-05.2006. URL: http://www.jneurosci.org/content/26/1/63 (visited on 10/21/2018).

Achard, Sophie et al. (2008). "Fractal connectivity of long-memory networks". In: *Physical Review E* 77.3, p. 036104.

Achard, Sophie et al. (2012). "Hubs of brain functional networks are radically reorganized in comatose patients". en. In: *Proceedings of the National Academy of Sciences* 109.50, pp. 20608–20613. ISSN: 0027-8424, 1091-6490. DOI: 10.1073/pnas.1208933109. URL: http://www.pnas.org/content/109/50/20608 (visited on 11/16/2016).

Aine, Cheryl J (1994). "A conceptual overview and critique of functional neuroimaging techniques in humans: I. MRI/FMRI and PET." In: *Critical reviews in neurobiology* 9.2-3, pp. 229–309.

Alstott, Jeffrey et al. (2009). "Modeling the Impact of Lesions in the Human Brain". en. In: *PLOS Computational Biology* 5.6, e1000408. ISSN: 1553-7358. DOI: 10.1371/journal.pcbi.1000408. URL: https://journals.plos.org/ploscompbiol/article?id=10.1371/journal.pcbi.1000408 (visited on 10/24/2018).

Ansari-Asl, Karim et al. (2006). "Quantitative evaluation of linear and nonlinear methods characterizing interdependencies between brain signals". In: *Physical Review E* 74.3, p. 031916.

Barabasi, Albert-László and Réka Albert (1999). "Emergence of Scaling in Random Networks". en. In: *Science* 286.5439, pp. 509–512. ISSN: 0036-8075, 1095-9203. DOI: 10.1126/science.286.5439.509. URL: http://science.sciencemag.org/content/286/5439/509 (visited on 11/20/2016).

Barttfeld, Pablo et al. (2011). "A big-world network in ASD: dynamical connectivity analysis reflects a deficit in long-range connections and an excess of short-range connections". In: *Neuropsychologia* 49.2, pp. 254–263.

Bassett, Danielle S. and Edward T. Bullmore (2017). "Small-World Brain Networks Revisited". en. In: *The Neuroscientist* 23.5, pp. 499–516. ISSN: 1073-8584. DOI: 10.1177/1073858416667720. URL: https://doi.org/10.1177/1073858416667720 (visited on 09/25/2018).

Bassett, Danielle S. and Olaf Sporns (2017). "Network neuroscience". en. In: *Nature Neuroscience* 20.3, pp. 353–364. ISSN: 1097-6256. DOI: 10.1038/nn.4502. URL: http://www.nature.com/neuro/journal/v20/n3/full/nn.4502.html (visited on 02/24/2017).

Bassett, Danielle S., Perry Zurn, and Joshua I. Gold (2018). "On the nature and use of models in network neuroscience". en. In: *Nature Reviews Neuroscience* 19.9, pp. 566–578. ISSN: 1471-003X, 1471-0048. DOI: 10.1038/s41583-018-0038-8. URL: http://www.nature.com/articles/s41583-018-0038-8 (visited on 08/22/2018).

Bassett, Danielle S. et al. (2008). "Hierarchical Organization of Human Cortical Networks in Health and Schizophrenia". In: *The Journal of neuroscience : the official journal of the Society for Neuroscience* 28.37, pp. 9239–9248. ISSN: 0270-6474. DOI: 10.1523/JNEUROSCI.1929-08.2008. URL: https://www.ncbi.nlm.nih.gov/pmc/articles/PMC2878961/ (visited on 09/25/2018).

Bassett, Danielle S. et al. (2011). "Dynamic reconfiguration of human brain networks during learning". en. In: *Proceedings of the National Academy of Sciences* 108.18, pp. 7641–7646. ISSN: 0027-8424, 1091-6490. DOI: 10.1073/pnas.1018985108. URL: http://www.pnas.org/content/108/18/7641 (visited on 06/25/2018).

Betzel, Richard F. et al. (2012). "Synchronization dynamics and evidence for a repertoire of network states in resting EEG". In: *Frontiers in Computational Neuroscience* 6.September, pp. 1–13. ISSN: 1662-5188 (Electronic)\n1662-5188 (Linking). DOI: 10.3389/fncom.2012.00074.

Betzel, Richard F. et al. (2016). "Generative models of the human connectome". In: *NeuroImage* 124, Part A, pp. 1054–1064. ISSN: 1053-8119. DOI: 10.1016/j.neuroimage.2015.09.041. URL: http://www.sciencedirect.com/science/article/pii/S1053811915008563 (visited on 11/15/2016).

Bonmassar, G et al. (2001). "Spatiotemporal brain imaging of visual-evoked activity using interleaved EEG and fMRI recordings". In: *Neuroimage* 13.6, pp. 1035–1043.

Braun, Urs et al. (2016). "Dynamic brain network reconfiguration as a potential schizophrenia genetic risk mechanism modulated by NMDA receptor function". In: *Proceedings of the National Academy of Sciences* 113.44, pp. 12568–12573.

Brown, Craig E., Charles Wong, and Timothy H. Murphy (2008). "Rapid morphologic plasticity of peri-infarct dendritic spines after focal ischemic stroke". eng. In: *Stroke* 39.4, pp. 1286–1291. ISSN: 1524-4628. DOI: 10.1161/STROKEAHA.107.498238.

Bullmore, Ed and Olaf Sporns (2009). "Complex brain networks: graph theoretical analysis of structural and functional systems". en. In: *Nature Reviews Neuroscience* 10.3, pp. 186–198. ISSN: 1471-003X. DOI: 10.1038/nrn2575. URL: http://www.nature.com/nrn/journal/v10/n3/full/nrn2575.html (visited on 11/17/2016).

— (2012). "The economy of brain network organization". en. In: *Nature Reviews Neuroscience* 13.5, pp. 336–349. ISSN: 1471-003X, 1471-0048. DOI: 10.1038/nrn3214. URL: http://www.nature.com/articles/nrn3214 (visited on 09/27/2018).

Cajal, R. S. (1995). *Histology of the Nervous System of Man and Vertebrates (History of Neuroscience, No 6)(2 Volume Set)*. Oxford: Oxford University Press.

Caplan, Louis R. and Jan Van Gijn (2012). *Stroke syndromes*. Cambridge University Press.

Carmichael, S. Thomas et al. (2001). "New patterns of intracortical projections after focal cortical stroke". In: *Neurobiology of disease* 8.5, pp. 910–922.

Carrera, Emmanuel and Giulio Tononi (2014). "Diaschisis: past, present, future". In: *Brain* 137.9, pp. 2408–2422.

Casdagli, Martin C et al. (1997). "Non-linearity in invasive EEG recordings from patients with temporal lobe epilepsy". In: *Electroencephalography and clinical Neurophysiology* 102.2, pp. 98–105.

Casey, BJ et al. (2005). "Imaging the developing brain: what have we learned about cognitive development?" In: *Trends in cognitive sciences* 9.3, pp. 104–110.

Chen, Andrew CN (2001). "New perspectives in EEG/MEG brain mapping and PET/fMRI neuroimaging of human pain". In: *International Journal of Psychophysiology* 42.2, pp. 147–159.

Chennu, Srivas et al. (2014). "Spectral Signatures of Reorganised Brain Networks in Disorders of Consciousness". In: *PLOS Computational Biology* 10.10, e1003887. ISSN: 1553-7358. DOI: 10.1371/journal.pcbi.1003887.

URL: http://journals.plos.org/ploscompbiol/article?id=10.1371/journal.pcbi.1003887 (visited on 11/16/2016).

Cole, Michael W. et al. (2013). "Multi-task connectivity reveals flexible hubs for adaptive task control". In: *Nature neuroscience* 16.9, p. 1348.

Corander, Jukka, Karin Dahmström, and Per Dahmström (1998). *Maximum likelihood estimation for Markov graphs*. Univ., Department of Statistics.

Crossley, Nicolas a et al. (2013). "Correction for Crossley et al., Cognitive relevance of the community structure of the human brain functional coactivation network". In: *Proceedings of the National Academy of Sciences* 110.38, pp. 15502–15502. DOI: 10.1073/pnas.1314559110. URL: http://www.pnas.org/cgi/doi/10.1073/pnas.1314559110.

Córdova-Palomera, Aldo et al. (2017). "Disrupted global metastability and static and dynamic brain connectivity across individuals in the Alzheimer's disease continuum". en. In: *Scientific Reports* 7, p. 40268. ISSN: 2045-2322. DOI: 10.1038/srep40268. URL: https://www.nature.com/articles/srep40268 (visited on 10/24/2018).

Dahmstrum, K. and P. Dahmstrum (1993). "ML-estimation of the clustering parameter in a Markov graph model". In: *Res. rep./Stockholm univ. Dep. of statist.*

Damasio, Hanna (1989). "Lesion Analysis". In: *Neuropsychology.*

Dancause, Numa et al. (2005). "Extensive cortical rewiring after brain injury". In: *Journal of Neuroscience* 25.44, pp. 10167–10179.

David, Olivier, Diego Cosmelli, and Karl J Friston (2004). "Evaluation of different measures of functional connectivity using a neural mass model". In: *Neuroimage* 21.2, pp. 659–673.

De Vico Fallani, Fabrizio, Vito Latora, and Mario Chavez (2016). "Filtering information in imaging connectomics". In: *arXiv:1603.08445 [q-bio]*. arXiv: 1603.08445. URL: http://arxiv.org/abs/1603.08445 (visited on 11/17/2016).

De Vico Fallani, Fabrizio et al. (2007). "Cortical functional connectivity networks in normal and spinal cord injured patients: evaluation by graph analysis". In: *Human brain mapping* 28.12, pp. 1334–1346.

De Vico Fallani, Fabrizio et al. (2014). "Graph analysis of functional brain networks : practical issues in translational neuroscience Graph analysis of functional brain networks : practical issues in translational neuroscience". In: September.

Deco, Gustavo et al. (2013). "Resting-state functional connectivity emerges from structurally and dynamically shaped slow linear fluctuations". ENG.

In: *The Journal of Neuroscience: The Official Journal of the Society for Neuroscience* 33.27, pp. 11239–11252. ISSN: 1529-2401. DOI: 10.1523/JNEUROSCI.1091-13.2013.

Deco, Gustavo et al. (2015). "Rethinking segregation and integration: contributions of whole-brain modelling". en. In: *Nature Reviews Neuroscience* 16.7, pp. 430–439. ISSN: 1471-003X. DOI: 10.1038/nrn3963. URL: http://www.nature.com/nrn/journal/v16/n7/abs/nrn3963.html (visited on 11/17/2016).

Ekman, Matthias et al. (2012). "Predicting errors from reconfiguration patterns in human brain networks". In: *Proceedings of the National Academy of Sciences*, p. 201207523.

Erd6s, Paul and A Rényi (1960). "On the evolution of random graphs". In: *Publ. Math. Inst. Hungar. Acad. Sci* 5, pp. 17–61.

Fingelkurts, Andrew A, Alexander A Fingelkurts, and Seppo Kähkönen (2005). "Functional connectivity in the brain—is it an elusive concept?" In: *Neuroscience & Biobehavioral Reviews* 28.8, pp. 827–836.

Fornito, Alex et al. (2011). "Genetic influences on cost-efficient organization of human cortical functional networks". ENG. In: *The Journal of Neuroscience: The Official Journal of the Society for Neuroscience* 31.9, pp. 3261–3270. ISSN: 1529-2401. DOI: 10.1523/JNEUROSCI.4858-10.2011.

Fox, Michael D. and Michael Greicius (2010). "Clinical applications of resting state functional connectivity". English. In: *Frontiers in Systems Neuroscience* 4. ISSN: 1662-5137. DOI: 10.3389/fnsys.2010.00019. URL: https://www.frontiersin.org/articles/10.3389/fnsys.2010.00019/full (visited on 10/22/2018).

Frank, O. (1991). "Statistical analysis of change in networks". en. In: *Statistica Neerlandica* 45.3, pp. 283–293. ISSN: 1467-9574. DOI: 10.1111/j.1467-9574.1991.tb01310.x. URL: http://onlinelibrary.wiley.com/doi/10.1111/j.1467-9574.1991.tb01310.x/abstract (visited on 11/19/2016).

Frank, O and David Strauss (1986). "Markov graphs". In: *Journal of the american Statistical ...* 81.395, pp. 832–842. ISSN: 0162-1459. DOI: 10.2307/2289017. URL: http://amstat.tandfonline.com/doi/abs/10.1080/01621459.1986.10478342.

Freeman, Linton C. (1978). "Centrality in social networks conceptual clarification". In: *Social networks* 1.3, pp. 215–239.

Friston, Karl J. (2011). "Functional and Effective Connectivity: A Review". In: *Brain Connectivity* 1.1, pp. 13–36. ISSN: 2158-0014. DOI: 10.1089/brain.

2011.0008. URL: http://online.liebertpub.com/doi/abs/10.1089/brain.2011.0008 (visited on 11/15/2016).

Fronczak, Agata (2012). "Exponential random graph models". In: *arXiv preprint*. URL: http://arxiv.org/abs/1210.7828.

Geyer, Charles J. and Elizabeth A. Thompson (1992). "Constrained Monte Carlo Maximum Likelihood for Dependent Data". In: *Journal of the Royal Statistical Society. Series B (Methodological)* 54.3, pp. 657–699. ISSN: 0035-9246. URL: https://www.jstor.org/stable/2345852 (visited on 09/20/2018).

Gilbert, E. N. (1959). "Random Graphs". EN. In: *The Annals of Mathematical Statistics* 30.4, pp. 1141–1144. ISSN: 0003-4851, 2168-8990. DOI: 10.1214/aoms/1177706098. URL: https://projecteuclid.org/euclid.aoms/1177706098 (visited on 09/15/2018).

Ginestet, Cedric E et al. (2011). "Brain network analysis: separating cost from topology using cost-integration". In: *PloS one* 6.7, e21570.

Goldenberg, Anna et al. (2009). "A survey of statistical network models". In: *arXiv:0912.5410 [physics, q-bio, stat]*. arXiv: 0912.5410. URL: http://arxiv.org/abs/0912.5410 (visited on 11/17/2016).

Gordon, Evan M. et al. (2014). "Generation and evaluation of a cortical area parcellation from resting-state correlations". In: *Cerebral cortex* 26.1, pp. 288–303.

Grefkes, Christian and Gereon R. Fink (2011). "Reorganization of cerebral networks after stroke: new insights from neuroimaging with connectivity approaches". In: *Brain* 134.5, pp. 1264–1276. ISSN: 0006-8950. DOI: 10.1093/brain/awr033. URL: http://www.ncbi.nlm.nih.gov/pmc/articles/PMC3097886/ (visited on 11/17/2016).

Hanneke, Steve, Wenjie Fu, and Eric P. Xing (2010). "Discrete temporal models of social networks". In: *Electronic Journal of Statistics* 4, pp. 585–605. DOI: 10.1214/09-EJS548. URL: http://projecteuclid.org/euclid.ejs/1276694116.

He, Biyu J. et al. (2007). "Breakdown of functional connectivity in frontoparietal networks underlies behavioral deficits in spatial neglect". In: *Neuron* 53.6, pp. 905–918.

Heuvel, Martijn P van den and Hilleke E Hulshoff Pol (2010). "Exploring the brain network: a review on resting-state fMRI functional connectivity." In: *European neuropsychopharmacology : the journal of the European College of Neuropsychopharmacology* 20.8, pp. 519–34. DOI: 10.1016/j.euroneuro.2010.03.008. URL: http://www.ncbi.nlm.nih.gov/pubmed/20471808.

Heuvel, Martijn P van den et al. (2008). "Small-world and scale-free organization of voxel-based resting-state functional connectivity in the human brain". In: *Neuroimage* 43.3, pp. 528–539.

Heuvel, Martijn P. van den and Olaf Sporns (2011). "Rich-Club Organization of the Human Connectome". en. In: *Journal of Neuroscience* 31.44, pp. 15775–15786. ISSN: 0270-6474, 1529-2401. DOI: 10.1523/JNEUROSCI.3539-11.2011. URL: http://www.jneurosci.org/content/31/44/15775 (visited on 09/25/2018).

Hilgetag, Claus C. and Marcus Kaiser (2004). "Clustered Organization of Cortical Connectivity". en. In: *Neuroinformatics* 2.3, pp. 353–360. ISSN: 1539-2791. DOI: 10.1385/NI:2:3:353. URL: http://link.springer.com/10.1385/NI:2:3:353 (visited on 09/25/2018).

Holland, Paul W. and Samuel Leinhardt (1981). "An Exponential Family of Probability Distributions for Directed Graphs". In: *Journal of the American Statistical Association* 76.373, pp. 33–50. ISSN: 0162-1459. DOI: 10.2307/2287037. URL: https://www.jstor.org/stable/2287037 (visited on 09/15/2018).

Holme, Petter (2003). "Network dynamics of ongoing social relationships". In: *EPL (Europhysics Letters)* 64.3, p. 427.

Holme, Petter and Jari Saramäki (2012). "Temporal networks". In: *Physics Reports* 519.3, pp. 97–125. DOI: 10.1016/j.physrep.2012.03.001. URL: http://linkinghub.elsevier.com/retrieve/pii/S0370157312000841.

Honey, C. J. et al. (2009). "Predicting human resting-state functional connectivity from structural connectivity". en. In: *Proceedings of the National Academy of Sciences* 106.6, pp. 2035–2040. ISSN: 0027-8424, 1091-6490. DOI: 10.1073/pnas.0811168106. URL: http://www.pnas.org/content/106/6/2035 (visited on 11/16/2016).

Huisman, T.A.G.M. (2010). "Diffusion-weighted and diffusion tensor imaging of the brain, made easy". In: *Cancer Imaging* 10.1A, S163–S171. ISSN: 1740-5025. DOI: 10.1102/1470-7330.2010.9023. URL: https://www.ncbi.nlm.nih.gov/pmc/articles/PMC2967146/ (visited on 10/13/2018).

Hunter, David R. (2007). "Curved exponential family models for social networks". In: *Social Networks* 29, pp. 216–230. ISSN: 0378-8733. DOI: 10.1016/j.socnet.2006.08.005.

Hunter, David R and Mark S Handcock (2006). "Inference in Curved Exponential Family Models for Networks". In: *Journal of Computational and Graphical Statistics* 15.3, pp. 565–583. ISSN: 1061-8600. DOI: 10.1198/106186006X133069.

URL: http://amstat.tandfonline.com/doi/abs/10.1198/106186006X133069 (visited on 11/17/2016).

Hutchison, R Matthew et al. (2013). "Dynamic functional connectivity: promise, issues, and interpretations." In: *NeuroImage* 80, pp. 360–78. DOI: 10.1016/j.neuroimage.2013.05.079. URL: http://www.pubmedcentral.nih.gov/articlerender.fcgi?artid=3807588&tool=pmcentrez&rendertype=abstract.

Kivela, M. et al. (2014). "Multilayer networks". In: *Journal of Complex Networks*. DOI: 10.1093/comnet/cnu016. URL: http://comnet.oxfordjournals.org/cgi/doi/10.1093/comnet/cnu016.

Latapy, Matthieu, Tiphaine Viard, and Clémence Magnien (2017). "Stream Graphs and Link Streams for the Modeling of Interactions over Time". In: *arXiv preprint arXiv:1710.04073*.

Latora, V and M Marchiori (2001). "Efficient behavior of small-world networks." In: *Physical review letters* 87, pp. 198701–198701. ISSN: 0031-9007. DOI: 10.1103/PhysRevLett.87.198701.

Lee, Jihui, Gen Li, and James D. Wilson (2017). "Varying-coefficient models for dynamic networks". In: *arXiv:1702.03632 [stat]*. arXiv: 1702.03632. URL: http://arxiv.org/abs/1702.03632 (visited on 10/24/2018).

Leifeld, Philip, Skyler J. Cranmer, and Bruce A. Desmarais (2015). "Temporal Exponential Random Graph Models with xergm: Estimation and Bootstrap Confidence Intervals". In: *Journal of Statistical Software*. URL: http://www.philipleifeld.com/cms/upload/btergm.pdf (visited on 02/22/2017).

Li, Aming et al. (2017). "The fundamental advantages of temporal networks". In: *Science* 358.6366, pp. 1042–1046.

Li, Siming et al. (2004). "A Map of the Interactome Network of the Metazoan C. elegans". In: *Science (New York, N.Y.)* 303.5657, pp. 540–543. ISSN: 0036-8075. DOI: 10.1126/science.1091403. URL: https://www.ncbi.nlm.nih.gov/pmc/articles/PMC1698949/ (visited on 10/24/2018).

Li, Wei et al. (2014). "Changes in brain functional network connectivity after stroke". In: *Neural Regeneration Research* 9.1, pp. 51–60. ISSN: 1673-5374. DOI: 10.4103/1673-5374.125330. URL: https://www.ncbi.nlm.nih.gov/pmc/articles/PMC4146323/ (visited on 10/24/2018).

Liljeros, Fredrik, Christofer R. Edling, and Luis A. Nunes Amaral (2003). "Sexual networks: implications for the transmission of sexually transmitted infections". In: *Microbes and infection* 5.2, pp. 189–196.

Liu, Yong et al. (2008). "Disrupted small-world networks in schizophrenia". In: *Brain* 131.4, pp. 945–961.

Lynall, Mary-Ellen et al. (2010). "Functional Connectivity and Brain Networks in Schizophrenia". en. In: *Journal of Neuroscience* 30.28, pp. 9477–9487. ISSN: 0270-6474, 1529-2401. DOI: 10.1523/JNEUROSCI.0333-10.2010. URL: http://www.jneurosci.org/content/30/28/9477 (visited on 11/17/2016).

Maldjian, Joseph A, Elizabeth M Davenport, and Christopher T Whitlow (2014). "Graph theoretical analysis of resting-state MEG data: identifying interhemispheric connectivity and the default mode". In: *Neuroimage* 96, pp. 88–94.

Mesulam, M.-Marsel (2000). *Principles of behavioral and cognitive neurology*. Oxford University Press.

Meunier, David, Renaud Lambiotte, and Edward T. Bullmore (2010). "Modular and Hierarchically Modular Organization of Brain Networks". English. In: *Frontiers in Neuroscience* 4. ISSN: 1662-453X. DOI: 10.3389/fnins.2010.00200. URL: https://www.frontiersin.org/articles/10.3389/fnins.2010.00200/full (visited on 09/25/2018).

Moody, James (2002). "The importance of relationship timing for diffusion". In: *Social Forces* 81.1, pp. 25–56.

Morris, Martina, Mark S Handcock, and David R Hunter (2008). "Specification of Exponential-Family Random Graph Models: Terms and Computational Aspects." In: *Journal of statistical software* 24.4, pp. 1548–7660. ISSN: 1548-7660 (Electronic)\n1548-7660 (Linking). URL: http://www.pubmedcentral.nih.gov/articlerender.fcgi?artid=2481518&tool=pmcentrez&rendertype=abstract.

Mostany, Ricardo and Carlos Portera-Cailliau (2011). "Absence of Large-Scale Dendritic Plasticity of Layer 5 Pyramidal Neurons in Peri-Infarct Cortex". en. In: *Journal of Neuroscience* 31.5, pp. 1734–1738. ISSN: 0270-6474, 1529-2401. DOI: 10.1523/JNEUROSCI.4386-10.2011. URL: http://www.jneurosci.org/content/31/5/1734 (visited on 10/23/2018).

Muldoon, Sarah Feldt and Danielle S. Bassett (2016). "Network and Multilayer Network Approaches to Understanding Human Brain Dynamics". In: *Philosophy of Science* 83.5, pp. 710–720. ISSN: 0031-8248. DOI: 10.1086/687857. URL: https://www.journals.uchicago.edu/doi/abs/10.1086/687857 (visited on 10/16/2018).

Newman, M. E. J. (2006). "Modularity and community structure in networks". en. In: *Proceedings of the National Academy of Sciences* 103.23, pp. 8577–8582.

ISSN: 0027-8424, 1091-6490. DOI: 10.1073/pnas.0601602103. URL: http://www.pnas.org/content/103/23/8577 (visited on 11/17/2016).

Newman, Mark (2010). *Networks: An Introduction*. en. Oxford University Press. ISBN: 978-0-19-920665-0.

Newman, Mark EJ, Steven H. Strogatz, and Duncan J. Watts (2001). "Random graphs with arbitrary degree distributions and their applications". In: *Physical review E* 64.2, p. 026118.

Nunez, Paul L and Ramesh Srinivasan (2006). *Electric fields of the brain: the neurophysics of EEG*. Oxford university press.

Obando, Catalina and Fabrizio De Vico Fallani (2017). "A statistical model for brain networks inferred from large-scale electrophysiological signals". en. In: *Journal of The Royal Society Interface* 14.128, p. 20160940. ISSN: 1742-5689, 1742-5662. DOI: 10.1098/rsif.2016.0940. URL: http://rsif.royalsocietypublishing.org/content/14/128/20160940 (visited on 10/24/2018).

Park, Hae-Jeong and Karl Friston (2013). "Structural and Functional Brain Networks: From Connections to Cognition". en. In: *Science* 342.6158, p. 1238411. ISSN: 0036-8075, 1095-9203. DOI: 10.1126/science.1238411. URL: http://science.sciencemag.org/content/342/6158/1238411 (visited on 11/17/2016).

Pattison, P. and S. Wasserman (1999). "Logit models and logistic regressions for social networks: II. Multivariate relations". eng. In: *The British Journal of Mathematical and Statistical Psychology* 52 (Pt 2), pp. 169–193. ISSN: 0007-1102.

Pattison, Philippa and Garry Robins (2002). "Neighborhood-Based Models For Social Networks". In: *Sociological Methodology* 32.1, pp. 301–337. ISSN: 00811750. DOI: 10.1111/1467-9531.00119. URL: http://www.blackwell-synergy.com/links/doi/10.1111/1467-9531.00119.

Pereira, Fernando et al. (2013). "Creating group-level functionally-defined atlases for diagnostic classification". In: *Pattern Recognition in Neuroimaging (PRNI), 2013 International Workshop on*. IEEE, pp. 29–32.

Quiroga, R Quian et al. (2002). "Performance of different synchronization measures in real data: a case study on electroencephalographic signals". In: *Physical Review E* 65.4, p. 041903.

Ramsey, Lenny E. et al. (2016). "Normalization of network connectivity in hemispatial neglect recovery". In: *Annals of neurology* 80.1, pp. 127–141.

Reus, Marcel A de and Martijn P Van den Heuvel (2013). "The parcellation-based connectome: limitations and extensions". In: *Neuroimage* 80, pp. 397–404.

Riolo, Christopher S., James S. Koopman, and Stephen E. Chick (2001). "Methods and measures for the description of epidemiologic contact networks". In: *Journal of Urban Health* 78.3, pp. 446–457.

Robb, R. A. and D. P. Hanson (1991). "A software system for interactive and quantitative visualization of multidimensional biomedical images". eng. In: *Australasian Physical & Engineering Sciences in Medicine* 14.1, pp. 9–30. ISSN: 0158-9938.

Robins, Garry and Philippa Pattison (2001). "Random Graph Models for Temporal Processes in Social Networks". In: *The Journal of Mathematical Sociology* 25.1, pp. 5–41. ISSN: 0022-250X, 0022-250X. DOI: 10.1080/0022250X.2001.9990243. URL: http://search.proquest.com/docview/60399651?accountid=13374.

Robins, Garry, Philippa Pattison, and Stanley Wasserman (1999). "Logit models and logistic regressions for social networks: III. Valued relations". en. In: *Psychometrika* 64.3, pp. 371–394. ISSN: 1860-0980. DOI: 10.1007/BF02294302. URL: https://doi.org/10.1007/BF02294302 (visited on 09/15/2018).

Robins, Garry et al. (2007). "An introduction to exponential random graph (p *) models for social networks". In: *Social Networks* 29, pp. 173–191. ISSN: 03788733. DOI: 10.1016/j.socnet.2006.08.002.

Robins, Garry L. et al. (2003). "Assessing Degeneracy in Statistical Models of Social Networks". In: *Journal of the American Statistical Association* 76.39, pp. 33–50. DOI: 10.1.1.81.5086. URL: http://citeseerx.ist.psu.edu/viewdoc/summary?doi=10.1.1.81.5086.

Rogers, Baxter P. et al. (2007). "Assessing Functional Connectivity in the Human Brain by FMRI". In: *Magnetic resonance imaging* 25.10, pp. 1347–1357. ISSN: 0730-725X. DOI: 10.1016/j.mri.2007.03.007. URL: https://www.ncbi.nlm.nih.gov/pmc/articles/PMC2169499/ (visited on 09/26/2018).

Rosvall, Martin and Carl T. Bergstrom (2010). "Mapping change in large networks". In: *PloS one* 5.1, e8694.

Rubinov, Mikail and Olaf Sporns (2010). "Complex network measures of brain connectivity: Uses and interpretations". In: *NeuroImage*. Computational Models of the Brain 52.3, pp. 1059–1069. ISSN: 1053-8119. DOI: 10.1016/j.neuroimage.2009.10.003. URL: http://www.sciencedirect.com/science/article/pii/S105381190901074X (visited on 11/17/2016).

Rubinov, Mikail and Olaf Sporns (2011). "Weight conserving characterization of complex functional brain networks". In: *Neuroimage* 56.4, pp. 2068–2079.

Sakkalis, Vangelis (2011). "Review of advanced techniques for the estimation of brain connectivity measured with EEG/MEG". In: *Computers in biology and medicine* 41.12, pp. 1110–1117.

Salvador, Raymond et al. (2005). "Neurophysiological architecture of functional magnetic resonance images of human brain". In: *Cerebral cortex* 15.9, pp. 1332–1342.

Siegel, Joshua S. et al. (2018). "Re-emergence of modular brain networks in stroke recovery". In: *Cortex* 101, pp. 44–59. ISSN: 0010-9452. DOI: 10.1016/j.cortex.2017.12.019. URL: http://www.sciencedirect.com/science/article/pii/S0010945217304276 (visited on 02/13/2018).

Siegel, Joshua Sarfaty et al. (2016). "Disruptions of network connectivity predict impairment in multiple behavioral domains after stroke". en. In: *Proceedings of the National Academy of Sciences* 113.30, E4367–E4376. ISSN: 0027-8424, 1091-6490. DOI: 10.1073/pnas.1521083113. URL: http://www.pnas.org/content/113/30/E4367 (visited on 06/25/2018).

Snijders, Tom A B (2002). "Markov Chain Monte Carlo Estimation of Exponential Random Graph Models". In:

Snijders TAB Robins GL & Handcock MS, Pattison P (2006). "New specifications for exponential random graph models". In: pp. 99–153. DOI: 10.1111/j.1467-9531.2006.00176.x. URL: http://onlinelibrary.wiley.com/doi/10.1111/j.1467-9531.2006.00176.x/abstract.

Sporns, Olaf (2013a). "Making sense of brain network data". en. In: *Nature Methods* 10.6, pp. 491–493. ISSN: 1548-7091, 1548-7105. DOI: 10.1038/nmeth.2485. URL: http://www.nature.com/articles/nmeth.2485 (visited on 10/16/2018).

— (2013b). "Structure and function of complex brain networks". In: *Dialogues in Clinical Neuroscience* 15.3, pp. 247–262. ISSN: 1294-8322. URL: https://www.ncbi.nlm.nih.gov/pmc/articles/PMC3811098/ (visited on 09/27/2018).

Sporns, Olaf and Richard F. Betzel (2016). "Modular Brain Networks". In: *Annual review of psychology* 67, pp. 613–640. ISSN: 0066-4308. DOI: 10.1146/annurev-psych-122414-033634. URL: https://www.ncbi.nlm.nih.gov/pmc/articles/PMC4782188/ (visited on 09/25/2018).

Sporns, Olaf, Christopher J. Honey, and Rolf Kötter (2007). "Identification and Classification of Hubs in Brain Networks". en. In: *PLOS ONE* 2.10,

e1049. ISSN: 1932-6203. DOI: 10.1371/journal.pone.0001049. URL: https://journals.plos.org/plosone/article?id=10.1371/journal.pone.0001049 (visited on 09/25/2018).

Sporns, Olaf and Jonathan D. Zwi (2004). "The Small World of the Cerebral Cortex". en. In: *Neuroinformatics* 2.2, pp. 145–162. ISSN: 1539-2791. DOI: 10.1385/NI:2:2:145. URL: http://link.springer.com/10.1385/NI:2:2:145 (visited on 09/25/2018).

Stam, C. J. (2004). "Functional connectivity patterns of human magnetoencephalographic recordings: a 'small-world' network?" In: *Neuroscience Letters* 355.1–2, pp. 25–28. ISSN: 0304-3940. DOI: 10.1016/j.neulet.2003.10.063. URL: http://www.sciencedirect.com/science/article/pii/S0304394003012722 (visited on 11/17/2016).

Stam, C. J. and E. C. W. van Straaten (2012). "The organization of physiological brain networks". In: *Clinical Neurophysiology* 123.6, pp. 1067–1087. ISSN: 1388-2457. DOI: 10.1016/j.clinph.2012.01.011. URL: http://www.sciencedirect.com/science/article/pii/S1388245712000570 (visited on 11/17/2016).

Stam, Cornelis J (2014). "Modern network science of neurological disorders". In: *Nature Publishing Group* September, pp. 1–13. DOI: 10.1038/nrn3801. URL: http://dx.doi.org/10.1038/nrn3801.

Stam, Cornelis J. and Jaap C. Reijneveld (2007). "Graph theoretical analysis of complex networks in the brain". In: *Nonlinear Biomedical Physics* 1.1, p. 3. ISSN: 1753-4631. DOI: 10.1186/1753-4631-1-3. URL: https://doi.org/10.1186/1753-4631-1-3 (visited on 09/25/2018).

Stanley, Matthew L et al. (2013). "Defining nodes in complex brain networks". In: *Frontiers in computational neuroscience* 7.

Strauss, David and Michael Ikeda (1990). "Pseudolikelihood estimation for social networks". In: *Journal of the American statistical association* 85.409, pp. 204–212.

Supekar, Kaustubh et al. (2008). "Network analysis of intrinsic functional brain connectivity in Alzheimer's disease". In: *PLoS Comput Biol* 4.6, e1000100.

Tang, J. et al. (2009). "Small-world behavior in time-varying graphs". In: pp. 5–5. DOI: 10.1103/PhysRevE.81.055101. URL: http://arxiv.org/abs/0909.1712.

Thompson, William Hedley, Per Brantefors, and Peter Fransson (2017). "From static to temporal network theory: Applications to functional brain connectivity". In: *Network Neuroscience* 1.2, pp. 69–99.

Tijms, Betty M. et al. (2013). "Alzheimer's disease: connecting findings from graph theoretical studies of brain networks". In: *Neurobiology of Aging* 34.8, pp. 2023–2036. ISSN: 0197-4580. DOI: 10.1016/j.neurobiolaging.2013.02.020. URL: http://www.sciencedirect.com/science/article/pii/S0197458013000997 (visited on 11/17/2016).

Tononi, G, O Sporns, and G M Edelman (1994). "A measure for brain complexity: relating functional segregation and integration in the nervous system." In: *Proceedings of the National Academy of Sciences of the United States of America* 91.May, pp. 5033–5037. ISSN: 0027-8424 (Print)\n0027-8424 (Linking). DOI: 10.1073/pnas.91.11.5033.

Tumminello, M. et al. (2005). "A tool for filtering information in complex systems". en. In: *Proceedings of the National Academy of Sciences of the United States of America* 102.30, pp. 10421–10426. ISSN: 0027-8424, 1091-6490. DOI: 10.1073/pnas.0500298102. URL: http://www.pnas.org/content/102/30/10421 (visited on 11/17/2016).

Valencia, Miguel et al. (2008). "Dynamic small-world behavior in functional brain networks unveiled by an event-related networks approach". In: *Physical Review E* 77.5, p. 050905.

Van Meer, Maurits PA et al. (2010). "Recovery of sensorimotor function after experimental stroke correlates with restoration of resting-state interhemispheric functional connectivity". In: *Journal of Neuroscience* 30.11, pp. 3964–3972.

Vergara, Victor M. et al. (2018). "Dynamic functional network connectivity discriminates mild traumatic brain injury through machine learning". In: *NeuroImage: Clinical* 19, pp. 30–37. ISSN: 2213-1582. DOI: 10.1016/j.nicl.2018.03.017. URL: http://www.sciencedirect.com/science/article/pii/S2213158218300871 (visited on 10/24/2018).

Vidal, Marc, Michael E. Cusick, and Albert-László Barabási (2011). "Interactome Networks and Human Disease". In: *Cell* 144.6, pp. 986–998. ISSN: 0092-8674. DOI: 10.1016/j.cell.2011.02.016. URL: http://www.sciencedirect.com/science/article/pii/S0092867411001309 (visited on 11/17/2016).

Wang, Liang et al. (2010a). "Dynamic functional reorganization of the motor execution network after stroke". In: *Brain* 133.4, pp. 1224–1238.

Wang, Liang et al. (2010b). "Impaired efficiency of functional networks underlying episodic memory-for-context in schizophrenia". In: *The Journal of Neuroscience* 30.39, pp. 13171–13179.

Wasserman, Stanley and Philippa Pattison (1996). "Logit models and logistic regressions for social networks: I. An introduction to Markov graphs andp". en. In: *Psychometrika* 61.3, pp. 401–425. ISSN: 0033-3123, 1860-0980. DOI: 10.1007/BF02294547. URL: http://link.springer.com/article/10.1007/BF02294547 (visited on 11/17/2016).

Watts, Duncan J. and Steven H. Strogatz (1998). "Collective dynamics of 'small-world' networks". en. In: *Nature* 393.6684, pp. 440–442. ISSN: 0028-0836. DOI: 10.1038/30918. URL: http://www.nature.com/nature/journal/v393/n6684/abs/393440a0.html?cookies=accepted (visited on 11/15/2016).

Weiller, Cornelius et al. (1992). "Functional reorganization of the brain in recovery from striatocapsular infarction in man". In: *Annals of Neurology: Official Journal of the American Neurological Association and the Child Neurology Society* 31.5, pp. 463–472.